AD 669251

VOL. I.--Technical Summary Report No. 1

Dec. 9, 1965 to Dec. 8, 1966

EQUATIONS OF STATE IN SOLIDS

by

G. E. Duvall, G. R. Fowles,
and Y. Horie

Contract No.
DA-04-200-AMC-1702(X)

WSU SDL 67-01
February, 1967

Research sponsored by the U.S. Army
Ballistics Research Laboratories
Aberdeen Proving Ground, Maryland

BEST AVAILABLE COPY

VOL. I.--Technical Summary Report No. 1

Dec. 9, 1965 to Dec. 8, 1966

EQUATIONS OF STATE IN SOLIDS

by

G. E. Duvall, G. R. Fowles,
and Y. Horie

Contract No.
DA-04-200-AMC-1702(X)

WSU SDL 67-01
February, 1967

Research sponsored by the U.S. Army
Ballistics Research Laboratories
Aberdeen Proving Ground, Maryland

TABLE OF CONTENTS

	Page
ABSTRACT	v
LIST OF TABLES	vii
LIST OF ILLUSTRATIONS	ix
FORWARD	xi
I. INTRODUCTION	1
II. CONSTITUTIVE RELATIONS	3
2.1 General Considerations	3
2.2 Equations of State for Fluids	3
2.3 Elastic Solids	10
III. PHASE TRANSITIONS	41
3.1 Introduction	41
3.2 General Constitutive Relations for Two-Phase Flow	46
3.3 Irreversible Thermodynamics and Phase Relaxation	50
IV. CONSTITUTIVE RELATIONS FOR IRON	61
4.1 Approximations for Two-Phase Flow	61
4.2 Review of Experimental Information	64
4.3 Equation of State of Iron	65
V. SHOCK PROPAGATION IN IRON	71
5.1 Difference Equations	71
5.2 FORTRAN Program	75
5.3 Numerical Results	76
LITERATURE CITED	101
DISTRIBUTION LIST	105
APPENDIX	
I. HEAT CAPACITY OF MIXTURE	109
II. PROGRAM FOR CALCULATING WAVE FLOW IN ONE SPACE DIMENSION FOR PLANE, CYLINDRICAL, OR SPHERICAL GEOMETRY	111
III. FLOW CHART FOR BURN	129

Abstract

A procedure is described for developing simple approximate equations of state of liquids from Hugoniot P-V relations determined in shock wave measurements. This is applied to a number of liquids and a table of coefficients is given.

The formalism of irreversible thermodynamics is applied to time-dependent phase transitions in iron and an approximate set of constitutive relations is obtained in a form suitable for numerical integration with the equations of continuum dynamics. These are applied in an approximate form to study the development of the two-wave structure in iron caused by the α-ϵ phase transition.

Finite strain theory is applied to the analysis of shock wave data for quartz, and the results supply enough information to estimate some of the fourth-order elastic constants.

LIST OF TABLES

Table		Page
I.	Equation of State Parameters for Liquids	9
II.	Summary of Experimental Data	19
III.	Elastic Moduli of Quartz	33
IV.	Stress-Kbar	38
V.	The Coefficient dp/dT from Static and Shock Wave Experiments	42
VI.	Physical Data for α - iron	67

LIST OF ILLUSTRATIONS

Figure		Page
2.1	Diagram of Experimental Assembly	12
2.2	Photograph of Experimental Assembly	14
2.3	Diagram Showing Relation of Experimental Assembly, Light Source and Camera	16
2.4	Streak Camera Photograph Showing Shock Arrival Times and Free-Surface Traces. Shock No. 7394	18
2.5	Definition of Parameters Used in Adjusting Streak Camera Data	21
2.6	Shock Velocity as Function of Particle Velocity. Curves labelled 3rd, 4th, are fits based on zero-pressure elastic constants up to 3rd and 4th order respectively for X and Z-cut crystals	23
2.7	Stress-Volume States Resulting From Shock Compression of X-cut Quartz. Solid curve is Bridgman's Hydrostatic Data. Curves labelled 3rd, 4th, are fits based on zero-pressure elastic constants to 3rd and 4th order	24
2.8	Stress-Volume States Resulting From Shock Compression of Y-cut Quartz. Solid curve is Bridgman's Hydrostatic Data	25
2.9	Stress-Volume States Resulting From Shock Compression of Z-cut Quartz. Solid curve is Bridgman's Hydrostatic Data. Curves labelled 3rd, 4th, are fits based on zero-pressure elastic constants to 3rd and 4th order. The curve labelled X represents the tangential stresses, calculated from constants up to and including 3rd order	26
3.1	Extended Metastable Region	44
4.1	Temperature Independent Equation of State of Iron and α^{eq}	68
5.1	Difference Scheme in Space	71
5.2	Computational Sequence	72
5.3	Flow Chart for the Constitutive Relation	77
5.4	Wave Propagation in Iron at Early Stages	78
5.5	Double Shock in Iron	79
5.6	Relative Magnitude of p and q for $C_L = .1$	80

List of Illustrations--(continued)

5.7 Wave Propagation with $C_L = .02$ 82

5.8 Wave Propagation with $C_L = .1$ 83

5.9 Wave Propagation with $C_L = .2$ 84

5.10 Effect of q at .4 μsec 85

5.11 Effect of q at 1. μsec 86

5.12 q and Speed of Transformation at Fifth Cell 88

5.13 Decay of First Shock in Iron Resulting from Phase Transition . . . 89

5.14 Pressure Profile and Total Stress with Respect to the Rayleigh Line 92

5.15 Total Stress (p+q) and Rayleigh Line 93

5.16 The Hugoniot Curve in and Beyond the Coexistence Region. . . . 95

5.17 Path of the Permanent Regime Solution 98

5.18 dp/dx for Permanent Regime Solution. 98

5.19 Comparison of Permanent Regime with Transient Profile of Second Shock. 99

Foreword

The work reported here represents the results and the state of understanding which had been achieved in December, 1966. Since that time some further progress has been made, and it will be described in later reports of this series. Particular attention is drawn to the approximate temperature calculation described in Section 4.1. The basis of this approximation is now thought to be unsound, so some skepticism should be maintained concerning temperature effects reported. Fortunately these are few and slight, and the general conclusions of the report are not affected by possible errors here.

A major shortcoming of the theory, but one which is very hard to evaluate, is the complete reliance on equilibrium thermodynamics to describe the static behavior. It is quite likely that metallurgical considerations govern the true progress of the α-ϵ transition in iron; consequently the static reference states to which dynamic effects are referred may be metastable and very different from the thermodynamic states. This is suggested by recent static pressure measurements by Bassett and co-workers (J. Appl. Phys., Jan. 1967) and by shock de-magnetization experiments by R. A. Graham of Sandia Corporation (private communication). Satisfactory metallurgical models for such processes are not presently available; it is hoped that shock wave measurements will help to stimulate the development of such models.

February, 1968

I. INTRODUCTION

Numerical methods for the integration of the equations of finite amplitude wave propagation have reached such a stage of development that the principal limitation on predictions of wave effects is more apt to be uncertainty in the constitutive relations of the material than inability to perform the integrations. The complete constitutive relations for a real solid may at present be regarded as unknowable. Practically useful relations can be obtained from a succession of approximations, to each of which is attached some uncertainty. For high amplitude compressive waves the predominant relation is the hydrostatic one between pressure, volume and temperature. To this may be added the effects of finite shear strength, which makes the pressure tensor anisotropic, strain-rate effects which cause deviations from equilibrium, and partition of internal energy among thermal, surface, and inhomogeneous effects.

In the present work the primary emphasis is on the effects of phase transitions on compressive wave forms, particularly when the rate of transition is too slow to exactly follow the changes in pressure, temperature, and density associated with the compressive wave which initiates the transition. In order to study these effects it has been necessary to develop computer programs for integration of the flow equations for the appropriate constitutive relations. In the course of this

development other useful results on equations of state have been produced, and these are described in the following sections.

II. CONSTITUTIVE RELATIONS

2.1 General Considerations

The term "constitutive relations" is used in a generic sense to encompass all material properties which must be combined with the equations of continuity, motion, and energy conservation to supply a complete set of flow equations. Constitutive relations in practice usually reduce to an equation of state relating pressure, volume, and temperature or internal energy. This simplification is partially enforced by ignorance of other material relations; it often yields, in addition, quite a good description of wave propagation over a wide range of parameters. The equation of state is necessarily accompanied by a statement about the variation of specific heat with pressure and temperature. It may on occasion include information about rigidity and yield or even rate effects. For the present we consider the equation of state as defined above. These considerations are themselves useful and they will provide insight into the requirements which must be satisfied by more general constitutive relations. The following remarks are necessarily limited in their scope. More detailed information will be found in various review articles (1,2).

2.2 Equations of State for Fluids (3)

A "complete" equation of state for a fluid is a relation between thermodynamic variables which is sufficient for

calculating any thermodynamic parameter of the material, given two. For example, if specific internal energy, E, is given as a function of specific entropy, S, and specific volume v, $E = E(S,v)$, then

$$p = -(\partial e/\partial v)_S$$

$$T = (\partial e/\partial S)_v$$

$$H = E + pv$$

etc.,

where p, T, H are pressure, temperature and specific enthalpy. On the other hand, if pressure is given as a function of T and v, as usually occurs, then neither internal energy nor enthalpy can be calculated without specifying the specific heat.

When partial equations of state are given, as in the last example, then certain limitations are placed on other thermodynamic quantities if all are to be compatible. This is illustrated by the following example. Suppose that specific heat at constant pressure is known as a function of temperature and assumed to be a function of temperature alone: $C_p = C_p(T)$. Then by the following argument we can see that the relation between p, v, and T must be that of Eq. (2.1) below:

$$(\partial H/\partial T)_p = C_p(T) \quad \text{by definition.} \tag{2.1}$$

If $H = H(p,T)$, then

$$dH = C_p dT + (\partial H/\partial p)_T \, dp$$

or

$$H = \int C_p(T) dT + f(p) \ .$$

We may thus write that

$$(\partial H/\partial p)_T = f'(p) = (\partial H/\partial p)_S + (\partial H/\partial S)_p(\partial S/\partial p)_T$$

$$= v - T\,(\partial v/\partial T)_p .$$

Dividing by T^2 we find that

$$f'(p)/T^2 = -(\partial(v/T)/\partial T)_p .$$

When integrated this yields the implied form for the equation of state:

$$v = f'(p) + Tg(p) \qquad (2.2)$$

where $$g(p) = (\partial v/\partial T)_p$$

In a similar way it can be shown that if specific heat at constant volume, C_v, is a function of T alone, $C_v = C_v\,(T)$, then it must follow that p, T, and v are related by a Grüneisen equation:

$$p = f(v) + Th(v) \qquad (2.3)$$

Both Eqs. (2.2) and (2.3) are remarkably simple. The (p, v, T) surfaces that can be represented by either of these can be constructed from a "bamboo-place-mat." In the first case the straight sticks lie in planes of constant p; in the second they lie in planes of constant v.

Eq. (2.3) has the same form as the Mie-Grüneisen equation:

$$p = p_k(v) + \Gamma C_v\,(T-T_o)/v \qquad (2.4)$$

where p_k is pressure on the isotherm $T = T_o$. With the assumption

that $C_v = C_v(T)$, Eqs. (2.2) and (2.3) then imply that

$$(\partial(\Gamma C_v)/\partial T)_v = 0.$$

This condition implies that $(\partial\Gamma/\partial T)_v \neq 0$ unless C_v = const. While it is very likely true that Γ does depend upon T (4), the only available theories of any generality suppose that $\Gamma = \Gamma(v)$ (1). Fowles has obtained a more general compatibility relation for Γ and C_v (5):

$$(\partial C_v/\partial \ln v)_T = (\partial(\Gamma C_v)/\partial \ln T)_v$$

It turns out that this is satisfied by the Debye theory of specific heats. However, any dependence of Debye temperature on temperature violates the condition.

Despite these difficulties, Eq. (2.3) has been commonly used to extend pressure-volume data determined from shock studies into off-Hugoniot regions (1). Doran (6) has gone even farther to show that quite reasonable representations of the equations of state of solids can be obtained with Γ/v = constant.

In view of the limitations on Γ and C_v, it is unlikely that the zero degree isotherms calculated using Eq. (2.4) and the Slater or Dugdale-McDonald relation for Γ are physically reliable. Their principal virtue is that they provide a consistent and reproducible procedure for determining a reference curve. An alternative procedure is to calculate the isotherm passing through the initial state of the Hugoniot. This avoids some of the difficulties associated with extrapolating to 0°K. It introduces some new ones inasmuch as there is now no theory for

calculating Γ. However, since the low temperature region is eliminated, the assumption Γ/v = constant may be a reasonable one. Then Eq. (2.4) becomes

$$p = p_i + b\,(E-E_i) \tag{2.5}$$

$$E_H = E_o + \tfrac{1}{2}\, p_H\,(v_o-v) \tag{2.6}$$

$$dE_i = (T_o\,(\partial p/\partial T)v - p_i)dv \tag{2.7}$$

$$= (bC_vT_o - p_i)dv$$

where $b = \Gamma/v$ = constant, C_v = constant, $p_i(v)$ and $E_i(v)$ are pressure and internal energy, respectively, on the T_o isotherm, and subscript "H" refers to the Hugoniot curve. Setting p and E in Eq. (2.5) equal to p_H and E_H and combining with Eqs. (2.6) and (2.7) yields a differential equation for p_i:

$$(dp_i/dv) + bp_i = (1 - b(v_o-v)/2)(dp_H/dv) + bp_H/2 + b^2C_vT_o \tag{2.8}$$

The solution of this equation is

$$p_i(v) = A\exp(-bv) + bC_vT_oB \tag{2.9}$$

$$A = f(v) - b\int_{v_o}^{v} f(v)dv$$

$$B = 1 - \exp(b(v_o-v))$$

$$f(v) = (1 - (b/2)(v_o-v))\,p_H\exp(bv).$$

Experience has shown that Hugoniot data for liquids and solids can be fitted quite well by curves of the form

$$p_h(v) = \sum_{n=1}^{3} a_n x^n \tag{2.10}$$

where $x = \rho v_o - 1$.

Equations of the form (2.10) have been fitted to shock data on liquids and used to calculate $p_i(v)$ and $E_i(v)$ from Eqs. (2.9) and (2.7), respectively. The numerical results are used in a least squares procedure to calculate the coefficients b_n in the equation for isothermal pressure:

$$p_i = \sum_{n=1}^{3} b_n x^n$$

where $x = \rho v_o - 1$ as in Eq. (2.10). The coefficients a_n and b_n are given in Table I.

Table I

Equation of State Parameters for Liquids

Liquid	v_o cc/g	b g/cc	C_v Mbcc/g	Mbars					
				a_1	a_2	a_3	b_1	b_2	b_3
Acetone	1.266	.7717	$.2210 \times 10^{-4}$	.011430	.066642	.06529	.0065389	.072453	.039347
Ethyl Alcohol	1.266	.500	.2390 "	.010664	.012718	.18343	.0084472	.022402	.15276
Hg	.07390	37.14	.0140 "	.28484	.33709	5.2384			
Glycerine	.7950	.9770	.2360 "	.045598	.18572	.39734	.04035	.20832	.29888
Benzene	1.139	1.105	.1700 "	.015154	.076136	.13401	.0082263	.089867	.075642
Ethyl Ether	1.405	.5270	.2260 "	.0072023	.036930	.082756	.0046190	.042386	.063185
Methanol	1.264	.4750	.2510 "	.0099446	.044929	.11398	.0078472	.050666	.092903
CCl_4	.6260	2.114	.08400 "	.014417	.0787315	.159736	.0075315	.095623	.088747
Water	1.002	.1070	.4180 "	.021950	.017078	.07004	.021810	.017614	.067912

2.3 Elastic Solids (G. R. Fowles)

The shock compression of quartz is of particular interest because of its importance to geophysics, its wide-spread use in shock wave studies as a pressure transducer, and because it represents a different class of materials from the more thoroughly studied metals. In this paper we describe measurements similar to those reported by Wackerle (15). The data are in substantial agreement; however, the recording techniques were somewhat different so that the present results* provide independent corroboration, in most respects, of Wackerle's data.

In addition to describing the experiments and the results, we examine the agreement between the uniaxial stress-strain data derived from shock experiments and predictions based on finite strain theory and the second and third-order elastic constants measured by McSkimin, et al. (39), and Thurston, et al. (40). From this comparison it is clear that shock-wave measurements and low pressure acoustic measurements are complementary methods for evaluating higher order elastic coefficients.

In Section 2.31 we describe the experimental technique and the experimental results; Section 2.32 gives a brief outline of finite strain theory and its application to the shock experiments. Conclusions are discussed in Section 2.33.

---

*These data were reported originally in the author's Ph.D. thesis (48).

2.31 Experiments

A. Experimental Method

In the experiments shock propagation velocities and associated free surface velocities were measured in alpha quartz crystals oriented as X, Y, or Z-cuts.* Shock waves of varying intensity were generated by plane-wave explosive lenses with or without additional explosive pads.

The experimental arrangement is shown schematically in Fig. 2.1. A four-inch diameter explosive lens (and in some cases an explosive pad) was cemented to one surface of a 1/2-inch thick, 5-inch diameter Dural plate. The quartz specimens (usually two) were cemented to the opposite, lapped surface of the plate. The specimens were accurately flat and polished; the tolerance on crystallographic orientation was ± 1°. The faces of the specimens in contact with the plate were vapor-plated with aluminum to yield a reflecting surface. Lucite mirrors, also aluminized on their inside faces were cemented to the outer surfaces of the specimens at angles of 3 to 8°. The edge of the lucite mirror in contact with the specimen was, in each case, set back from the edge of the specimen at least one specimen thickness to avoid interference from edge effects. The X, Y, or Z orientation refers to the smallest linear dimension and also designates the direction of shock propagation. The X-cut crystals were measured in both the + and - orientations because of the large differences observed in electrical experiments (41).

In some of the experiments an inclined lucite mirror was cemented directly to the aluminum plate. Its function was to measure the free-surface velocity of the aluminum to permit impedance-match solutions to the final shocked states (1).

---

*Synthetic crystals supplied by Valpey Corporation.

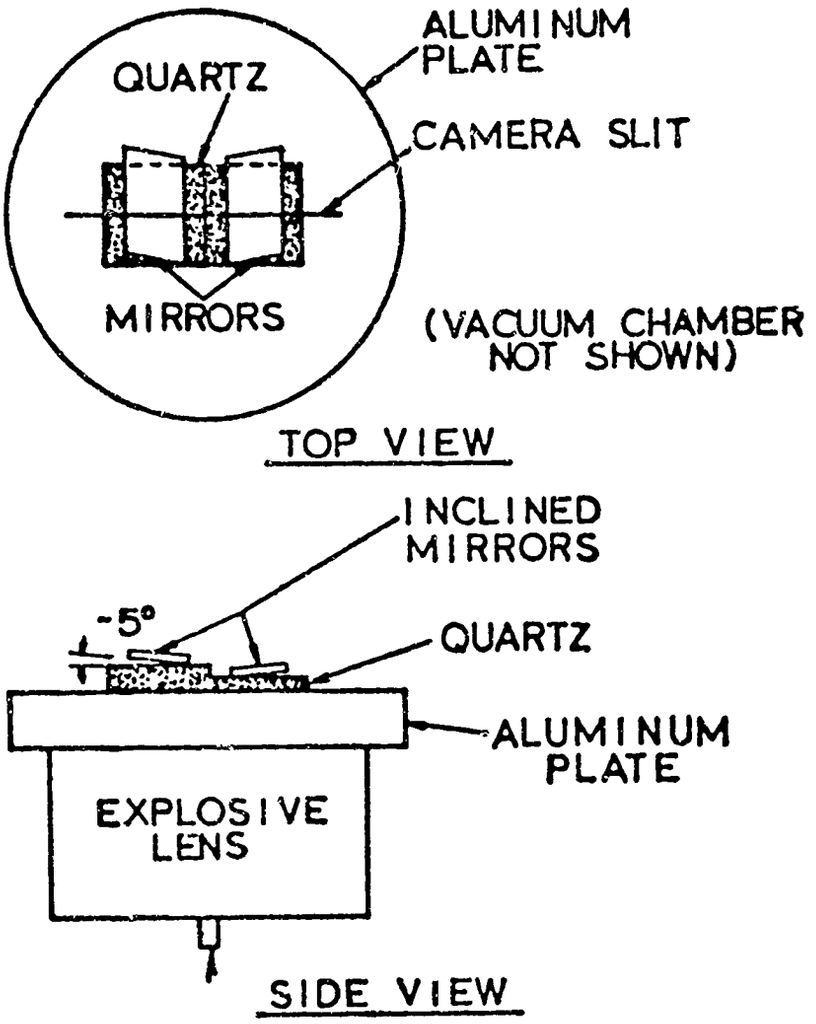

Fig. 2.1 Diagram of experimental assembly

The angles of the inclined mirrors with respect to the quartz surfaces were measured after assembly by mounting the assembly on a mill table and observing with a telescope the superposition of a cross-hair and its image reflected alternately in the quartz and lucite surfaces. The angles could thus be measured to a precision of 0.1%. Some difficulty was encountered in keeping the lucite mirrors extremely flat. It was necessary to allow angular deviations of up to ± one minute of arc. In each case this amounted to less than 1/2% of the total angle.

In order to obtain the desired accuracy in shock velocity, ± 1%, good contact (0.0002 inch) between the inside edge of the inclined mirror and the outer quartz surface was required. A contact such that no transmitted light was visible was considered satisfactory.

In order to avoid complications due to air shocks the assembly was evacuated prior to firing to a pressure of less than 0.05 torr. A hemicylindr section of lucite tubing cemented to the aluminum plate served as a vacuum chamber.

A photograph of an assembly, without explosive, prior to firing is shown as Fig. 2.2.

The assembly was viewed through a slit of a rotating mirror streak camera aligned along the centers of the inclined mirrors in the direction of maximum inclination (i.e., the direction in which the mirror angles were previously measured). The slit width was 0.05 mm; the time resolution, determined from the slit width and the camera writing speed (3.81 mm/μs), was approximately 0.01 μs.

Illumination was provided by an explosive argon light source consisting of a 4-inch diameter, 18-inch long cardboard tube with a one-inch pad of composition C-3 explosive at one end. A ground glass diffusing screen was placed over the other end and argon was flowed through the tube continuously.

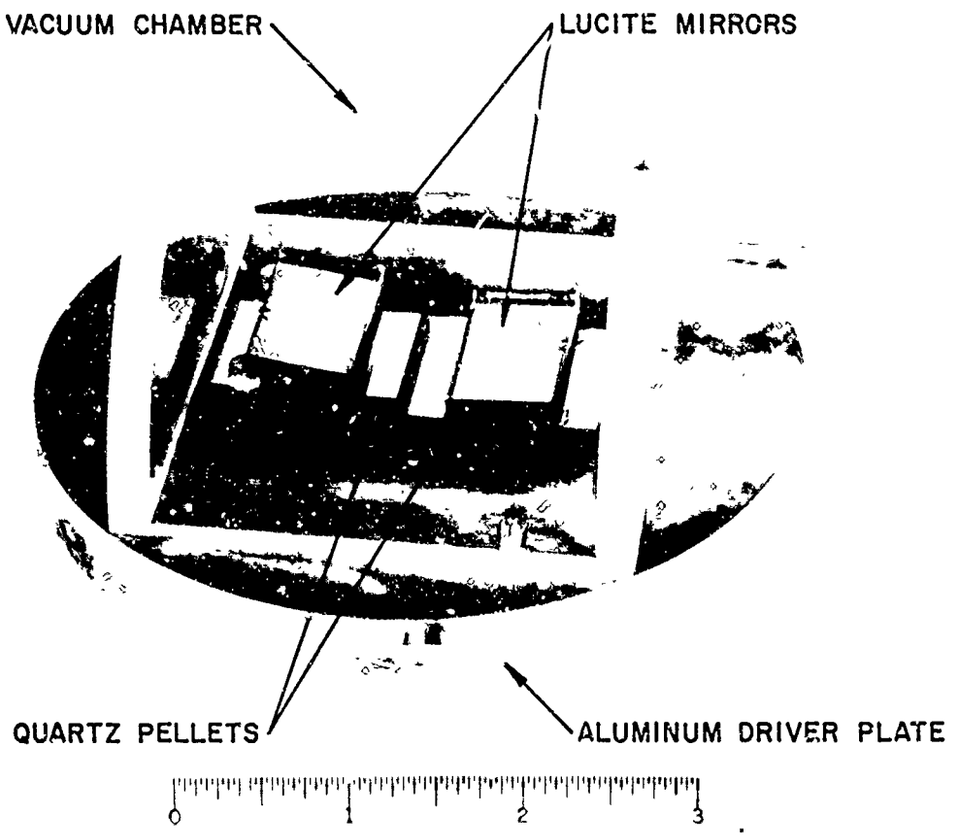

Fig. 2.2.--Photograph of Experimental Assembly

The light source explosive was initiated simultaneously with the plane wave lens of the experimental assembly; the resulting strongly luminuous shock in the argon produced a bright reflection from the aluminized surfaces a few microseconds before the first arrival to be recorded in the quartz.

A drawing of the complete arrangement as it appeared before firing is shown as Fig. 2.3.

An abrupt change in intensity of the light reflected from the aluminized surfaces of the assembly showed arrival times of the shock fronts and free surfaces upon impact with the mirrors.

A streak camera photograph taken in this manner is shown in Fig. 2.4. The two specimens in this shot were Z-cut; the upper one was 1/8-inch thick and the lower 1/4-inch thick. The final pressure was approximately 200 kbar. At time, T_0, the reflection from the rear (aluminized) face of the quartz extinguishes abruptly as the shock arrives at the quartz-aluminum interface. At time, T_1, the first shock arrives at the quartz free surface. The traces are relatively smooth until the change in slope caused by the arrival of the second shock at time T_2; thereafter the traces are slightly irregular. A slight curvature to the trace of the first shock can be detected. This slowing up of the free-surface is due to stress-relaxation effects, as was pointed out by Wackerle(15).

For reliable results the point of collision of the quartz free surface with the inside surface of the mirror must travel with supersonic velocity with respect to both quartz and lucite (non-jetting configuration). Consequently, the initial mirror angle must be less than approximately

$$\alpha \max = \sin^{-1} \frac{u_f}{U_s}$$

where u_f is the quartz free-surface velocity and U_s is the larger of the two shock wave velocities in quartz and lucite. This criterion restricted the usable mirror angles to less than about 8°.

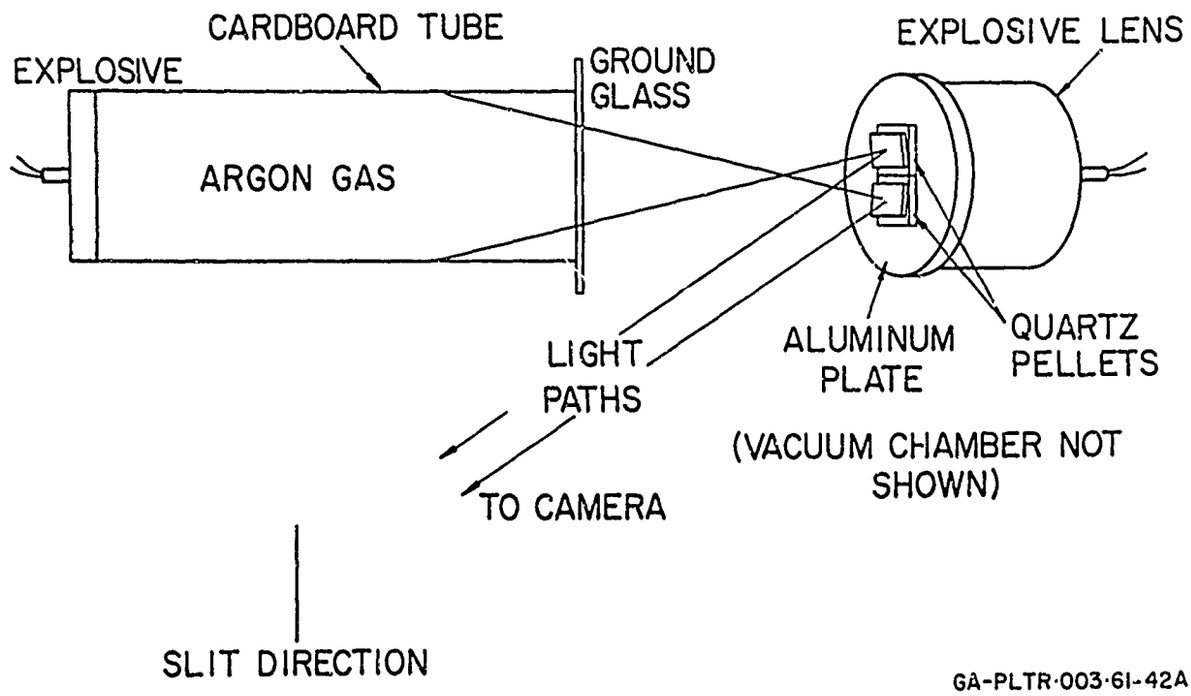

Fig. 2.3.--Diagram Showing Relation of Experimental Assembly, Light Source and Camera.

B. Data Reduction

The shock velocities were determined from distances measured on the film and the known writing speed of the camera. The velocity of the second shock requires corrections because of the motion of the free surface and because of the interaction of the second shock with the reflection of the first shock. The first of these is straightforward and a simple derivation gives:

$$U_2 = \frac{d + u_{f1}(T_2 - T_1)}{T_2 - T_0} \tag{2.11}$$

where d is the initial specimen thickness, u_{f1} is the free-surface velocity due to the first shock, and T_0, T_1, and T_2 are the arrival times of the shock fronts as shown in Fig. 2.4.

The correction due to the interaction of the second shock with the reflection of the first requires knowledge of the state (and constitutive relation) of the quartz in the region between the two fronts and cannot be made unequivocally. However, the assumption that the material is stressed and relieved only elastically by the first wave leads to a large correction and unreasonably high compression for the state behind the second shock in shot No. 7394 (Table II) The results from that shot are the most sensitive to this correction because the second shock was relatively slow with respect to the first. For the other experiments the correction is smaller and does not appreciably affect the conclusions.

It should be emphasized, however, that the result for shot 7394 implies that an irreversible change in the material properties occurs between the two shock fronts. This conclusion is consistent with the observed relaxation of the state of the first shock. It is not consistent with an assumption of conventional elastic-plastic behavior.

Because of the arbitrariness regarding the interaction correction the data are here reported without such a correction. The correction used by WACKERLE (15) is plausible, but does not significantly change the data of this paper.

Fig. 2.4.--Streak Camera Photograph Showing Shock Arrival Times and Free-Surface Traces. Shock No. 7394.

Table II

SUMMARY OF EXPERIMENTAL DATA

SHOT NO.	EXPLOSIVE SYSTEM	ORIENTATION	PELLET THICKNESS (mm)	ARRIVAL TIMES		FREE-SURFACE VELOCITIES		FIRST SHOCK					SECOND SHOCK				
				$t_1 - t_0$ (μs)	$t_2 - t_0$ (μs)	u_{f_1} (mm/μs)	u_{f_2} (mm/μs)	Shock Velocity U_1 (mm/μs)	Particle Velocity u_1 (mm/μs)	Stress σ_1 (kb)	$\frac{V_1}{V_0}$	Internal Energy $E_1 - E_0$ (cal/gm)	Shock Velocity U_2 (mm/μs)	Particle Velocity u_2 (mm/μs)	Stress σ_2 (kb)	$\frac{V_2}{V_0}$	Internal Energy $E_2 - E_0$ (cal/gm)
5648	P-40 lens	X (−) to (+)	6.378	1.057	1.296	0.692	1.62	6.03	0.346	55.5	0.9426	14.3	5.05	0.810	117.0	0.8[illegible]5	86.6
		X (−) to (+)	6.388	1.075	1.308	0.807	1.62	5.94	0.403	63.7	0.9320	19.5	5.03	0.810	117.4	0.8[illegible]0	86.4
5807	P-40	X (+) to (−)	6.388	1.079	1.320	0.836	1.52	5.92	0.418	65.7	0.9294	20.9	4.99	0.758	110.1	0.8[illegible]93	75.6
		Z	6.383	0.876		1.02		7.28	0.508	98.4	0.9302	30.9	not observed				
5880	P-40	X (+) to (−)	6.391	1.078	1.322	0.754	(1.66)	5.93	0.377	59.4	0.9364	17.0	4.97	(0.828)	118.1	0.8[illegible]24	90.5
	Initial state in Al					1.47											
5921	P-40 + 1" Comp B	Y (+) to (−)	6.380	1.079	1.146	(0.786)	2.630	5.91	0.393	(61.8)	(0.9335)	18.5	5.61	1.315	198.8	0.7[illegible]35	212.0
		Y	6.347	1.020	1.144	0.994	2.56	6.22	0.497	82.2	0.9201	29.6	5.66	1.281	199.0	0.7[illegible]33	205.6
5920	P-40 + 1" Comp B	X (−) to (+)	6.391	1.063	1.139	(0.687)	2.63	5.98	0.344	(54.6)	(0.9426)	14.1	5.65	1.315	199.9	[illegible]732	211.7
		Z	6.380	0.876		1.40		7.28	0.698	135.1	0.9041	58.3	not observed				
6009	P-40	Y	6.358	1.058	1.363	0.819	1.43	6.01	0.410	65.3	0.9320	20.0	4.85	0.713	103.7	0.8[illegible]31	68.4
		Z	6.388	0.893		1.12		7.15	0.560	106.6	0.9215	38.2	not observed				
5997	P-40 + 2" Comp B	Y	6.360	1.011	1.158	1.03	3.00	6.29	0.515	86.2	0.9180	58.5	5.62	1.50	231.9	0.7211	311.9
		Z	6.386	0.871	1.201	1.40	(2.63)	7.33	0.700	136.1	0.9046	34.0	5.70	(1.32)	(227.2)	(0.7524)	217.6
7363	P-40	Z	6.599	0.914	1.824	1.04	1.58	7.22	0.520	99.8	0.9280	32.4	4.14	0.79	127.4	0.8593	102.2
		Z	3.3[illegible]5	0.469	0.958	1.09	1.65	7.24	0.545	104.8	0.9247	35.5	4.10	0.82	133.4	0.8519	113.6
7394	P-40 + 1" Comp B	Z	6.607	0.899	1.336	1.27	2.32	7.35	0.635	123.6	0.9139	47.9	5.36	1.16	195.8	0.8124	193.9
		Z	3.411	0.462	0.691	1.51	2.47	7.38	0.751	147.6	0.8981	67.7	5.49	1.23	215.3	0.8[illegible]36	217.2
7395	P-40	Y	6.601	1.088	1.448	0.836	1.60	6.07	0.418	67.7	0.9308	22.2	4.77	0.800	114.9	0.8195	85.3
		Y	3.399	0.562	0.745	0.862	1.58	6.05	0.431	69.3	0.9287	22.2	4.77	0.790	113.9	0.8519	85.5

Initial density, $\rho_0 = 2.657$ gm/cm^3

( ) points in parentheses are less reliable

The free-surface velocities were calculated from the measured slopes of the traces by means of the relation:

$$u_f = \frac{\tan \alpha'}{MF \tan \gamma'} \tag{2.12}$$

where α' is the effective angle of the inclined mirror with respect to the quartz surface, γ' is the angle of the trace on the film with respect to the space axis, M is the magnification or ratio of distance on the film to the corresponding distance on the shot, and F is the writing speed of the camera. The parameters, α', and γ', of this relation are not identical to their nominal values, α and γ because of tilt of the incident shock and slight departures from orthogonality of the slit and sweep directions. The corrections are given by

$$\tan \alpha' = \tan \alpha \, (1 + \theta'/\tan \gamma)$$

and

$$\tan \gamma' = \tan \gamma \sec \delta \, (1 - \tan \gamma \tan \delta)$$

where α is the angle of the inclined mirror with respect to the quartz surface, θ' is the angle of shock tilt as measured on the film, δ is the angle of the slit with respect to the normal to the sweep direction, and γ is the angle of the trace with respect to the slit direction (Fig. 2.5).

The observed shock wave velocities and associated free-surface velocities are given in Table II, along with the initial conditions for each experiment and other quantities derived from the measured velocities.

The experimental precision, based on assembly tolerances, camera resolution, and film reading errors is estimated to be ±1% in shock velocity and ±5% in free-surface velocity. Most of the error in free-surface velocity is due to uncertainty in reading the angle γ'(± 1°).

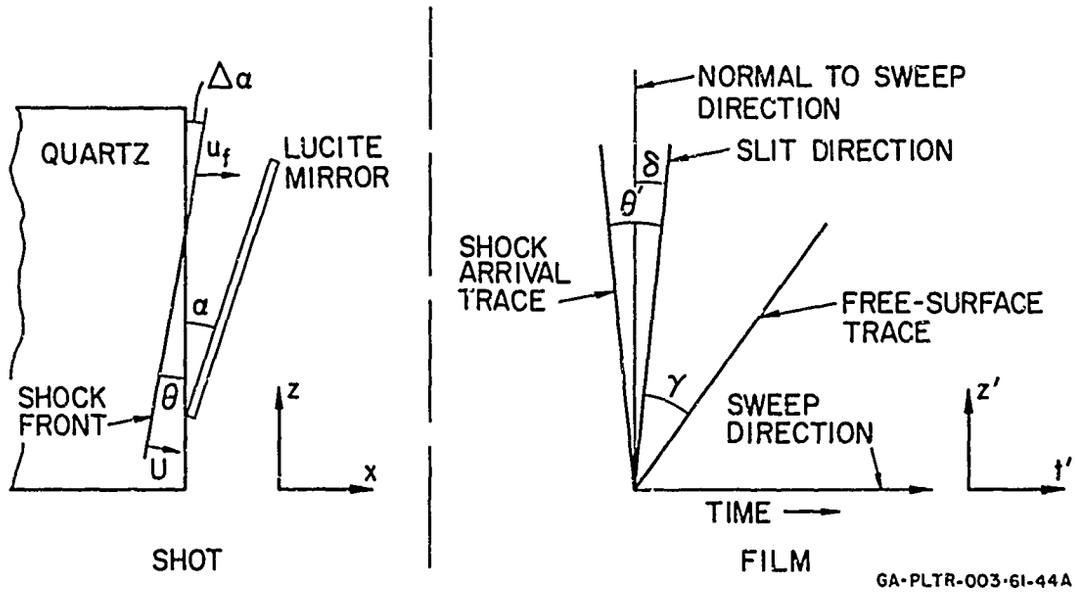

Fig. 2.5.--Definition of Parameters Used in Adjusting Streak Camera Data.

C. Experimental Results

The observed shock velocities are plotted as functions of the shock particle velocities (taken to be one half the free-surface velocities) in Fig.2.6. Data by WACKERLE (15) and GREGSON (42) are also shown. The data of Wackerle are his "average" values, shown for comparison because they were determined on the same basis as the present results. The solid curves are predicted from finite strain theory, to be discussed in Section 2.33.

The agreement among the experimental data is seen to be generally satisfactory. The only significant disagreement occurs for Z-cut crystals at a particle velocity of 1.23 mm/μs. The source of this discrepancy is unknown. A shot fired by Gregson to remeasure this state agrees better with the present data*. However, if the present data are correct (rather than Wackerle's) some anomalous behavior is noted in the pressure-volume plane, as discussed below.

The stress-compression states were calculated from the measured velocities by means of the Rankine-Hugoniot jump conditions (1):

$$V/V_0 = 1 - \frac{u_I - u_0}{U_I - u_0}$$

$$\sigma_I - \sigma_0 = \rho_0(U_I - u_0)(u_I - u_0)$$

In these equations, V is specific volume, u is particle velocity, U is shock velocity, σ is stress normal to the shock front, and ρ is density. Subscripts 0 refer to the state ahead of the shock; subscripts I refer to the state behind the shock. Velocities are with respect to laboratory coordinates. Figs. 2.7, 2.8, and 2.9 show the results in the stress, specific-volume plane for X, Y, and Z crystals respectively. Bridgman's

---

*Shown in Fig. 2.9.

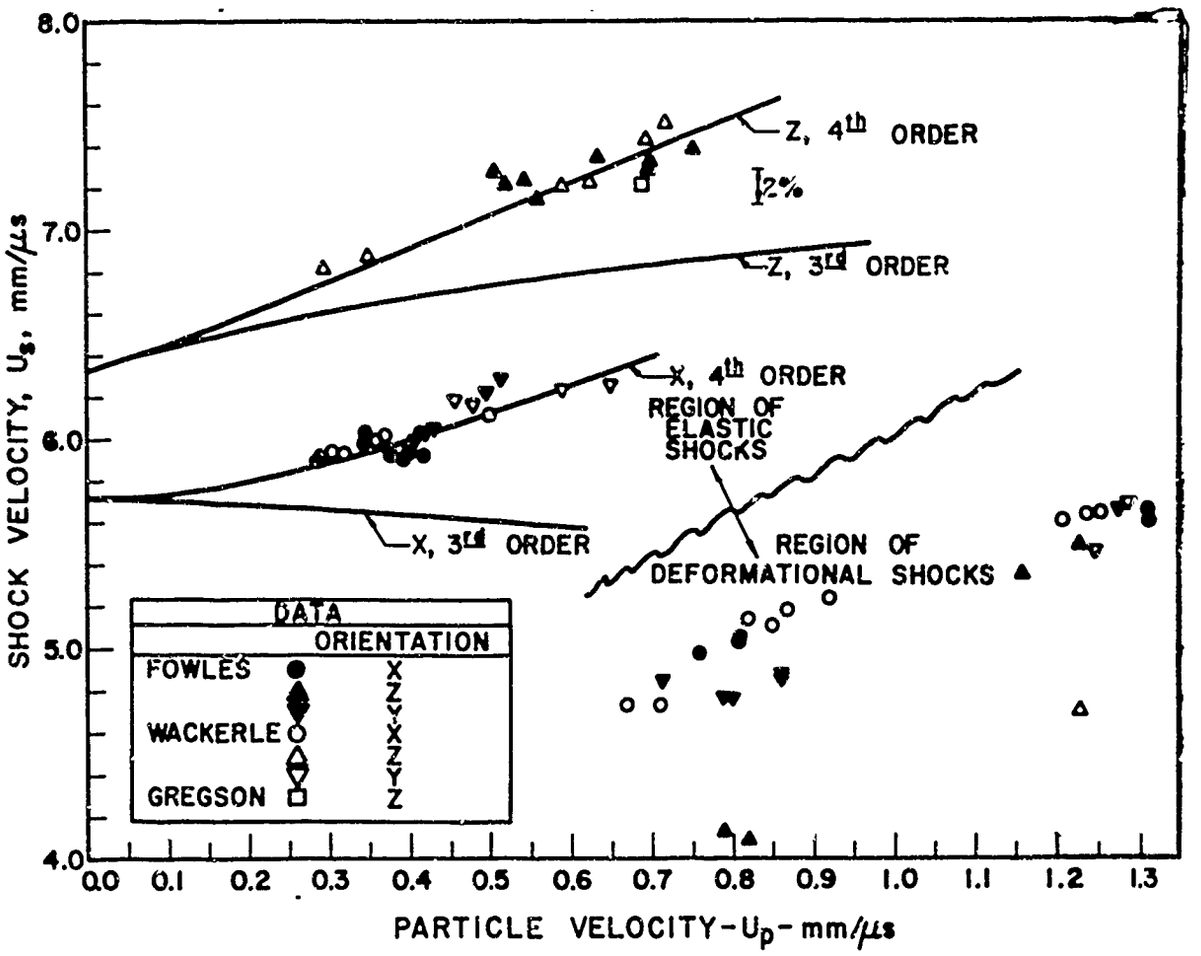

Fig. 2.6.--Shock Velocity as Function of Particle Velocity. Curves labelled 3rd, 4th, are fits based on zero-pressure elastic constants up to 3rd and 4th order respectively for X and Z-cut crystals.

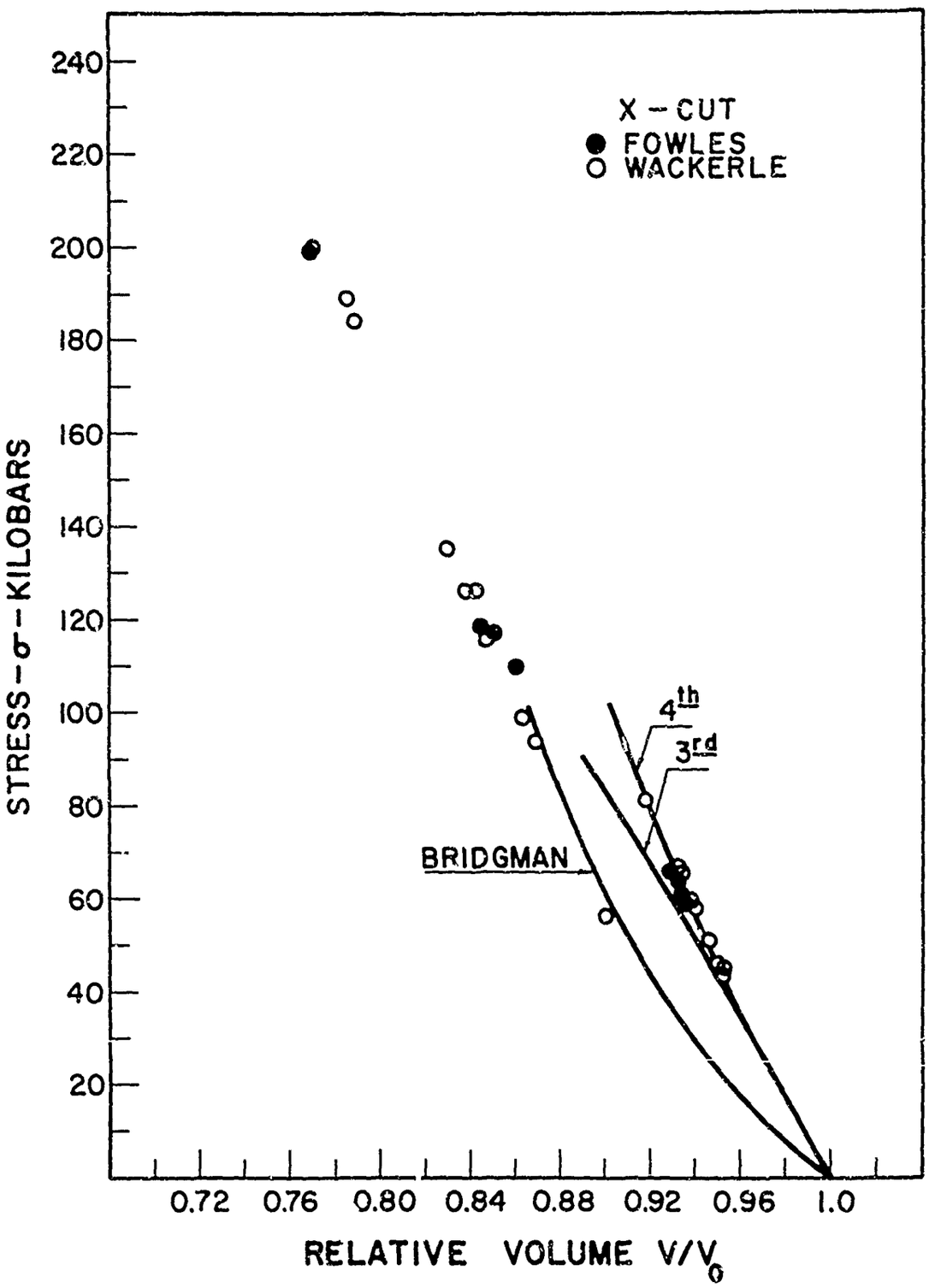

Fig. 2.7.--Stress-Volume States Resulting From Shock Compression of X-cut Quartz. Solid curve is Bridgman's Hydrostatic Data. Curves Labelled 3rd, 4th, are fits based on zero-pressure elastic constants to 3rd and 4th order.

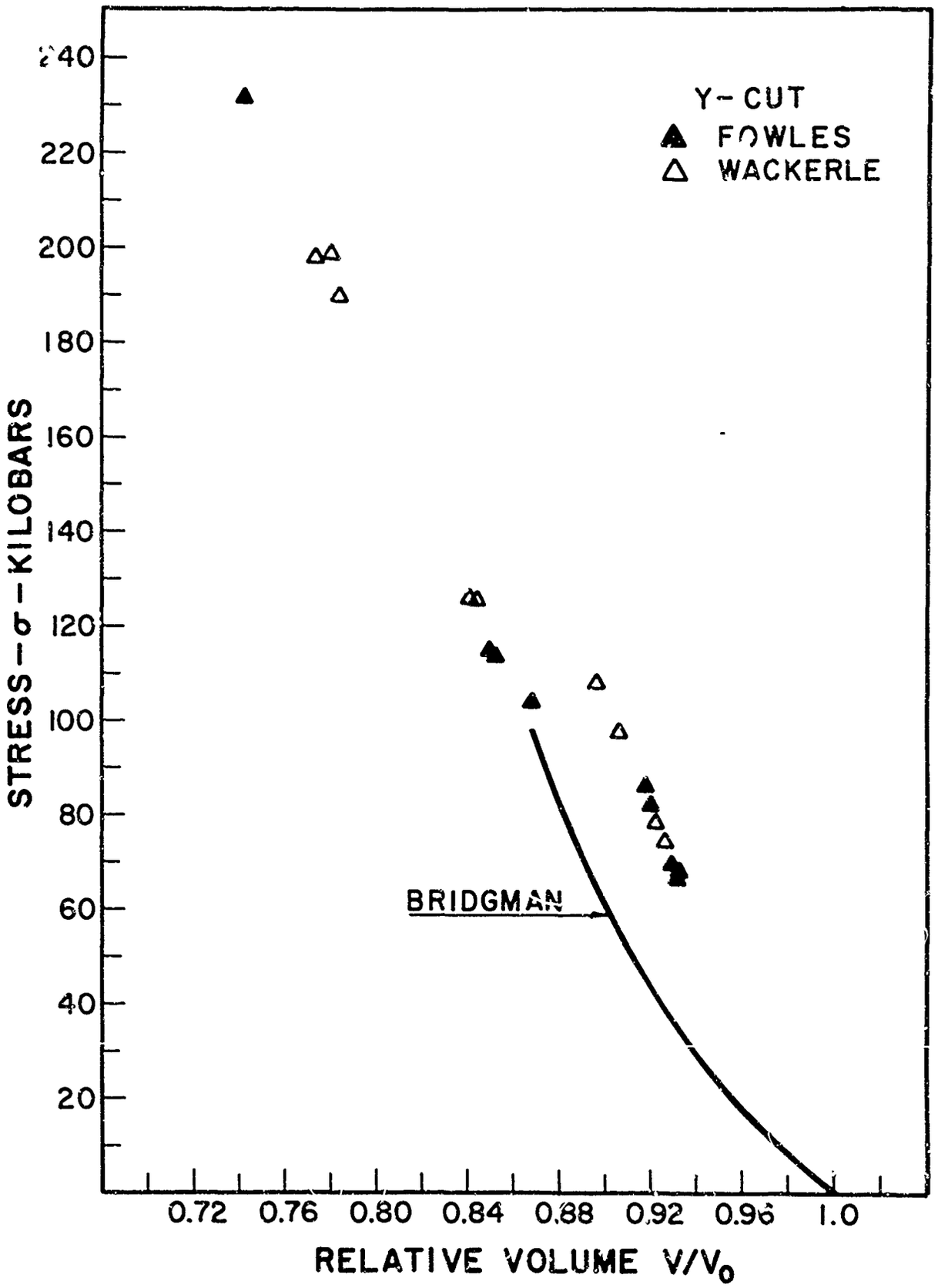

Fig. 2.8.--Stress-Volume States Resulting From Shock Compression of Y-cut Quartz. Solid curve is Bridgman's Hydrostatic Data.

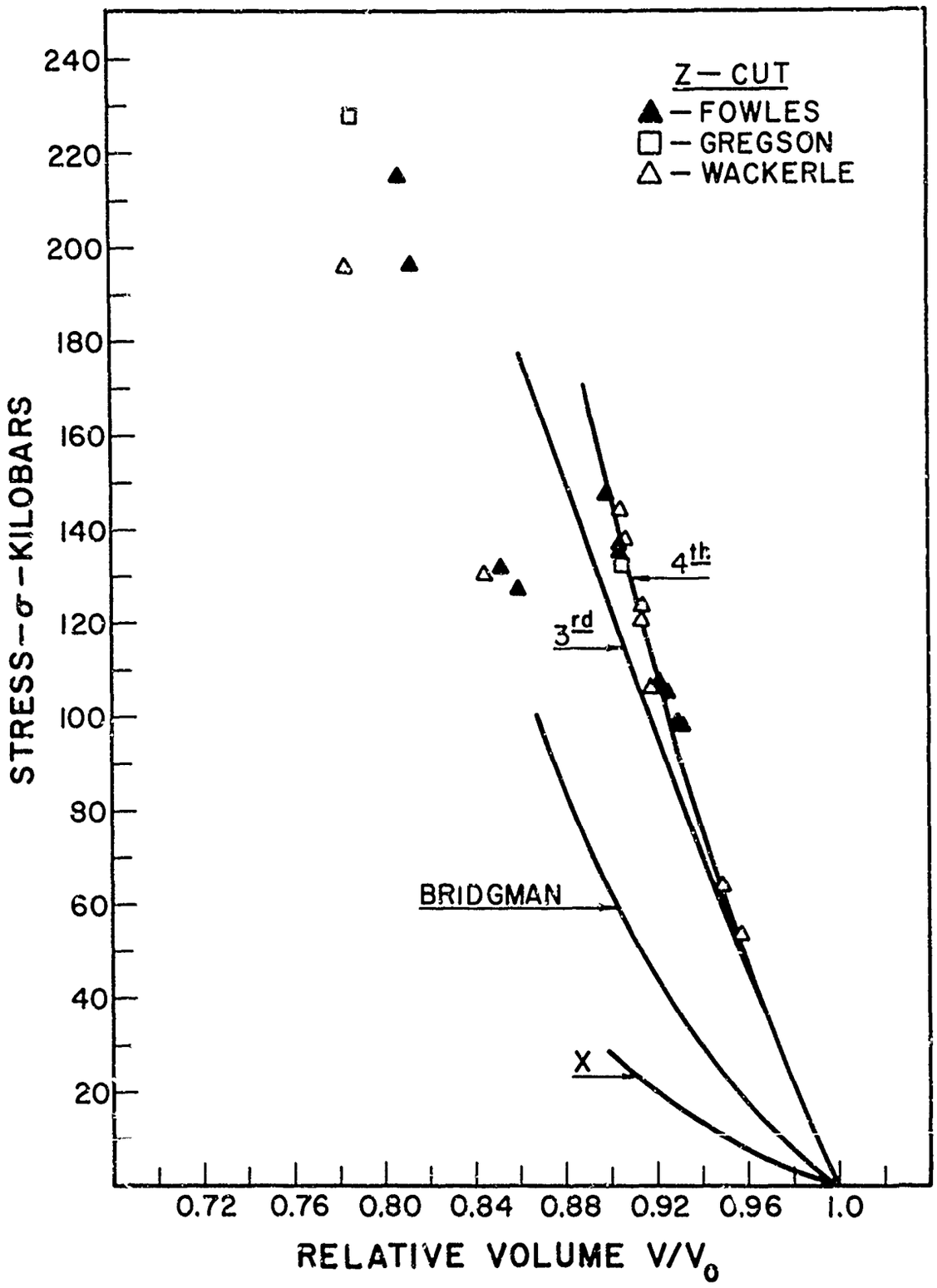

Fig. 2.9.--Stress-Volume States Resulting From Shock Compression of Z-cut Quartz. Solid curve is Bridgman's Hydrostatic Data. Curves labelled 3rd, 4th, are fits based on zero-pressure elastic constants to 3rd and 4th order. The curve labelled X represents the tangential stresses, calculated from constants up to and including 3rd order.

hydrostatic curve based on measurements to 98 kbar is shown for comparison (43). The curves labelled 3rd, 4th, are fits based on low pressure acoustic measurements and finite elastic strain theory (Section 2.33).

These plots show clearly the important features of the compression, namely:

(1) extremely high amplitude elastic waves, up to 150 kbar in Z-cut quartz

(2) loss of rigidity above the elastic limit, as shown by the agreement of the higher pressure shock data with extrapolation of the hydrostatic data

(3) lack of a unique value for the Hugoniot elastic limit.

This behavior implies that yielding is not due to dislocation motion as in a metal, but is analogous (or identical) to fracture. It is shown below that the shear stresses behind the elastic shocks approach the theoretical shear strength of the crystal lattice.

The range of the present data is not sufficient to show clearly the transformation to stishovite, as indicated by Wackerle's higher pressure measurements.

2.33 Finite Strain Theory

Because the strains behind the elastic shocks are relatively large, it is of interest to examine the agreement of the data with predictions of finite strain theory. Predictions are made possible by the work of THURSTON (40) and McSKIMIN (39) and their co-workers on the third-order elastic constants of quartz. Such comparisons should indicate the extent to which third-order constants are sufficient to describe the stress-strain behavior at strains of the order of 5 - 10%. The constants are determined from precise acoustic measurements at strains of less than 0.1%. ANDERSON (44)

has already shown that the second and third-order constants alone give reasonably good predictions for hydrostatic compressions of up to about 15% in quartz, provided the constants are used in the Murnaghan logarithmic equation or the Birch equation of state.

Discrepancies between the observed and predicted stress-strain curves can be used alternatively to evaluate fourth and higher order constants, or to examine the effects of adopting alternate definitions of strain, as suggested by KNOPOFF (45). Finally, to the extent that the third-order constants give adequate predictions, the stresses tangential to the shock fronts can be calculated from the observed stresses normal to the fronts and, hence, the shear stresses sustained (momentarily) by the crystal can be deduced.

A. Finite Strain Fundamentals*

Denote the coordinates of a mass element in an initial (unstrained) coordinate system by a_i, and the coordinates in a final (strained) system by x_i, with the transformation given by,

$$x_i = x_i(t, a_1, a_2, a_3), \; i = 1, 2, 3$$

where (2.13)

$$a_i = x_i(t_0, a_1, a_2, a_3)$$

and t_0 is a reference time. The x_i are thus Eulerian, or spatial, coordinates and the a_i Lagrangian, or material, coordinates.

For this transformation one can derive an expression for the ratio of specific volumes:

$$V/V_0 = J = \frac{\partial x_i}{\partial a_s} \tag{2.14}$$

---

*This section is a summary of portions of the theory as presented by THURSTON (46).

J is thus the determinant of the Jacobian of the transformation, or the "functional determinant."

The strain, N_{jk}, is defined, somewhat arbitrarily, from the difference in the squares of the lengths of line elements by:

$$2N_{jk}\, da_j\, da_k = dx_i\, dx_i - da_i\, da_i$$

$$N_{jk} = 1/2\, \left(\frac{\partial x_i}{\partial a_j}\frac{\partial x_i}{\partial a_k} - \delta_{jk}\right) \tag{2.15}$$

Here and in the following the Einstein summation convention for repeated subscripts applies. δ_{jk} is the Kronecker delta.

Expanding the internal (strain) energy in a power series in the strains, one obtains (at constant entropy):

$$\rho_o[E(N,S) - E(0,S)] = 1/2\, c^s_{ijkl}\, N_{ij}\, N_{kl} + 1/6\, c_{ijklmn}\, N_{ij}\, N_{kl}\, N_{mn}$$

$$+ 1/24\, c^s_{ijklmnpq}\, N_{ij}\, N_{kl}\, N_{mn}\, N_{pq} + \ldots \tag{2.16}$$

In this expression the c^s_{ijk} . . . , represent the second and higher order isentropic elastic stiffness coefficients. The first-order term is missing since the reference state is considered to be one of zero stress and strain.

We now define quantities, called thermodynamic tensions, by

$$t_{ij} = \rho_o\left(\frac{\partial E}{\partial N_{ij}}\right)_s \quad . \tag{2.17}$$

In terms of these quantities the elastic constants are

$$c^s_{ijkl} = \left(\frac{\partial t_{ij}}{\partial N_{kl}}\right)_s = \frac{\partial^2 E}{\partial N_{ij}\, \partial N_{kl}}$$

and similarly for the higher order coefficients. Consequently,

$$\rho_o \, dE = t_{ij} \, dN_{ij} \; (dS = 0) \quad .$$

Finally, the equilibrium (non-dissipative) components of the stress are obtained from the thermodynamic tensions by the relations,

$$t_{ij} = (1/j) \frac{\partial x_k}{\partial a_j} \frac{\partial x_m}{\partial a_i} t_{ij} \quad . \tag{2.18}$$

The above formulas provide isentropic constitutive relations in terms of the elastic stiffness coefficients. Other forms of constitutive relations can, of course, be derived in a similar fashion.

Low pressure acoustic measurements yield a mixed third-order constant of the form:

$$C_{ijkmpq} = \left(\frac{\partial c^S_{ijkm}}{\partial N_{pq}}\right)_T$$

where the subscript T means the derivative is taken at constant temperature. The corresponding purely isentropic constant is given by:

$$c^S_{ijkmpq} = C_{ijkmpq} + (T/\rho_o \, C_t) \, c^S_{kmpq} \, \alpha_{uv} [C_{ijkmrs} \, \alpha_{rs} - \left(\frac{\partial c^S_{ijkm}}{\partial T}\right)_t] \tag{2.19}$$

where C_t is the specific heat at constant tension and the α_{uv} are thermal expansion coefficients,

$$\alpha_{uv} = \left(\frac{\partial N_{uv}}{\partial T}\right)_t \quad .$$

In view of the symmetry of the stress and strain tensors, the number of subscripts can be reduced by adopting the following convention:

11 → 1	32 → 4
22 → 2	31 → 5
33 → 3	21 → 6

This convention is employed in the following.

B. Application to Uniaxial Strain in Quartz

We assume the deformation to occur in the X direction only. The coordinate transformation is accordingly,

$$x_1 = (1 - \gamma)a_1$$

$$x_2 = a_2$$

$$x_3 = a_3$$

Formulas (2.14) through (2.18) then give:

$$J = V/V_0 = 1 - \gamma$$

$$N_1 = \gamma(\gamma/2 - 1)$$

$$\rho_0[E - E_0] = 1/2\ c_{11}\ N_1^2 + 1/6\ c_{111}\ N_1^3 + 1/24\ c_{1111}\ N_1^4 + \ldots$$

$$t_k = c_{1k}\ N_1 + 1/2\ c_{11k}\ N_1^2 + 1/6\ c_{111k}\ N_1^3 + \ldots \quad (k = 1, 2 \ldots 6)$$

or writing out the components:

$$t_1 = c_{11}\ N_1 + 1/2\ c_{111}\ N_1^2 + 1/6\ c_{1111}\ N_1^3 +$$

$$t_2 = c_{12}\ N_1 + 1/2\ c_{112}\ N_1^2 + \ldots$$

$$t_3 = c_{13}\ N_1 + 1/2\ c_{113}\ N_1^2 + \ldots$$

$$t_4 = c_{14}\ N_1 + 1/2\ c_{114}\ N_1^2 + \ldots$$

$$t_5 = c_{15}\ N_1 + 1/2\ c_{115}\ N_1^2 + \ldots$$

$$t_6 = c_{16}\ N_1 + 1/2\ c_{116}\ N_1^2 + \ldots$$

The stress components are then:

$$\sigma_1 = (1 - \gamma)t_1 \qquad \sigma_4 = (1 - \gamma)^{-1}\, t_4$$

$$\sigma_2 = (1 - \gamma)^{-1}\, t_2 \qquad \sigma_5 = t_5 \tag{2.20}$$

$$\sigma_3 = (1 - \gamma)^{-1}\, t_3 \qquad \sigma_6 = t_6$$

For alpha quartz compressed in the X-direction the above formulas are correct as they stand. For compression in other directions the proper translation of subscripts must, of course, be made to indicate the correct constants.

The above formulas have been applied to uniaxial compression of X and Z-cut quartz, using the second and third order constants determined by McSKIMIN, et al. (39) and THURSTON, et al. (40). Values of these constants are shown in Table III.

The resulting curves are plotted in Figs. 2.6, 2.7 and 2.9. The values of shock velocity, U_s and particle velocity, u_p, of Fig. 2.6 were obtained from the Hugoniot relations:

$$U_s = V_0\left(\frac{\sigma}{V_0 - V}\right)^{1/2}$$

and

$$u_p = [\sigma(V_0 - V)]^{1/2} \quad .$$

The predictions are seen to fall outside the estimated error of the shock data, indicating that the fourth-order term contributes significantly to the energy (and the stress) at larger values of strain. Although it might be thought that the discrepancy is due in part to the use of isentropic second-order moduli and mixed isentropic-isothermal third-order moduli to predict Hugoniot states, for which internal energy is greater than for isentropic compression, a straightforward calculation shows that the errors

TABLE III

Elastic Moduli of Quartz*

Modulus	Value (10^{11} dyne/cm^2)	Reference
2nd-order		
c_{11}**	8.757	(39)
c_{12}	0.704	"
c_{13}	1.191	"
c_{14}	-1.804	"
c_{33}	10.575	"
3rd-order		
c_{111}	-21.0	(40)
c_{112}	-34.5	"
c_{113}	1.2	"
c_{114}	-16.3	"
c_{133}	-31.2	"
c_{333}	-81.5	"
4th-order		
c_{1111}	1705	Present Work
c_{3333}	1849	"

*The second-order constants are isentropic, the third-order are mixed isothermal, isentropic constants, and the fourth-order are Hugoniot constants, (see text).

**The c_{11} constant used is appropriate for open circuit compression, i.e., at constant electric displacement, D.

thus produced are negligible.

The differences between the purely isentropic third-order moduli and the mixed moduli given in Table III can be calculated from Eq. (2.19)

The temperature coefficients of expansion, as given by MASON (47) are:

$$\alpha_3 = 7.8 \times 10^{-6}, \ \alpha_1 = \alpha_2 = 14.3 \times 10^{-6}$$

and the expression, due to Westrum, reported by McSKIMIN (39) for the specific heat is:

$$C_p\,(T) = C_p\,(T_c) + (T - T_c)C_1 + (T + T_c)^2 C_2 + (T - T_c)^3 C_3 + \ldots$$

$$(77.4°K < T < 298°K)$$

where

$$T_c = 190°K$$

$$C_p\,(T_c) = 5.189 \times 10^6 \text{ erg/g°K}$$

$$C_1 = 2.444 \times 10^4 \text{ erg/g°K}$$

$$C_2 = -4.126 \times 10^1 \text{ erg/g°K}$$

$$C_3 = 5.327 \times 10^{-2} \text{ erg/g°K}$$

taking

$$T = 25°C, \ \rho_o = 2.6485 \text{ g/cm}^3, \ C_p = 7.42 \times 10^6 \text{ erg/g°K},$$

and estimating $\left(\frac{\partial C^S_{33}}{\partial T}\right)$ from McSkimin's data taken at 25°C and -195.8°C to be of the order of -1×10^8 dyne/cm^2 °K we find the difference given by Eq. (2.19) for the c_{333} constant, for example, to be of the order of 5×10^3 dyne/cm^2.

This is four orders of magnitude less than c_{333}. Hence, although the above calculation is hardly accurate for the cases under consideration, only pathological behavior of some of the thermodynamic variables, α, C_p or $(\frac{\partial c_{33}^S}{\partial T})$ could significantly influence the results.

The difference between Hugoniot and isentropic compressions can also be shown to be negligible. For compression in the Z direction to a relative volume of 0.9 the strain energy given by Eq.(2.16) to terms of third-order is 2.5×10^9 erg/gm. The internal energy on the Hugoniot is 2.8×10^9 erg/gm. Taking Grüneisen's ratio, Γ, to be approximately 1*, the stress difference due to this difference in thermal energy is less than 1 kbar--very much less than the observed stress difference, and within the experimental scatter.

C. Fourth-Order Constants

The discrepancies between the observed data and the predictions based on low pressure data can be used to evaluate fourth-order coefficients. This was done for X and Z-cut crystals to yield the values of c_{1111} and c_{3333} shown in Table II. The procedure followed was to fit differences between the data and the third-order predictions with a straight line. Because of the large differences in pressure range and experimental precision, this method proved to give an adequate fit to both the high and low pressure data. No adjustment of the second or third-order constants was necessary.

The fits obtained using the constants up to fourth-order are shown in Figs. 26, 27, and 29. Note that for X-cut crystals the slope of the curve in the shock velocity-particle-velocity plane (Fig. 26) is always negative when constants only up to and including third-order are used. This would imply

---

*ANDERSON (44) gives a value of 0.746 for hydrostatic compression. Calculated for the individual components with the assumption $C_p = C_v$ gives $\Gamma_{11} = \Gamma_{22} = 1.17$; $\Gamma_{33} = 0.53$.

that a shock wave in this direction is unstable and spreads as it travels. With the addition of the fourth-order constant, however, the slope is always slightly positive. Thus, the addition of the fourth-order term results in a qualitative difference in predicted behavior.

The U_s - U_p plot for Z-cut crystals is nearly a straight line; however it is easily shown that a straight line does not accurately fit the slope at zero particle velocity. Thus the straight line relation often assumed in shock studies is only an approximation for quartz shocked in either the X or Z direction.

It is also easily shown that the Murnaghan form of equation of state, when fitted to the correct slope and curvature of the σ - V curve, (utilizing second and third-order constants), does not accurately fit the higher pressure data and is therefore an approximation only.

These statements can be illustrated by examining the derivatives of each function. Expanding the relation for σ, in Eq. 2.20 in terms of γ yields:

$$\sigma = c_{11}\,\gamma[1 - 1/2\,(3 + \frac{c_{111}}{c_{11}})\gamma + 1/6\,(3 + 6\,\frac{c_{111}}{c_{11}})\gamma^2 + \ldots] \qquad (2.21)$$

A linear relation between shock and particle velocity of the form

$$V_s = a + b\,u_p$$

can be written, by means of the Rankine-Hugoniot jump conditions, as

$$\sigma = \rho_0 \frac{a^2\,\gamma}{(1 - b\gamma)^2} ,$$

where ρ_0 is initial density, and can be expanded to give

$$\sigma = \rho_0 a^2\,\gamma[1 + 2b\gamma + 3b^2\,\gamma^2 + \ldots] \qquad (2.22)$$

Finally, the one-dimensional-strain analogue of the Murnaghan equation

$$\sigma = \frac{A}{B}\,[(V_0/V)^B - 1]$$

can be expanded to give

$$\sigma = A\,\gamma[1 + 1/2\,(B + 1)\gamma + 1/6\,(B + 1)(B + 2)\gamma^2 + \ldots] \qquad (2.23)$$

Equating the derivatives up to second-order, we have

$$c_{11} = \rho_0\, a^2 = A \qquad \text{(1st order)}$$

$$-(3 + \frac{c_{111}}{c_{11}}) = 4b = (B + 1) \qquad \text{(2nd order)}$$

Evaluating the parameters A, b, and B from these equations gives

X-cut: $A = \rho_0 a^2 = c_{11} = 8.68 \times 10^{11}$

$b = -0.15$

$B = 1.6$

Z-cut: $A = \rho_0 a^2 = c_{33} = 10.575 \times 10^{11}$

$b = 1.177$

$B = 3.71$

With these values all three expressions have the same slope and curvature at zero stress. The predicted stresses for various compressions are shown in Table IV.

That the closed form expressions are approximate is hardly surprising inasmuch as they are both empirical with no known physical basis. Their value is that they both are two-parameter functions that have physically reasonable shapes, and they are therefore convenient for interpolation and extrapolation when experimental information is lacking.

Knopoff's suggestion that, because of the arbitrariness in the definition of strain, alternative definitions may prove more suitable for representing constitutive relations would seem to be worthy of further consideration. However, some guidance from physical reasoning is necessary to provide any degree of generality to a given definition.

TABLE IV

Stress-Kbar

V/V_0	X			Z		
	Murnaghan	Linear $U_s - U_p$	Finite Strain	Murnaghan	Linear $U_s - U_p$	Finite Strain
0.99	8.6	8.8	8.7	10.7	10.8	10.8
0.98	17.2	17.5	17.5	21.8	22.2	22.3
0.97	25.8	26.3	26.5	32.0	34.0	34.5
0.96	34.4	35.0	35.9	47.1	46.5	47.6
0.95	42.7	43.7	45.7	60.3	59.7	61.6
0.94	51.2	52.5	56.1	73.9	72.5	75.5
0.93	59.0	61.3	67.1	87.9	88.0	92.6
0.92	67.9	70.0	78.9	103.4	106.0	109.7
0.91	76.2	78.8	91.4	119.0	119.0	127.9
0.90	84.4	87.6	104.7	136.4	135.8	147.3

2.34 Conclusions

The behavior of quartz under shock loading conditions is very much different from that of metals, as was pointed out by Wackerle. The elastic precursor waves are an order of magnitude higher and, correspondingly, so are the shear stresses. The curve labelled X in Fig. 2.9 is the stress component (based on constants to third-order) parallel to the shock front when the shock propagates in the Z direction. The maximum stress difference is seen to exceed 100 kbar. This is of the same order of magnitude as the effective shear modulus; consequently, it appears that quartz momentarily exhibits theoretical yield strength under dynamic conditions.

That cohesion of the material is destroyed upon yielding is indicated by the close agreemen he second shocked states with Bridgman's hydrostatic data. There is no indication of a residual shear stress, in contrast to the case for metals (49).

The pronounced stress relaxation shown by the observed variation in amplitude of the elastic waves and the apparent dependence on the final pressure is quantitatively larger than for metals, although similar qualitatively.

Evidently shock wave methods provide a valuable supplement to low pressure acoustic measurements in determining higher order elastic constants, at least for ceramic type materials which sustain large amplitude elastic waves. Shock waves are inherently more suitable for higher pressure measurements than are acoustic methods, but are less suitable for the high precision, low pressure measurements required to evaluate second-order constants. To what extent shock wave techniques are capable of measuring coefficients other than the principal coefficients, i.e., those directions for which the elastic wave is purely longitudinal, requires additional study.

III. PHASE TRANSITIONS

3.1 Introduction

Solid-solid phase transitions are classified as first order if a volume discontinuity exists at constant temperature and as second or higher order if discontinuities exist only in various thermodynamic derivatives. We are concerned here only with first order changes. If such a change occurs reversibly, the transition region is characterized by the equality of the Gibbs energies of the two phases. This leads to the Clausius-Clapeyron equation which relates changes in pressure and temperature in the mixed-phase region:

$$dp/dT = \Delta S/\Delta v \tag{3.1}$$

The consequences of this relation to shock wave propagation have been developed in some detail in Reference (7). One of the important results is a relation between dp/dT and the slope of the Hugoniot in the coexistence region (8):

$$(dp/dT)^2 + A(dp/dT) + B = 0 \tag{3.2}$$

where

$$A = 2\alpha_1/\beta_M-\beta_1)$$

$$B = - C_{p1}/Tv_1(\beta_M-\beta_1)$$

$$\beta_M = - (1/v)(dv/dp)_M = \text{Hugoniot compressibility in mixed phase}$$

β_1 = isothermal compressibility

α_1 = volume expansion coefficient at constant pressure

C_{p1} = specific heat at constant pressure

Subscript "1" denotes evaluation in phase one at the phase boundary.

Measurements made on bismuth, iron and quartz allow dp/dT to be estimated from Eq. (3.2). Results are entered in Table V where static values are also given for comparison. Values of α_1 and C_{p1} at atmospheric pressure and room temperature were used in the estimates, and β_1 was estimated from shock measurements.

TABLE V

The Coefficient dp/dT from Static and Shock Wave Experiments

Type of Experiment	Sample		
	Bismuth	Iron	Quartz
Static measurements	-.05 (9)*	-.065 (10)*	.018 (11)*
Shock wave measurements (calculated from Eq. (3.2))	-.067 ±.045 (7)*	-.29 ±.115 (7)*	.225 (7)*

*Refer to sources in "Literature Cited."

From the table it is apparent that shock wave data for iron and quartz do not agree with those of static experiments. The errors in shock measurements shown in the table are estimated upper bounds based on rors in measurements of β_M. Therefore

it is very difficult to attribute the discrepancies for iron and quartz to experimental errors in determining the slope of the Hugoniot at the phase boundary. Conceivable reasons for the discrepancies are:

1. Inaccuracies in thermodynamic data (α_1 and C_{p1}) at high pressures. Values used in the preceding table are those at atmospheric pressures.
2. The experimental Hugoniot curve in the coexistence region is not at equilibrium. There may be some non-equilibrium rate-dependent effects influencing the measurements.

In order to explain the discrepancies of Table II, either of the coefficients α_1 or C_{p1} must exhibit a two- to four-fold difference between its value at high pressure and that at atmospheric pressure. Information for estimating such differences is not generally available. Measurements by Bridgman below 20 kb show changes of not more than 20 per cent (12). It seems unlikely that changes of the required magnitude will occur at these higher pressures.

If there exist rate dependent effects in phase transition, we should be able to observe other dynamic evidence in wave propagation. For example, if the phase transition exhibits a relaxation process, then we expect a decay of the first shock wave with travel distance. This arises because the delay in transition allows a mass in the first phase to momentarily support a higher pressure than its transition pressure; i.e., the mass exists in the extended metastable region (Fig. 3.1). This is similar to stress relaxation of an elastic precursor.

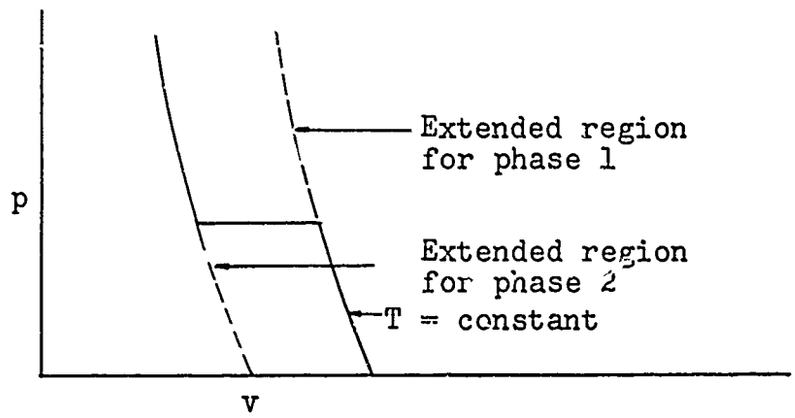

Fig. 3.1--Extended Metastable Region

There are two experimental observations of the decay of the first wave for iron (13,14).

For α-quartz Wackerle (15) did not observe a two-wave structure corresponding to the stishovite transformation. This may indicate that the transition is neither rapid nor complete.

In order to study transient effects in shock wave propagation, we must solve the flow equations. In Lagrange coordinates for plane, one-dimensional, time-dependent flow these are:

1. Newton's second law

$$\rho_o(\partial u/\partial t)_h + (\partial(p+q)/\partial h)_t = 0 \qquad (3.3)$$

where h = Lagrangian space coordinate

t = time

ρ_o = initial density = $1/v_o$

q = viscous stress

Introduction of q makes the flow continuous through the shock front and the jump conditions unnecessary.

2. Continuity equation

$$\rho_o(\partial v/\partial t) - \partial u/\partial h = 0 \qquad (3.4)$$

3. Energy conservation

$$\partial E/\partial t + (p+q)\ (\partial v/\partial t) = 0 \qquad (3.5)$$

4. Constitutive relation

In order to solve the above differential equations in four independent variables (p, v, u, E), constitutive relations are required. Ignoring solid rigidity, which

should play a secondary role in the problems considered here, these will consist of an equation of state, $p = p(v,E)$, an expression for q, and, in the mixed phase, a statement of the kinetics of transition.

3.2 General Constitutive Relations for Two-Phase Flow

We assume the following conditions to apply in a small mass element when both phases coexist:

1. Equal pressure exists in both phases.
2. Temperatures of the two phases are equal, i.e., the heat released by the transition is instantly redistributed.
3. Particle velocities are the same for each phase.
4. No surface energy is associated with the interface between the two phases.
5. No heat is transferred between mass elements by conduction.

Conditions 1 and 3 insure that Eqs. (3.3)-(3.5) apply for the coexistence region as well as for a single phase. The only change needed is a reinterpretation of v and E. This can be done as follows:

Regardless of phase transition, the total mass of a given Lagrangian volume is conserved. Therefore, if we denote by v the total specific volume of the mixture of two phases, then from condition 3 above, v satisfies Eq. (3.4) on p. 3.4. But the variable v must also satisfy the following relation in the coexistence region:

$$v(p,T) = (1-\alpha)\, v_1(p,T) + \alpha v_2(p,T) \qquad (3.6)$$

where α is defined as the mass fraction of the second phase and v_i is specific volume of the i-th phase at p and T.

Conditions 4 and 5 imply that the total internal energy of a mass element is the sum of the internal energies of the two phases:

$$E = (1-\alpha)E_1 + \alpha E_2 \tag{3.7}$$

where E_i is specific internal energy of the i-th phase at p and T.

In order to obtain a suitable constitutive relation when the phase transition has a finite reaction rate, we assume first that the p,v,E surfaces in each phase can be extended smoothly into metastable regions overlapping the equilibrium region of mixed phase, as in Fig. 3.1.

Then we have the following functional forms:

$$\begin{aligned} v_1 &= v_1(p,T) \\ v_2 &= v_2(p,T) \\ E_1 &= E_1(p,T) \\ E_2 &= E_2(p,T). \end{aligned} \tag{3.8}$$

Then from Eqs. (3.6) and (3.7) we have

$$dv = (1-\alpha)dv_1 + \alpha dv_2 + (v_2-v_1)d\alpha \tag{3.9}$$

$$dE = (1-\alpha)dE_1 + \alpha dE_2 + (E_2-E_1)d\alpha. \tag{3.10}$$

From Eq. (3.8):

$$dv_i = (\partial v_i/\partial T)_p dT + (\partial v_i/\partial p)_T dp \tag{3.11}$$

$$i = 1 \text{ or } 2.$$

With E a function of T and p we have:

$$dE_i = (\partial E_i/\partial T)_p dT + (\partial E_i/\partial p)_T dp$$

$$= (C_{pi} - p(\partial v_i/\partial T)_p)dT - (T(\partial v_i/\partial T)_p + p(\partial v_i/\partial p)_T)dp \tag{3.12}$$

$$i = 1 \text{ or } 2$$

where C_{pi} = specific heat of i-th phase at constant pressure.

Substituting (3.11) and (3.12) into (3.9) and (3.10), we get

$$dv = \ell_1 dp + m_1 dT + n_1 d\alpha \tag{3.13}$$

$$dE = \ell_2 dp + m_2 dT + n_2 d\alpha \tag{3.14}$$

where

$$\ell_1 = (1-\alpha)\ (\partial v_1/\partial p)_T + \alpha(\partial v_2/\partial p)_T \tag{3.15}$$

$$m_1 = (1-\alpha)\ (\partial v_1/\partial T)_p + \alpha(\partial v_2/\partial T)_p \tag{3.16}$$

$$n_1 = v_2 - v_1 \tag{3.17}$$

$$\ell_2 = -(1-\alpha)\ (T(\partial v_1/\partial T)_p + p(\partial v_1/\partial p)_T)$$

$$- \alpha\ (T(\partial v_2/\partial T)_p + p(\partial v_2/\partial p)_T) \tag{3.18}$$

$$m_2 = (1-\alpha)\ (C_{p1} - p(\partial v_1/\partial T)_p) + \alpha(C_{p2} - p(\partial v_2/\partial T)_p) \tag{3.19}$$

$$n_2 = E_2 - E_1 \tag{3.20}$$

and

$$dE = -(p+q)dv \text{ from Eq. (3.5).} \tag{3.21}$$

Therefore, in principle, (3.13) and (3.14) can be solved for dp and dT if $d\alpha$ is given.

Now we assume the following relaxation

relation, whose derivation is the subject of the next section,

$$d\alpha = f(v,T,\alpha)dt. \tag{3.22}$$

Then substituting Eqs. (3.21) and (3.22) into (3.13) and (3.14) and solving for dp and dT, we get

$$dp = F/G \tag{3.23}$$

$$dT = -M/G \tag{3.24}$$

where

$$F = \left[m_2 + m_1(p+q)\right]dv + (m_1n_2-m_2n_1)\ f(v,T,\alpha)dt$$

$$M = \left[\ell_2 + \ell_1(p+q)\right]dv + (\ell_1n_2-\ell_2n_1)\ f(v,T,\alpha)dt$$

$$G = \ell_1m_2 - m_1\ell_2$$

In Eq. (3.8) it is assumed that E_1 and E_2 are known functions of p and T. These can be calculated by integrating Eq. (3.12) along two paths, provided specific heats are known:

1. Integrate over T at p = 0
2. Integrate over p at constant temperature, T.

Then

$$E_i = E_i^{oo} + \int_o^T C_{pi}^o dT - \int_o^p Q dp \tag{3.25}$$

where

$$Q = T(\partial v_i/\partial T)_p + p(\partial v_i/\partial p)_T$$

$$i = 1, 2$$

E_i^{oo} = specific internal energy at absolute zero Kelvin and p = 0 (this is zero-point energy),

and

C^{o}_{pi} = specific heat capacity at zero pressure.

In summary, the generalized constitutive relations now consist of:

1. Equations of state

$$v_i = v_i(p,T)$$

2. Specific heat capacities

$$C_{pi} = C_{pi}(p,T)$$

3. Zero-point energy difference

$$E_1^{oo} - E_2^{oo}$$

4. Relaxation relation

$$d\alpha/dt = f(v,T,\alpha)$$

5. Artificial viscosity, q.

To complete the above description we must find a relaxation relation and an expression for q.

3.3 Irreversible Thermodynamics and Phase Relaxation

This section is concerned with the mechanism of phase transformations in the solid state. It should be possible to describe the mechanism of phase change in solids in terms of interatomic forces by use of kinetic theory. Actually, because of the problem's complexity, no such quantitative description has been achieved. However, very successful phenomenological theories for the kinetics of phase change have been developed (16,17,18,19). Such theories are of two kinds, known as

nucleation and growth processes and martensitic transformations. This nomenclature is rather unfortunate, as pointed out by Christian, because growth from nuclei also occurs during martensitic reactions.

In nucleation and growth processes a new phase grows from critical nuclei at the expense of the old phase. The reaction proceeds to completion by a slow migration of the interphase boundary, the velocity of which varies markedly with temperature. Most atoms have different neighbors in a new phase. On the other hand in martensitic transformation the reaction takes place by coordinated atom movements (e.g., shear-like), and atoms have the same neighbors after transformation. The latter is often observed in rapid cooling of alloys.

The basic model for describing nucleation and growth phenomena is based on the following conditions:

1. Steady state reaction
2. Isothermal and isobaric process
3. Thermal fluctuations as driving force
4. Boltzman's law for the relative probability of different energy states.

The expression of this theory is:

1. Nucleation

   I (nucleation frequency) α $\exp(-\Delta G^*/kT)$

   where ΔG^* is defined to be the critical net free energy change on forming the nucleus of the new phase.

2. Growth

There are many expressions for the growth law. An often used form is:

$$x = 1 - \exp(-kt^n)$$

where x = the volume fraction transformed

k = a complicated function of the nucleation frequency I

t = time

n = constant of magnitude 3 to 4.

The principal difficulties in applying this model to the shock-induced transition are the conditions imposed in deriving the rate equation. In a shock front the situation is neither isothermal nor isobaric, nor is it steady state.

A description of the nucleation of martensitic transformation is given (20) for an athermal case (e.g., quenching), but the result is less conclusive than that for a nucleation and growth process. This transformation has a negligible free energy barrier (21) and proceeds very rapidly to completion. Therefore at present the quantitative information obtained is mainly concerned with the amount of transformation with respect to the cooling rate but not with time.

It is tempting to use the martensitic transformation in describing shock-induced transformations because of its high speed. There are some who suggest the martensitic transition for iron ($\alpha \rightarrow \epsilon$) in shocks (22,23). However, a quantitative description of the rate equation is not yet available for inclusion in the constitutive relations.

As more and better data on shock-induced transition become available, it will become important to develop some of the above models to describe the kinetics of phase transformation in shock waves. At present it is barely established that rate effects in shock-induced transformation exist, and we seek no more than a qualitative description of the effects of kinetics on the wave structure and some rough numbers for the magnitude of the reaction rate involved in the observed processes.

To this end we select a quite different approach, which is in some sense better founded, though formally limited to small deviations from equilibrium, in irreversible thermodynamics. In this approach there exist none of the conditions imposed in the above models, and it suggests a simple relaxation law for the transformation.

$$d\alpha/dt = (\alpha^{eq} - \alpha)/\tau \tag{3.26}$$

where

α^{eq} = equilibrium value of α, or a completely relaxed value

τ = relaxation time.

The derivation of the above relation from irreversible thermodynamics follows.

When a solid-solid transition occurs reversibly (or in equilibrium) by adiabatic compression, the entropy of a given system is constant and the process is called isentropic. If the transition is not reversible, the entropy will increase. However, ordinary thermodynamics does not give the precise amount

of increase; rather, it tells only the direction of increase:

$$ds_{\text{irreversible}} \geq 0 .$$

Basically, the idea of irreversible thermodynamics is to replace the inequality by an equality so that we can determine the increase of entropy caused by irreversible processes.

To establish the desired equality we assume that, although the total system is not in equilibrium, there exists within a small mass element a state of local equilibrium for which the total entropy change per unit mass, ds, is expressed by the Gibb's relation (24).

$$Tds = de + pdv - \sum_{i=1}^{n} \mu_i d\alpha_i \tag{3.27}$$

where

μ_i = partial specific Gibb's function

α_i = mass fraction of the i-th component.

This means, for the case of a single-component phase transition, that when two phases are not in equilibrium with one another, we interpret them as if they are two different components with different specific Gibb's functions and each is in local equilibrium satisfying Eq. (3.27).

There is an additional constraint on Eq. (3.27) for a single-component system from total mass conservation. Since the total mass is constant:

$$d\alpha_1 + d\alpha_2 = 0. \tag{3.28}$$

We redefine $\alpha_2 = \alpha$, $\alpha_1 = 1 - \alpha$ and use α hereafter as the sole reaction variable. Then from Eqs. (3.27) and (3.28) we get:

$$Tds = de + pdv - (\mu_2 - \mu_1)d\alpha. \tag{3.29}$$

So far we have been looking at an isolated element of mass. But if we assume that this mass element is part of a continuous medium which is in a state of non-uniform stress, strain and motion, then the variables e and v must satisfy the energy and mass conservation equations, (3.4) and (3.5). Substituting these equations into Eq. (3.29) we get:

$$T(ds/dt)_{irrev.} = -vq(\partial u/\partial x) - (\mu_2 - \mu_1)d\alpha/dt \tag{3.30}$$

We assume no heat to be deposited from the outside, so the entropy change is entirely due to the internal irreversible process. It should be noted that the Lagrangian derivative used in Eqs. (3.4) and (3.5) is identical to the convective derivative implied in Eq. (3.30). If we look closely at Eq. (3.30), we can see the sources of irreversibility. These are a chemical affinity $(\mu_2 - \mu_1)$, (25), and a velocity gradient. These quantities are called "forces" in irreversible thermodynamics and are denoted by $X_i (i=1,2...)$. The phenomena caused by these forces, such as phase changes, are called "fluxes" and are described by $J_i (i=1,2...)$. Then Eq. (3.30) becomes:

$$T(ds/dT)_{irrev.} = \sum_{i=1}^{2} J_i X_i \tag{3.31}$$

where

$$X_1 = -\partial u/\partial x \tag{3.32}$$

$$X_2 = -(\mu_2 - \mu_1) \tag{3.33}$$

$$J_1 = qv \tag{3.34}$$

$$J_2 = d\alpha/dt. \tag{3.35}$$

There is some arbitrariness in the choice of terms for forces and fluxes. The above choice is taken from Hirschfelder et al. (26). Another possible combination is:

$$X_1 = -qv$$

$$X_2 = -(\mu_2-\mu_1)$$

$$J_1 = \partial u/\partial x$$

$$J_2 = d\alpha/dt.$$

When the irreversible entropy change is expressed in terms of forces and fluxes, there are two basic assumptions made. The first is called the linear phenomenological law and the second the Onsager reciprocal relation:

1. Phenomenological law

$$J_i = \sum_{j=1}^{n} g_{ij}X_j \tag{3.36}$$

where g_{ij} are constant.

2. Onsager's reciprocal relation

$$g_{ij} = g_{ji}. \tag{3.37}$$

Then from Eqs. (3.32) through (3.35):

$$d\alpha/dt = g_{11}(\mu_2-\mu_1) + g_{12}(\partial u/\partial x) \tag{3.38}$$

$$vq = g_{21}(\mu_2-\mu_1) + g_{22}(\partial u/\partial x) \tag{3.39}$$

where $g_{12} = g_{21}$.

Furthermore, from Eqs. (3.36) and (3.37) we get:

$$T(ds/dt)_{irrev.} = g_{11}X_1^2 + (g_{12}+g_{21})X_1X_2 + g_{22}X_2^2.$$

The second law of thermodynamics requires that the left-hand side is always positive or zero, so we must have the following relations for the constants g_{ij}:

$$g_{11} \geq 0, \quad g_{22} \geq 0$$

$$2\sqrt{g_{11}g_{22}} \geq |g_{12} + g_{21}|.$$

But this is all we get from thermodynamics; it will not give us the magnitudes of the coefficients, because they are characteristic numbers which depend upon materials. A complete understanding of the reaction mechanisms would provide a foundation for calculating the g_{ij}. For the present we assume the reaction rate to be independent of shear stress and set $g_{12} = 0$. g_{11} and g_{22} are chosen from available data and for computational convenience, respectively. Then Eqs. (3.38) and (3.39) reduce to:

$$d\alpha/dt = g_{11}(\mu_2-\mu_1) \tag{3.40}$$

$$q = g_{22}(1/v)(\partial u/\partial x). \tag{3.41}$$

Since we know the chemical affinity $(\mu_2-\mu_1)$ is zero at the equilibrium state, we can find the equilibrium value α^{eq} of α as a function of two independent thermodynamic parameters. For example:

$$\alpha^{eq} = \alpha^{eq}(v, T).$$

Then for a small deviation from equilibrium, we can expand the affinity in a Taylor's series:

$$\mu_2-\mu_1 = (\mu_2-\mu_1)^{eq} + \left(\frac{\partial(\mu_2-\mu_1)^{eq}}{\partial\alpha}\right)_{v,T}(\alpha-\alpha^{eq}) \quad \ldots .$$

Neglecting the higher-order terms:

$$\mu_2-\mu_1 = \left(\frac{\partial(\mu_2-\mu_1)^{eq}}{\partial\alpha}\right)_{v,T}(\alpha-\alpha^{eq}). \tag{3.42}$$

Equations (3.40) and (3.42) give:

$$d\alpha/dt = (\alpha-\alpha^{eq})/\tau \tag{3.43}$$

Where τ is a new constant to be determined from comparisons of calculations with experiments.

Eq. (3.41) shows that q has the character of a viscous force, as stated earlier. It is necessarily proportional to the first power of the strain rate because of the use of the linear phenomenological law. This first-power dependence is retained in the computations, but since its primary purpose is to smooth the shock transition it will be artificially modified after the manner described by Richtmyer and von Neumann (27): The coefficient g_{22} is made proportional to the cell thickness used in the computation.

Then

$$q = C_L(\Delta x/v)\ |\partial u/\partial x| \tag{3.44}$$

where C_L = constant.

This completes our general description of non-equilibrium two-phase flow. In the following section we approximate the constitutive relations in order to apply them in numerical calculations.

IV. CONSTITUTIVE RELATIONS FOR IRON

4.1 Approximations for Two-Phase Flow

Three approximations were made in order to simplify the application of the principles of Section III to the $\alpha \rightarrow \epsilon$ transition in iron. First, the equilibrium volume change at constant p was assumed constant in the coexistence region. This approximation is supported by compressibility measurements at room temperature which result in the following values (10,28):

$$\beta_2 \text{ (at 192 Kb)} = 4.94 \times 10^{-1} (\text{Mb})^{-1}$$

$$\beta_1 \text{ (at 132 Kb)} = 5.1 \times 10^{-1} (\text{Mb})^{-1}$$

where β_i is the compressibility of the i-th phase.
Then

$$v_2(p,T) - v_1(p,T) = -.004 \text{ cc/g at every p and T.} \tag{4.1}$$

Then from Eqs. (3.6), (3.26) and (4.1) we get:

$$dv_1 = dv - (v_2 - v_1) d\alpha \tag{4.2}$$

$$d\alpha = (\alpha^{eq} - \alpha) dt/\tau \tag{4.3}$$

Then v_1 can be calculated from the above equations provided v and α^{eq} are known. In the computation process v is given by the continuity equation and α^{eq} by Eq. (3.6).

$$\alpha^{eq} = ((v-v_1)/(v_2-v_1))^{eq} = (v-v_1^{eq}(T))/(v_2-v_1)^{eq} \qquad (4.4)$$

Since $(v_2-v_1)^{eq}$ is constant, the temperature dependence of α^{eq} is in $v_1^{eq}(T)$. Our second approximation is to replace $v_1(T)$ by the value $v_1(T_o)$ at room temperature (T_o). Since the temperature is only slightly greater than room temperature, the error involved in this approximation is negligible except in the immediate vicinity of the transition pressure, 130 Kb.

Since v_1 can be determined from Eqs. (4.2) and (4.3) we can use the form $p = p(v_1,T)$ to calculate pressure if we know the temperature. The third approximation we made is the temperature calculation.

If the phase transition is made at equilibrium, pressure and temperature in the coexistence region must satisfy the relation:

$$dp/dT = \text{constant at fixed } p \text{ or } T.$$

Over a wide range of temperatures the coefficient is practically constant (10). But if we assume that the coefficient dp/dT is constant even in the non-equilibrium coexistence region, we shall see presently that the energy conservation law alone is then sufficient to determine the temperature change. Since E is given by Eq. (3.7) the internal energy is a function of p, T and α. On replacing α by Eq. (3.6), it is a function of p, T and v. But if we assume that dp/dT is constant, p and T are no longer independent and E is a function of T and v only. The

error resulting from this approximation has not yet been evaluated. It should be small since ΔT is small. From this assumption we relate changes in temperature to changes in specific volume as follows:

$$dE = (\partial E/\partial T)_v dT + (\partial E/\partial v)_T dv$$

Substituting into this relation from Eq. (3.21), we find in the mixed phase region:

$$(\partial E/\partial T)_v dT = -(p+q)dv - (\partial E/\partial v)_T dv.$$

Defining $(\partial E/\partial T)_v$ as $C_{v,m}$ and using the following identity,

$$T(\partial p/\partial T)_v = p + (\partial E/\partial T)_v ,$$

this becomes

$$dT = -(T(\partial p/\partial T)_v + q)dv/C_{v,m} . \qquad (4.4)$$

The calculation of $C_{v,m}$ in the coexistence region is given in Appendix I. It should be noted that in the coexistence region $(\partial p/\partial T)_v$ is equal to dp/dT because of the assumed dependence of p and T.

Our assumption or internal energy dependence $(E(v,T))$ is certainly true for a single phase, so the form of Eq. (4.4) is valid, and if we know the values of C_v and $(\partial p/\partial T)_v$ in either a single phase or a mixed phase, the temperature calculation is only a matter of substituting different values of these parameters, depending on the phase region.

4.2 Review of Experimental Information

There are three main static experiments on the equation of state (12,10,29) and the isothermal p-v relations are in close agreement, within the range of experimental errors, with shock wave measurements of the Hugoniot at low pressures. We use the equations of state determined from shock experiments.

There are four major measurements on shock wave propagation in iron. The one by Bancroft et al. (28), is on the Hugoniot pressure-volume relations above the transition pressure and it reveals a discrepancy in the magnitude of the gradient dp/dT compared with the static value (7). The other three are concerned with transient effects and the thickness of the second shock:

1. Bancroft et al. observed the two-wave structure and determined the pressure-volume relation in the second shock by jump conditions.
2. Smith measured the thickness (.02 mm) of the second shock front in recovery experiments by hardness methods and concluded that the duration of the transition zone is in the order of .001 μsec (30).
3. Novikov et al. observed the two-wave structure in iron by a capacitance method (14). They concluded, from the rise time of the second shock, that the duration of the transition region is .2 - .3 μsec. This duration is not exactly equal to the relaxation time τ, but as it is essentially governed by the relaxation of the phase transition, it should be of the same order of magnitude. They also observed a pressure drop behind the

first shock for thinner samples (no information is given about the thickness), and explain that it is due to relaxation processes.

4. Minshall observed, by a pin technique, decay of the first shock over a distance of 5 cm (.8 cm - 5.8 cm) (13). No estimation of transformation time is given, nor is the explanation of the decay. However, if we assume this decay to be due to the relaxation, the order of relaxation time must be about 5-10 μsec.

All of the above reports agree about the existence of the transition, but as far as the relaxation time is concerned, they make no suggestion of a particular value to be used in the calculation.

In numerical procedures we can use any relaxation time to study the effect of phase change on shock wave propagation, but we made an arbitrary choice of 1/3 μsec for most of the calculations, based on consideration of the experiments by Novikov. In the study of the decaying precursor we used three relaxation times, .1, 1/3, and 1 μsec.

4.3 Equation of State of Iron

The equation of state of the first phase is taken to be:

$$p(v_1,T) = a_1(\eta_1-1)+a_2(\eta_1-1)^2+a_3(\eta_1-1)^3+C_{v1}(T-T_o)\Gamma/v_1 \qquad (4.5)$$

where

C_{v1} = specific heat at constant volume, phase 1, assumed constant

T_o = some temperature above which C_{v1} is constant, taken as room temperature here.

a_i = constants

Γ = Grüneisen function, assumed constant

$\eta_1 = v_o/v_1$.

This is a form of the Mie-Grüneisen equation used by Al'tshuler et al. (31).

The coefficients a_i can be determined from the polynomial fits of the Hugoniot curve (1) or from static measurements. However, for the case of iron there is no appreciable difference, below 200 Kb, between the isotherm and the Hugoniot centered at room temperature. For example, the temperature rise along the Hugoniot from 0 to 130 Kb is 20°C (28), which contributes only about 1.3 Kb to the total pressure. This difference is less than experimental error for static and shock measurements in general (29). Therefore, we can substitute the Hugoniot as a room temperature isotherm in the equation of state. These and other equation of state parameters are given in Table VI. The values of a_i listed in Table VI are determined from the least square fit of existing data below 130 Kb (32). Since errors in the experiments are larger than the thermal pressure, this will not give any inconsistency in the equation of state. When we speak of the temperature-independent equation of state, we mean the isotherm at T_o.

Fig. 4.1 shows the isotherm at T_o in terms of relative volume. Bridgman's data at room temperature, extrapolated to high pressures, are drawn for comparison. The difference at high pressures is mainly due to inaccuracies encountered in extending Bridgman's data to such high pressures. Since the

volume change is constant at fixed p and T, the isotherm of the second phase (ϵ - phase) can be easily found by shifting the first phase by the amount of the volume change (v_2-v_1).

TABLE VI

Physical Data for α - iron

Parameter	Values	Dimension	Reference
v_o (initial volume)	.1275	cc/g	(33)
α_1 (thermal expansion coefficient)	36.3×10^{-6}	$1/K^o(degK)^{-1}$	(33)
C_{v1} (heat capacity)	$.4447 \times 10^{-5}$	$Mbcc/g^oK$	(33)
P_M (transition pressure)	.130	Mb	(10)
$(dp/dT)_m$ (equilibrium)	-.000065	Mb/K^o	(10)
Δv (volume difference)	-.004	cc/g	(10)
a_1	1.667	Mb	(32)
a_2	3.4	Mb	(32)
a_3	0	Mb	(32)
Γ	1.6	. . .	(34)
$C_{v,m}$	$.46 \times 10^{-5}$	$Mbcc/g^oK$	*
T_o	300^oK	^oK	

*See Appendix III.

Once the equation of state is known, the expression for α^{eq} can be easily found from Eq. (4.4), which includes the room temperature approximation for $v_1(T)$. Suppose we specify the room temperature transformation by the isotherm AB in Fig. 4.1;

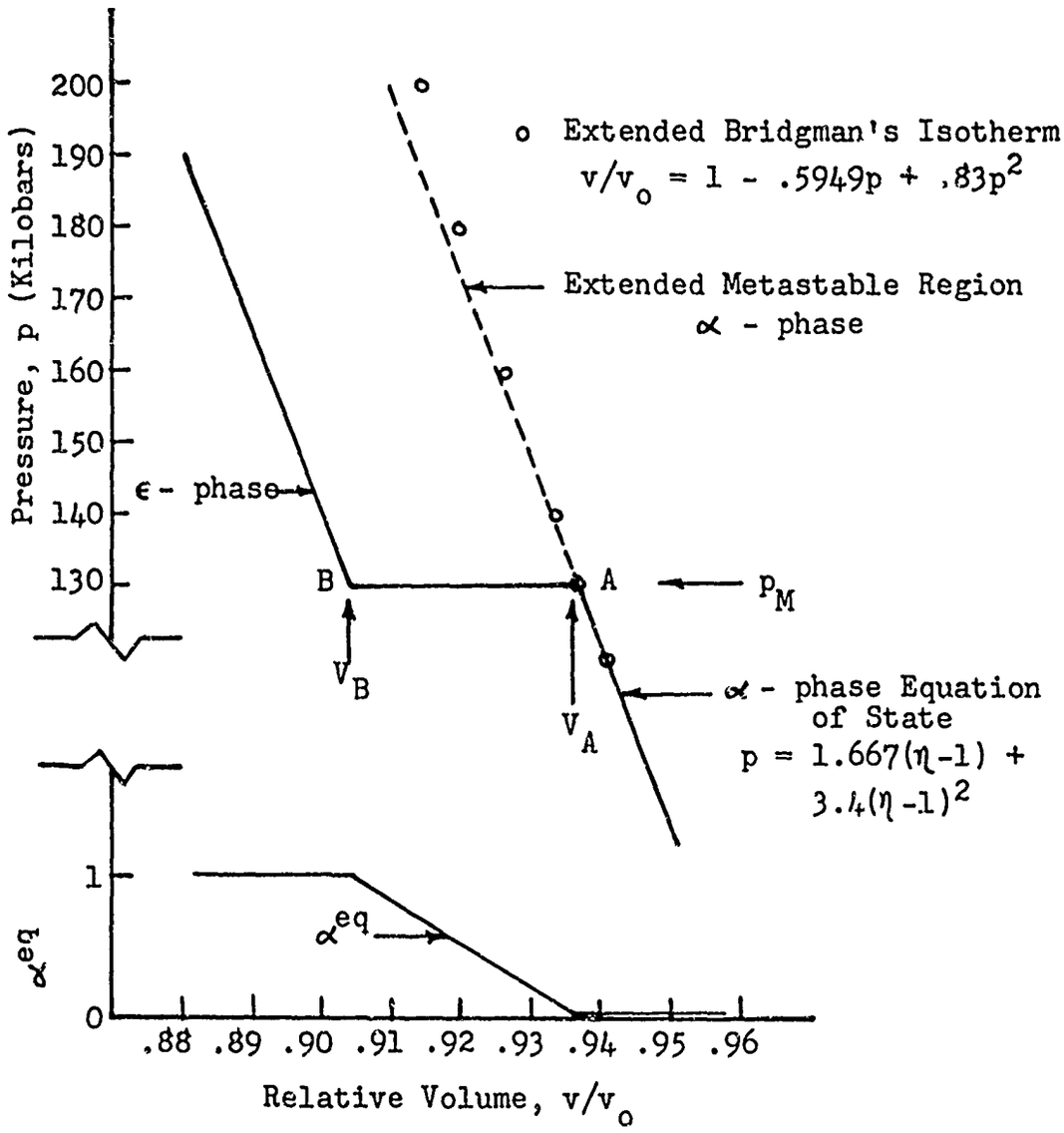

Fig. 4.1--Temperature Independent Equation of State of Iron and α^{eq}

α^{eq} is given by the relations:

$$\begin{aligned} \alpha^{eq} &= 0 && \text{if} \quad v > v_A \\ \alpha^{eq} &= (v-v_A)/(v_B-v_A) && \text{if} \quad v_B < v < v_A \\ \alpha^{eq} &= 1 && \text{if} \quad v < v_B . \end{aligned} \tag{4.6}$$

The graph of α^{eq} is given in Fig. 4.1.

As seen in Table VI, we assume the constancy of physical data, such as C_{vl}, Γ and so on, regardless of pressure. We use the equilibrium value (-.065 Kb/^{o}K) for dp/dT in the coexistence region unless otherwise stated.

V. SHOCK PROPAGATION IN IRON

5.1 Difference Equations

The system of difference equations used here is based on one described by Wilkins (35), with the yield stress set to zero. Space is divided into points and cells as in Fig. 5.1. The particle velocity and the current position of the Lagrangian coordinate are defined on the points with integer label j, and other variables are assigned to the cells with half-integer labels $j+\frac{1}{2}$, etc.

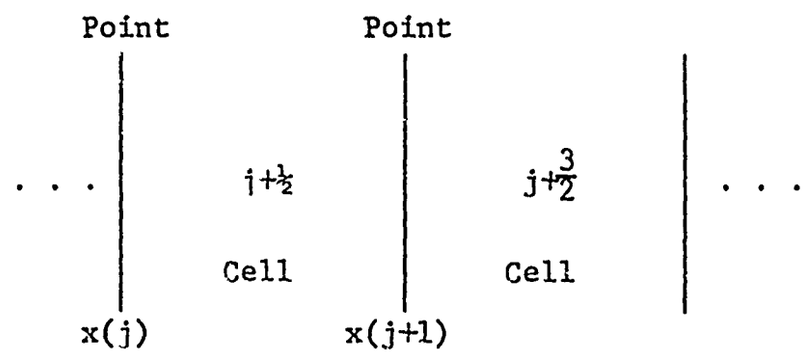

Fig. 5.1.--Difference Scheme in Space

Time differences are also staggered. Particle velocity and q are defined at half-integer times, $n+\frac{1}{2}$, and other variables are defined at integer times, n.

The computational sequence for general interior points and cells is given in Fig. 5.2.

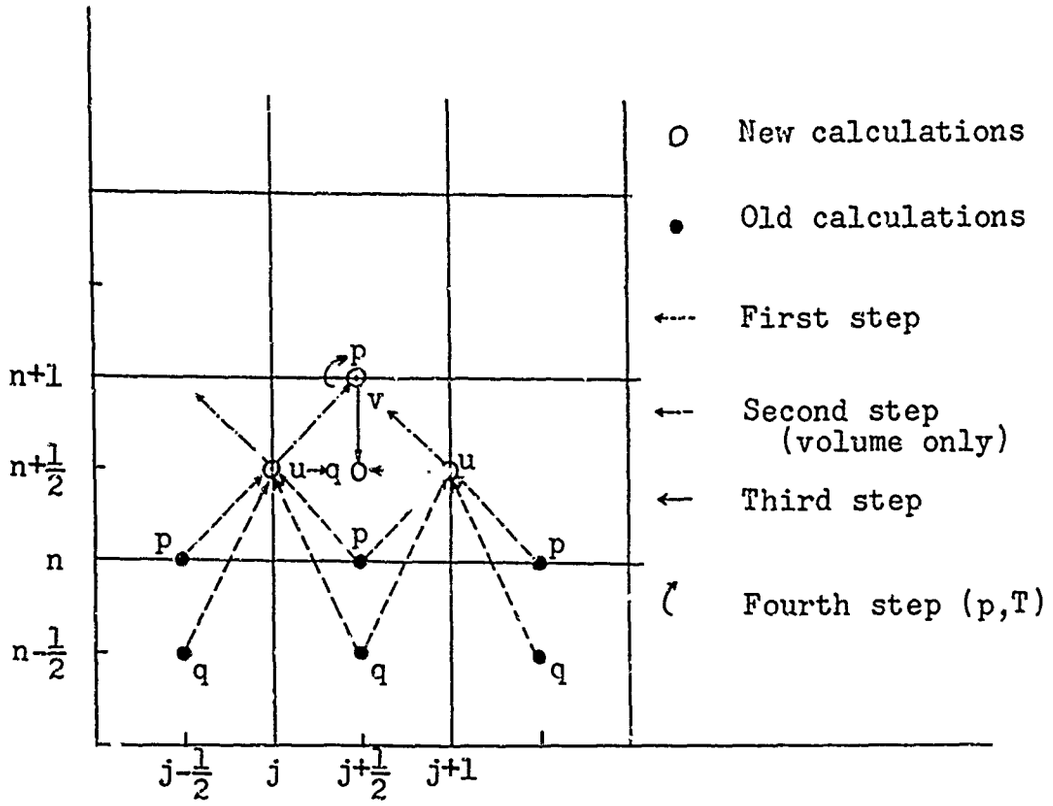

Fig.5.2.--Computational Sequence

The flow equations and the constitutive relations are approximated according to the above difference scheme. The difference equations are given in the order of computation. The subscript or superscript "o" refers to the initial state (p=0) of the first phase.

1. Equation of motion, Eq. (3.3):

$$u_j^{n+\frac{1}{2}} = u_j^{n-\frac{1}{2}} + \frac{\Delta t}{\Phi_j^n}\left(\Sigma_{j+\frac{1}{2}}^n - \Sigma_{j-\frac{1}{2}}^n\right) \tag{5.1}$$

where

$$\Sigma_{j+\frac{1}{2}}^n = -\left(p^n + q^{n-\frac{1}{2}}\right)_{j+\frac{1}{2}} \tag{5.2}$$

= total stress in the x-direction.

$$\Phi_j^n = \tfrac{1}{2}\left[\left(\frac{x_{j+1}^n - x_j^n}{v_{j+\frac{1}{2}}^n}\right) + \left(\frac{x_j^n - x_{j-1}^n}{v_{j-\frac{1}{2}}^n}\right)\right] \tag{5.3}$$

$$= \text{average mass at } j.$$

At the left boundary

$$\Phi_o^n = (\tfrac{1}{2})(x_1^n - x_o^n)/v_{\frac{1}{2}}^n \tag{5.4}$$

The new coordinate is given by:

$$x_j^{n+1} = x_j^n + u_j^{n+\frac{1}{2}}\,\Delta t. \tag{5.5}$$

2. Continuity equation:

$$v_{j+\frac{1}{2}}^{n+1} = v_{j+\frac{1}{2}}^n + \Delta t\left(\frac{\rho o}{m}\right)_{j+\frac{1}{2}}\left(u_{j+1}^{n+\frac{1}{2}} - u_j^{n+\frac{1}{2}}\right) \tag{5.6}$$

where

$$m_{j+\frac{1}{2}} = \rho_{j+\frac{1}{2}}^o(x_{j+1}^o - x_j^o) = \text{mass in the cell } j+\tfrac{1}{2}, \tag{5.7}$$

$$\rho o = \text{initial density.}$$

3. Linear viscosity:

$$q_{j+\frac{1}{2}}^{n+\frac{1}{2}} = C_L\,\rho_{j+\frac{1}{2}}^o\,\eta_{j+\frac{1}{2}}^{n+\frac{1}{2}}\,|u_{j+1}^{n+\frac{1}{2}} - u_j^{n+\frac{1}{2}}|\ \text{for}\left\{\begin{matrix} u_{j+1}^{n+\frac{1}{2}} < u_j^{n+\frac{1}{2}} \\ v_{j+\frac{1}{2}}^{n+1} < v_{j+\frac{1}{2}}^n \end{matrix}\right. \tag{5.8}$$

$$= 0 \text{ otherwise.}$$

Here

$$\eta_{j+\frac{1}{2}}^{n+\frac{1}{2}} = 2v_o/(v_{j+\frac{1}{2}}^{n+1} + v_{j+\frac{1}{2}}^n). \tag{5.9}$$

4. Constitutive relations:

The relaxation equation:

$$\alpha_{j+\frac{1}{2}}^{n+1} = \alpha_{j+\frac{1}{2}}^{n} + \left(\frac{\alpha^{eq}-\alpha}{\tau}\right)_{j+\frac{1}{2}}^{n} \Delta t. \tag{5.10}$$

τ is the characteristic relaxation time and is assumed to be constant.

The specific volume of the first phase is:

$$v_{1,j+\frac{1}{2}}^{n+1} = v_{j+\frac{1}{2}}^{n+1} - (v_2 - v_1)\alpha_{j+\frac{1}{2}}^{n+1} \tag{5.11}$$

Temperature calculation:

$$T_{j+\frac{1}{2}}^{n+1} = T_{j+\frac{1}{2}}^{n} + [CT]_{j+\frac{1}{2}}^{n}(v_{j+\frac{1}{2}}^{n+1} - v_{j+\frac{1}{2}}^{n})$$

$$- \left(\frac{q}{C_v}\right)_{j+\frac{1}{2}}^{n+\frac{1}{2}}(v_{j+\frac{1}{2}}^{n+1} - v_{j+\frac{1}{2}}^{n}) \tag{5.12}$$

where $C = -(1/C_v)(\partial p/\partial T)_v$ (convenient for a mixed phase)

or $C = -\Gamma/v$ (convenient for a single phase), and Γ is the Grüneisen coefficient. The value of C_v depends on the phase region as described in the last section. The formula for $C_{v,m}$ in a mixed phase is given in Appendix II.

Equation of state:

$$p_{j+\frac{1}{2}}^{n+1} = [p(v_1,T)]_{j+\frac{1}{2}}^{n+1} \tag{5.13}$$

where $p(v_1,T)$ is given by Eq. (4.5).

The boundary between a single and a two-phase region is distinguished by the transition pressure p_M, at which the relative volume of the first phase is given by v_A.

5.2. FORTRAN Program

The FORTRAN IV program used for the calculations is given in Appendix III. This program is set up specifically for the problem of a constant driving pressure and a semi-infinite slab of material so it does not treat an unloading rarefaction problem nor the reflection of a shock wave.

The heart of the program, insofar as we are concerned, is in the calculation of α, p and T, following that of v and q (Eqs. (5.10) through (5.13) above); therefore we consider it in detail.

When the material of cell j is in the region of phase 1, as determined by a test on p, the numerical computation proceeds to Eqs. (5.12) and (5.13) from Eq. (5.8). When the pressure in cell j reaches the transition value p_M and overshoots it, temperature and the relative specific volume of phase 1 must be readjusted by use of Eqs. (5.11) and (5.12). At this time the special program parameter NSA(J) is set equal to 2 for the cell j and kept at that value until the material is all converted to phase 2. Calculation of pressure is accomplished by substituting v_1 and T from Eqs. (5.11) and (5.12) into (5.13). Once the given cell becomes pure phase 2, NSA(J) is set equal to 3, and the calculation again proceeds as for phase 1. However, as long as we use the relaxation relation (Eq. (3.26)), with the approximation (v_2-v_1 = constant), we always have:

$$\alpha < 1$$

$$v_1 = v - \alpha(v_2 - v_1). \tag{5.14}$$

If we are reminded that pressure is essentially calculated from v_1, then from Eq. (5.14), regardless of whether we set α to unity when it is close to unity, the value of v_1 is practically the same. Therefore we can, for the present case, discard the case for NSA(J) = 3, which is enclosed by the dotted lines in the flow chart.

The expanded flow chart for this part of the program is given in Fig. 5.3.

5.3. Numerical Results

5.31 Transient Case

The particular concern here is with development of the double wave structure associated with the phase transition. A uniform pressure is applied at time t = 0 to the surface of a half space, x = 0, and maintained constant as the plane wavefront develops and propagates inward. For an applied pressure of 0.200 Mbar*, Figs 5.4 and 5.5 show pressure profiles of the developing wave at times measured from the first application of pressure. Fig. 5.4 illustrates the development and decay of the first wave caused by the α - ε phase transition. After about ten relaxation times the profile has the clear double-wave structure shown in Fig. 5.5.

The thickness of the first wave front is determined by q and by the choice of space increment, Δx (Fig. 5.1). The width of the second front is controlled by the relaxation time of the phase transition. When it is well separated from the first wave,

*1 Megabar = 10^{12} dynes/cm^2

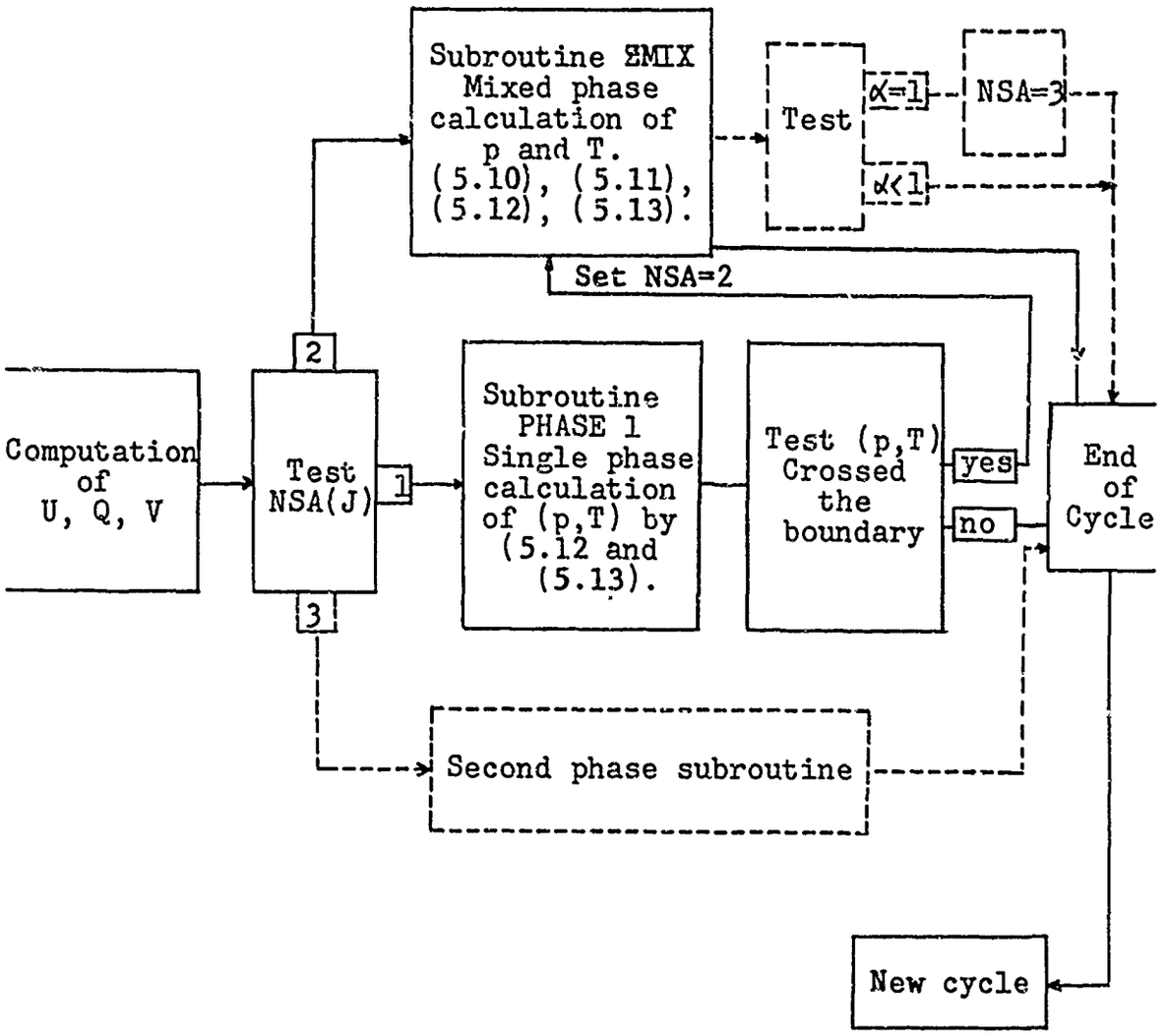

Fig. 5.3--Flow Chart for the Constitutive Relation

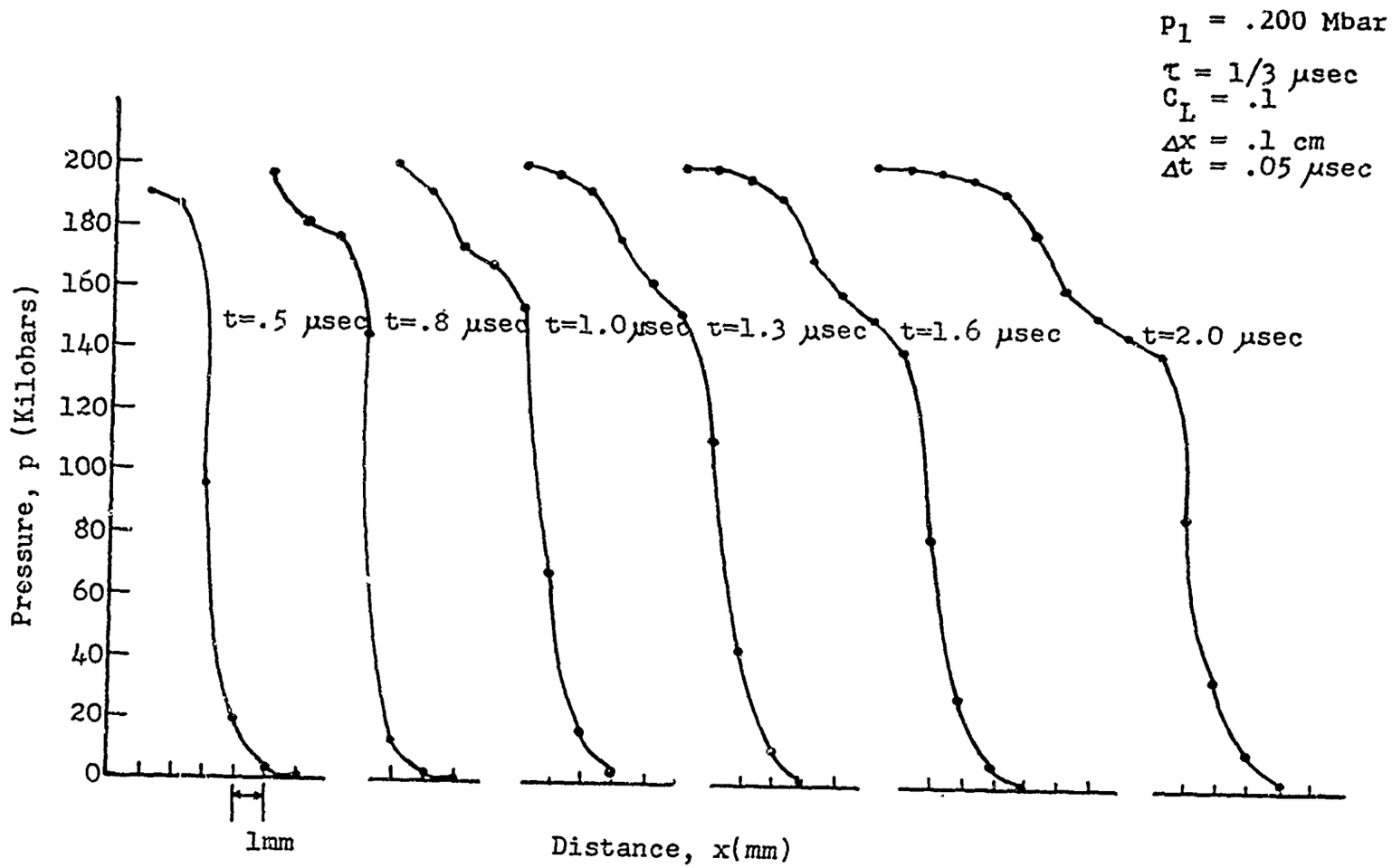

Fig. 5.4--Wave Propagation in Iron at Early Stages.
Δx and Δt are space and time increments used in the numerical integration.

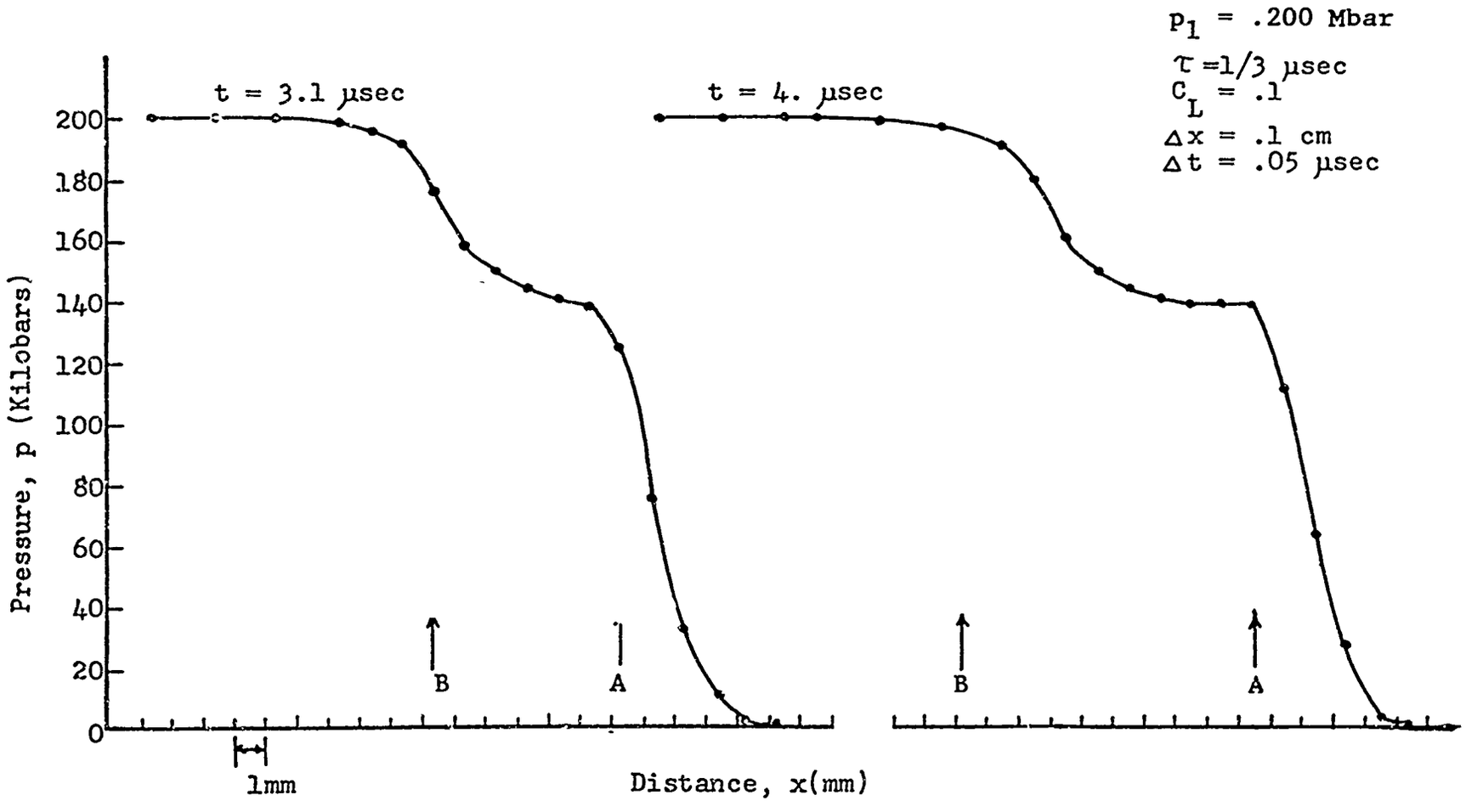

Fig. 5.5. --Double-Shock in Iron.
Δx and Δt are space and time increments used in the numerical integration.

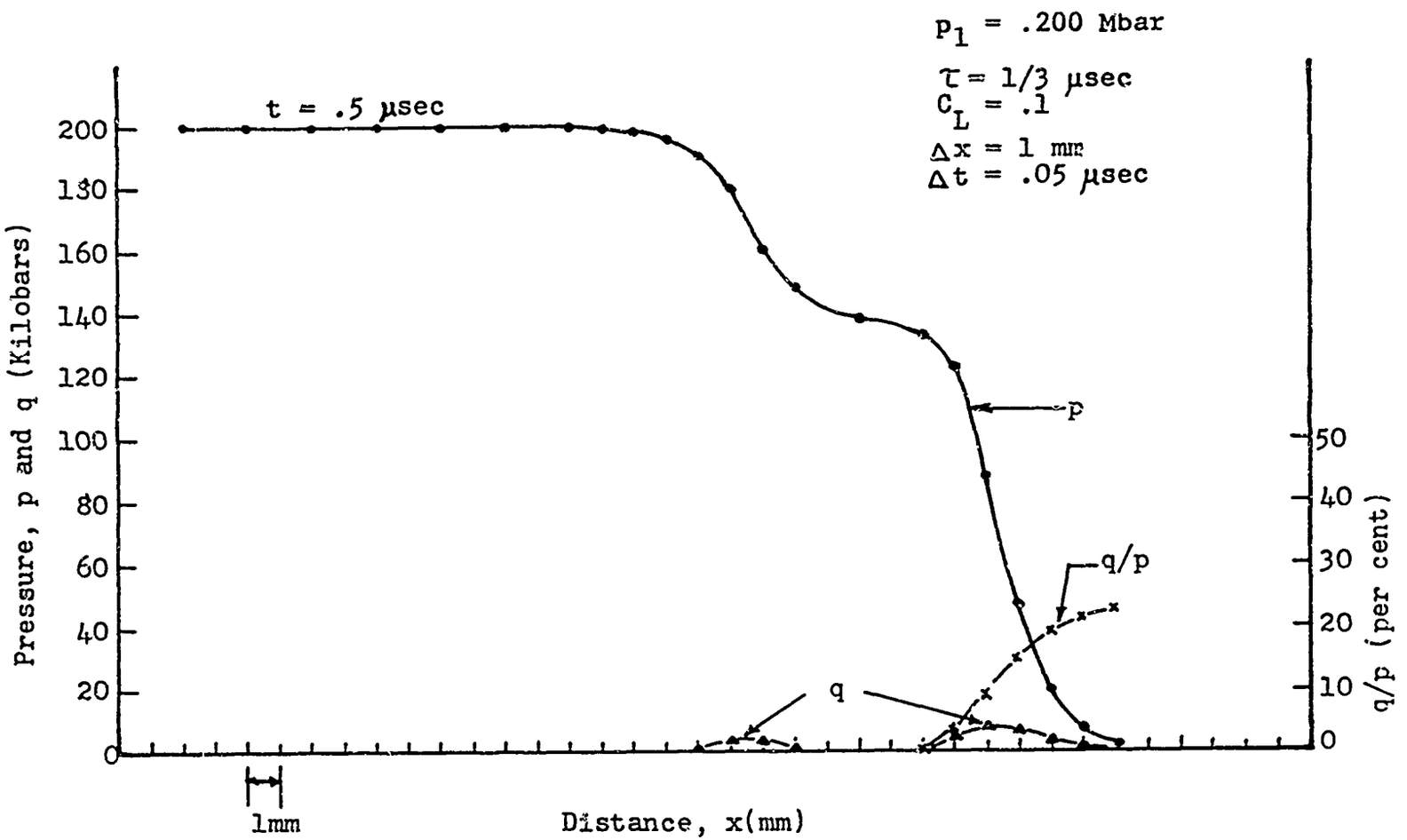

Fig. 5.6.--Relative Magnitude of p and q for C_L = .1. Δx and Δt are space and time increments used in the numerical integration.

the relative magnitude of q in the second front is negligible, as shown in Fig. 5.6. The coefficients C_L are varied to determine effects of q on the transient wave profiles.

Richtmyer (36) has shown, using quadratic q, that a small coefficient of pseudo-viscosity produces an ocillatory output even when the stability condition ($\Delta x/\Delta t$) is satisfied. Figs. 5.7 through 5.9 show similar changes in profiles for various C_L. Figs. 5.10 and 5.11 give the profile at fixed times for three different values of C_L. From these it is quite clear that the shock profile converges to the same form after about three relaxation times. Details of the relaxation process at early times can be obscured by oscillations when C_L is too small as these figures show. A very large C_L produces so much damping that sudden changes in profile are prevented. This can allow q to control the profile of the second shock as well as the first. A value of $C_L = 0.1$ was found satisfactory for most of the calculations described here.

Novikov observed a drop in pressure behind the first shock. These calculations sometimes show such a drop, but it is more likely due to oscillations in the output than to a physical effect.

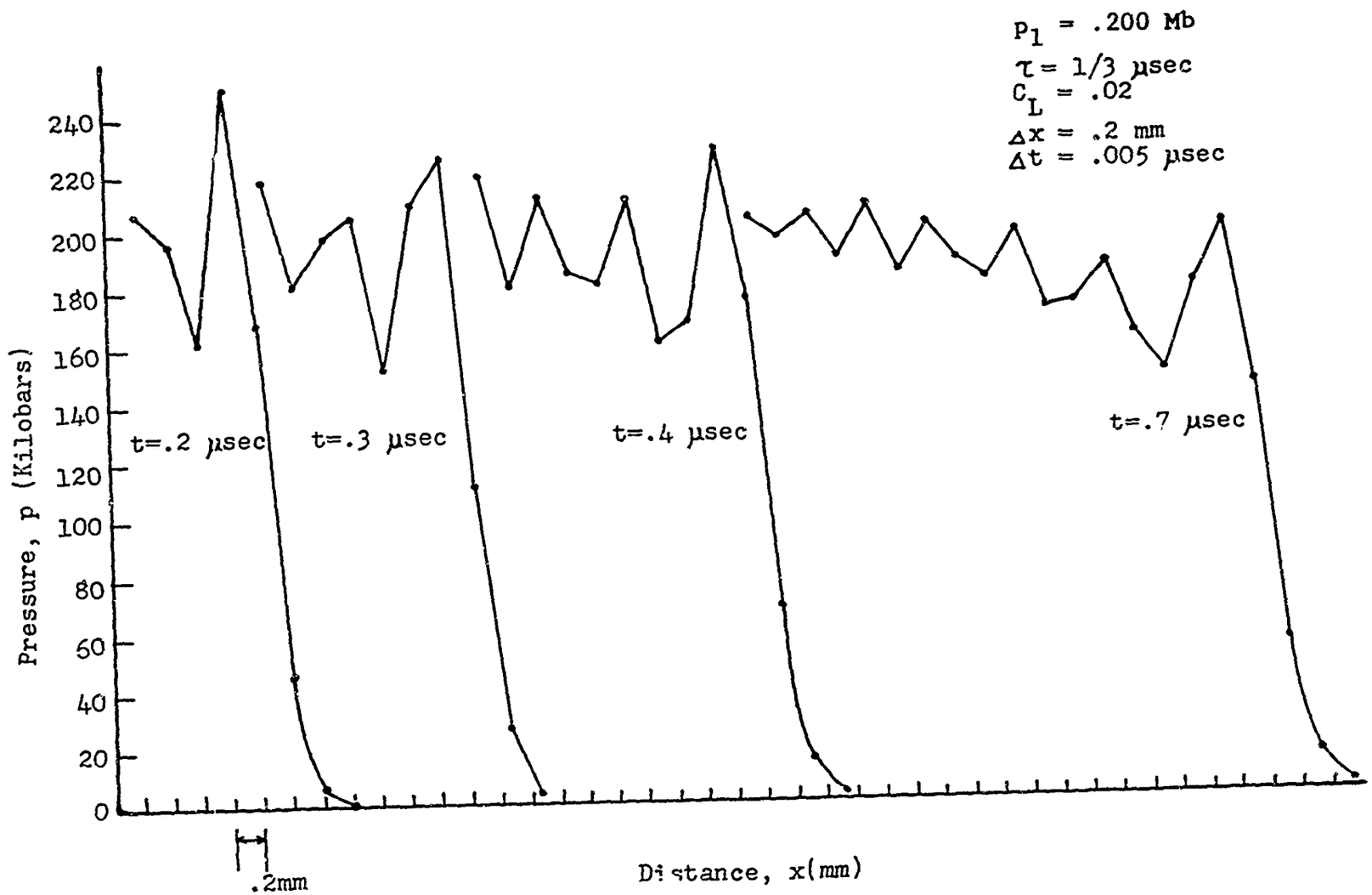

Fig. 5.7.--Wave Propagation with C_L = .02.
Δx and Δt are space and time increments used in the numerical integration.

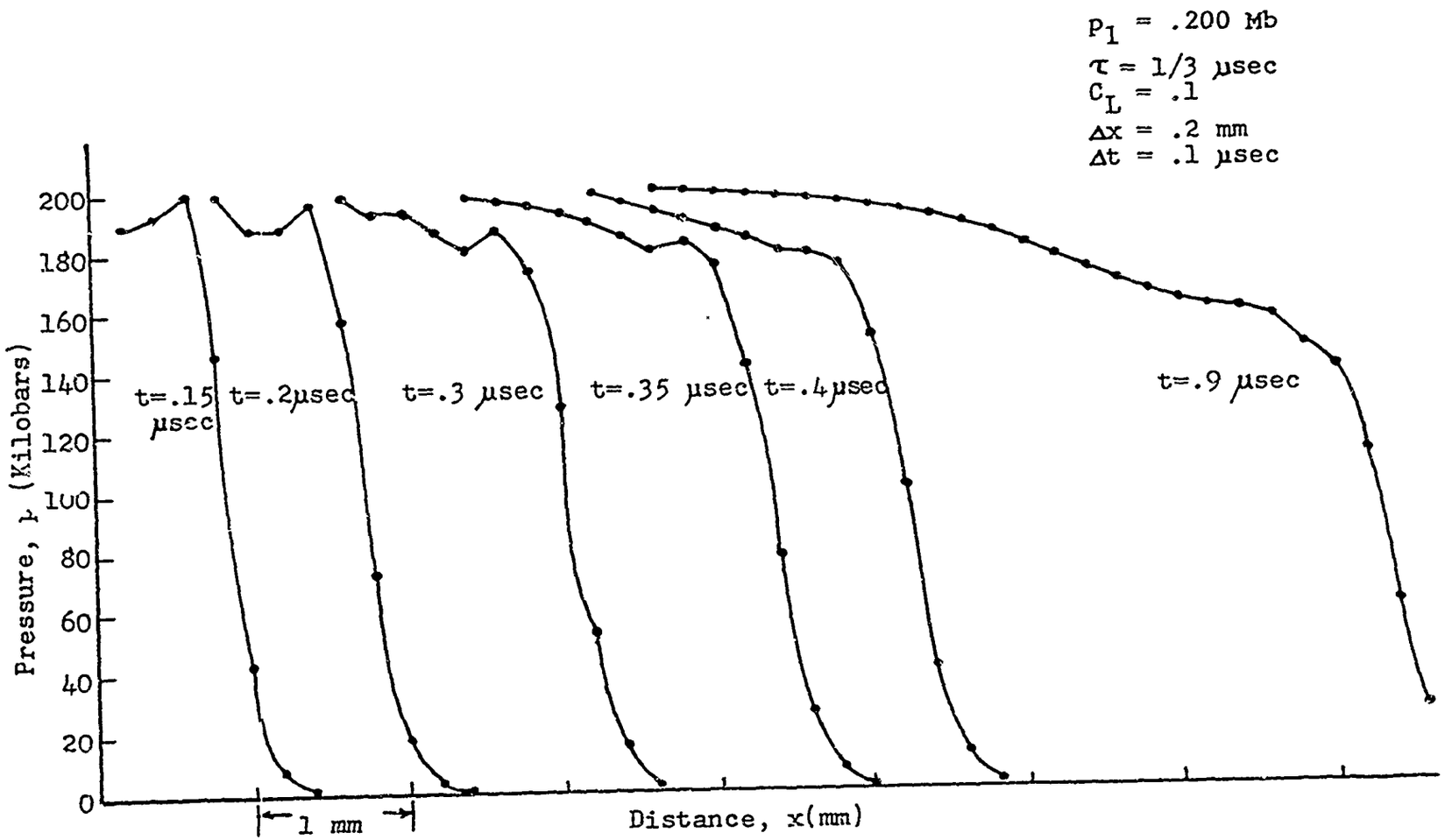

Fig.5.8.--Wave Propagation with C_L = .1.
Δx and Δt are space and time increments used in the numerical integration.

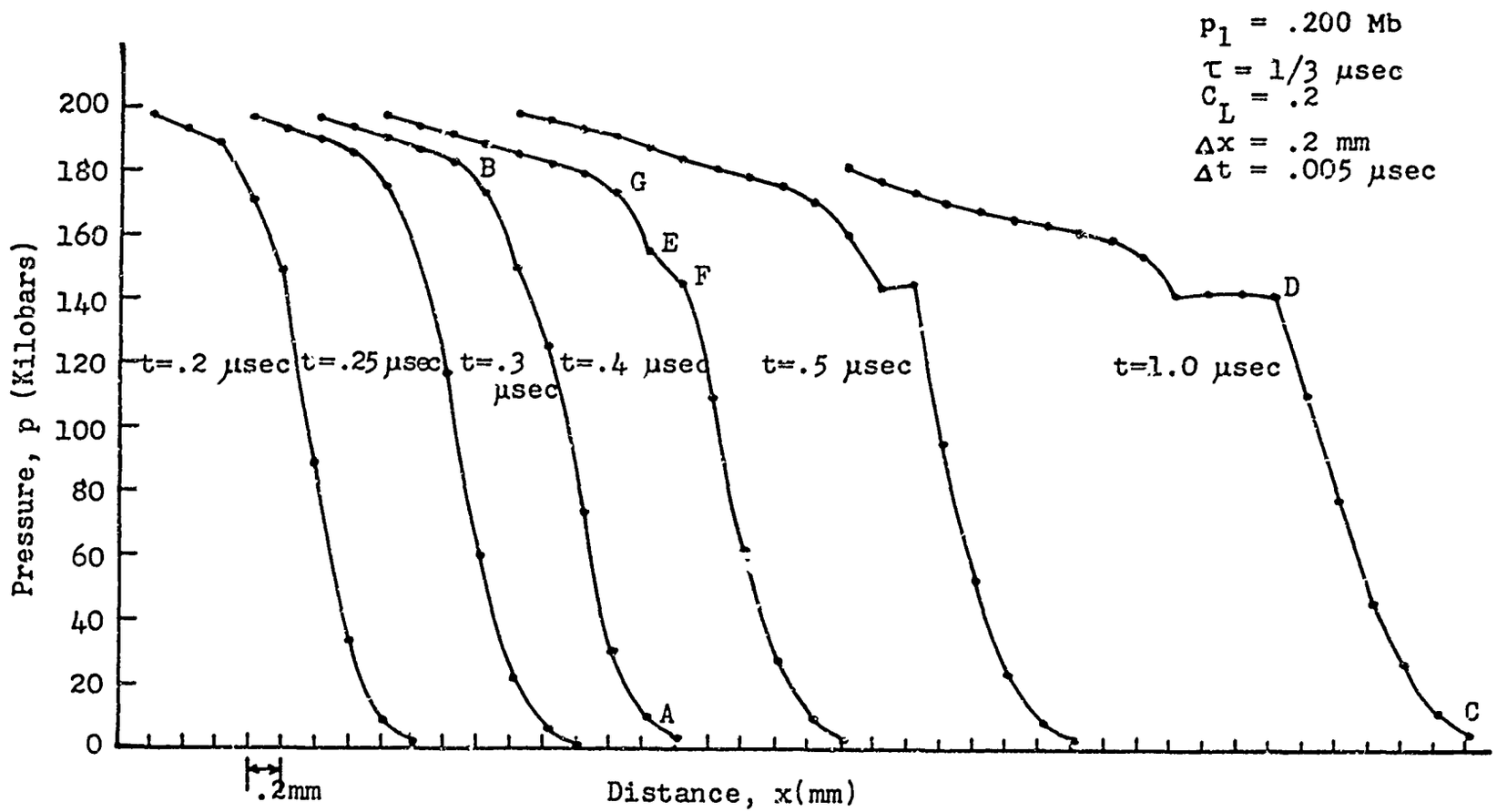

Fig. 5.9.--Wave Propagation with C_L = .2.
Δx and Δt are space and time increments used in the numerical integration.

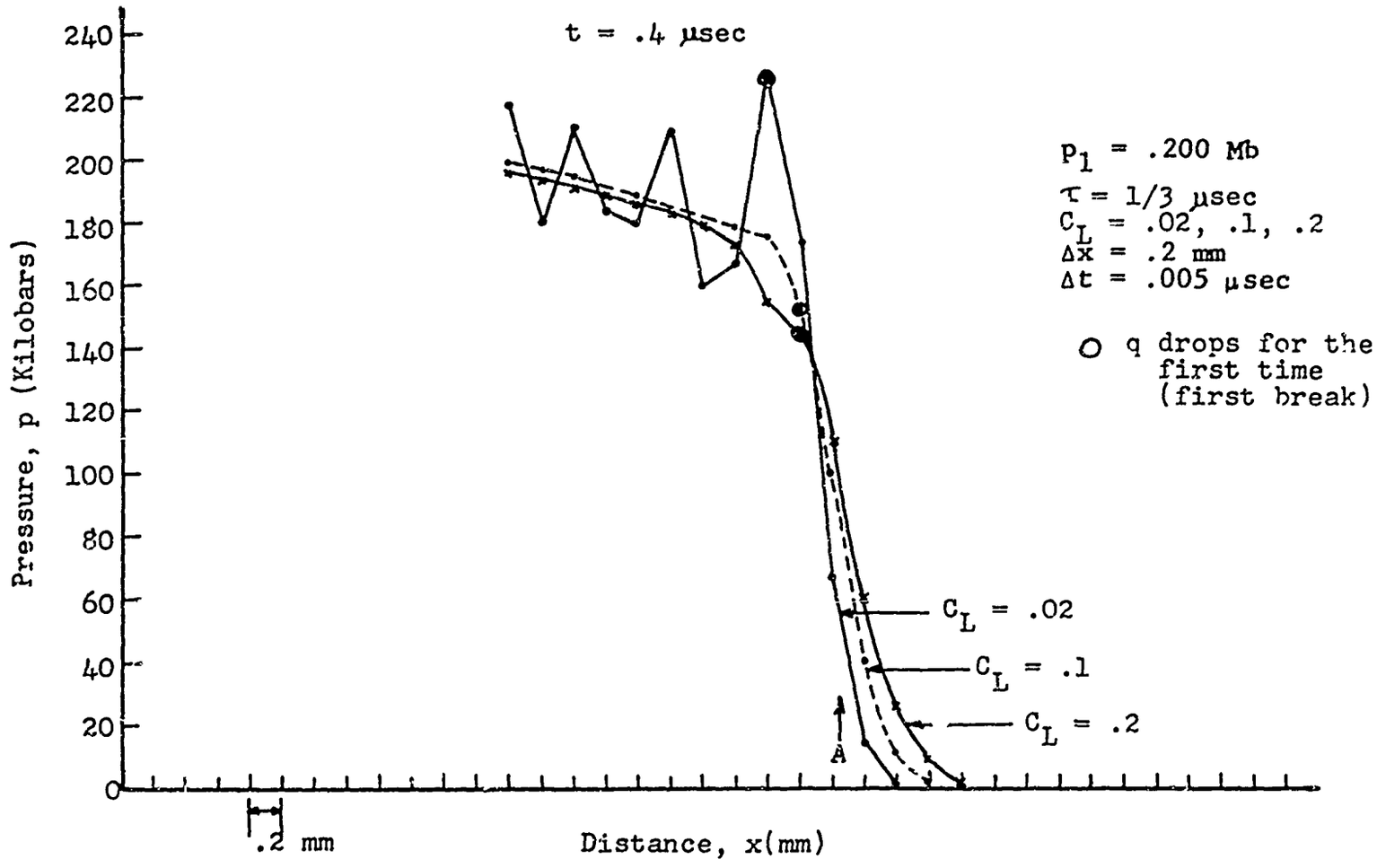

Fig. 5.10--Effect of q at .4 μsec.
Δx and Δt are space and time increments used in the numerical integration.

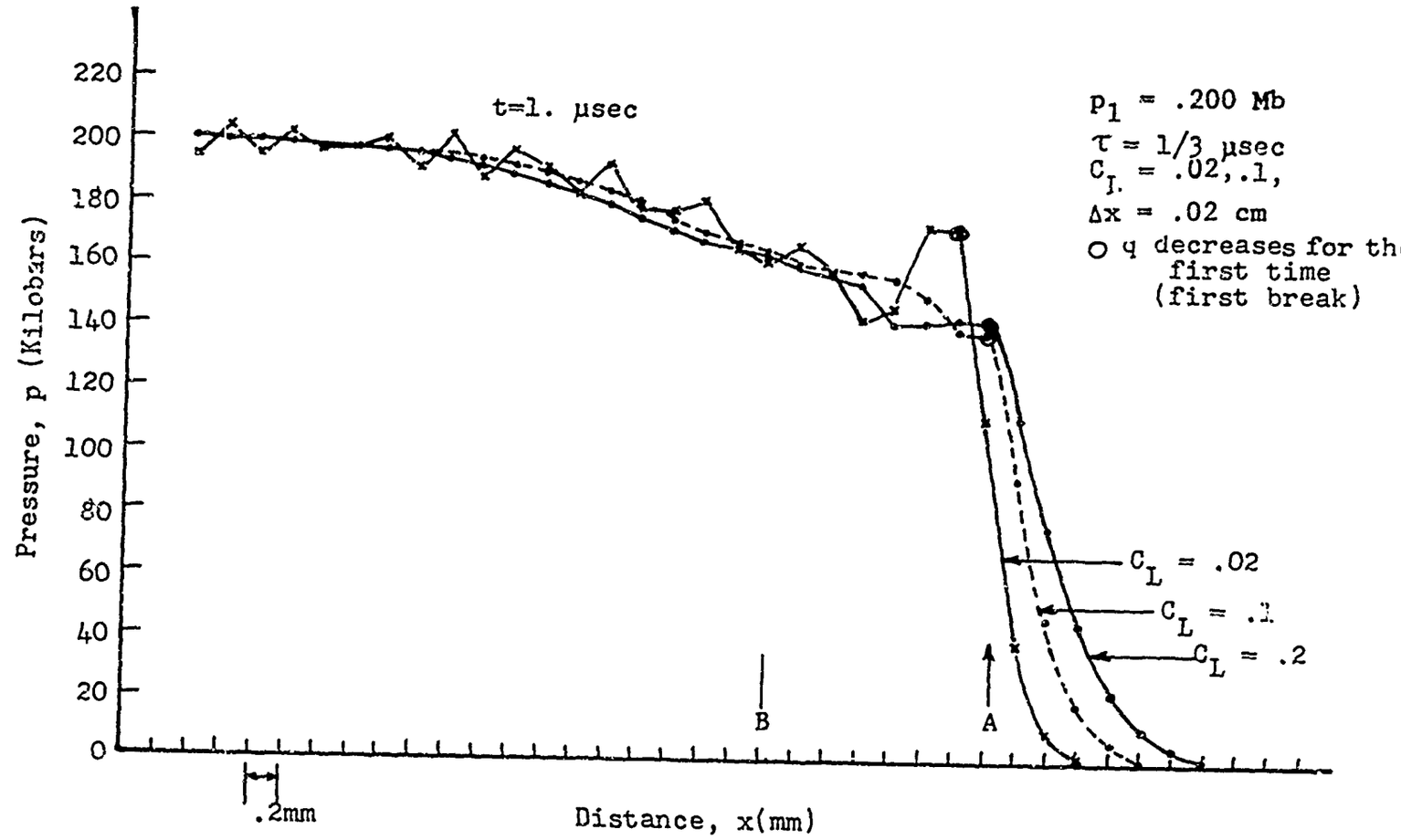

Fig.5.11--Effect of q at 1. μsec.
Δx and Δt are space and time increments used in the numerical integration.

Both pressure and α are shown in Fig. 5.12 as functions of time at .01 cm from the surface for 3 values of C_L. The behavior of α^{eq} is sensitive to C_L; it reflects the fluctuations in p. α, on the other hand, is relatively independent of C_L; its behavior is controlled by the relaxation time τ. This suggests that the decay in amplitude of the first wave is essentially independent of the artificial viscosity.

The decay of the precursor is shown in Fig. 5.13. The rate of decay at early times is closely related to a simple exponential, as shown.

This behavior is plausible on the basis of the following model. Eq. (3.23) can be written

$$dp/dt = a^2\, d\rho/dt + (m_1 n_2 - m_2 n_1) f(v_1\tau,\alpha)/G$$

This is the analog of Eq. (9) in reference (50). By the same arguments used there, we can arrive at the analog of Eq. (19) of ref. (50):

$$dp_1/dt = -(m_1 n_2 - m_2 n_1)(\alpha_{eq} - \alpha)/\tau G$$

providing the path of the number one shock lies along a characteristic, which is nearly true. Here p_1 is pressure at the peak of the first shock, assumed to be a discontinuity, hence it lies on the metastable surface $v_1(p,T)$. With this condition, $\alpha \equiv 0$. Now with the sweeping approximations that $v_1 - v_2 = \Delta v$ = constant, that the entire process is temperature independent, and that $C_{p1} = C_{p2}$, we obtain for the decay equation:

$$dp_1/dt = (\Delta v\, \alpha_{eq}/2\tau)\, dp/dv_1 \ .$$

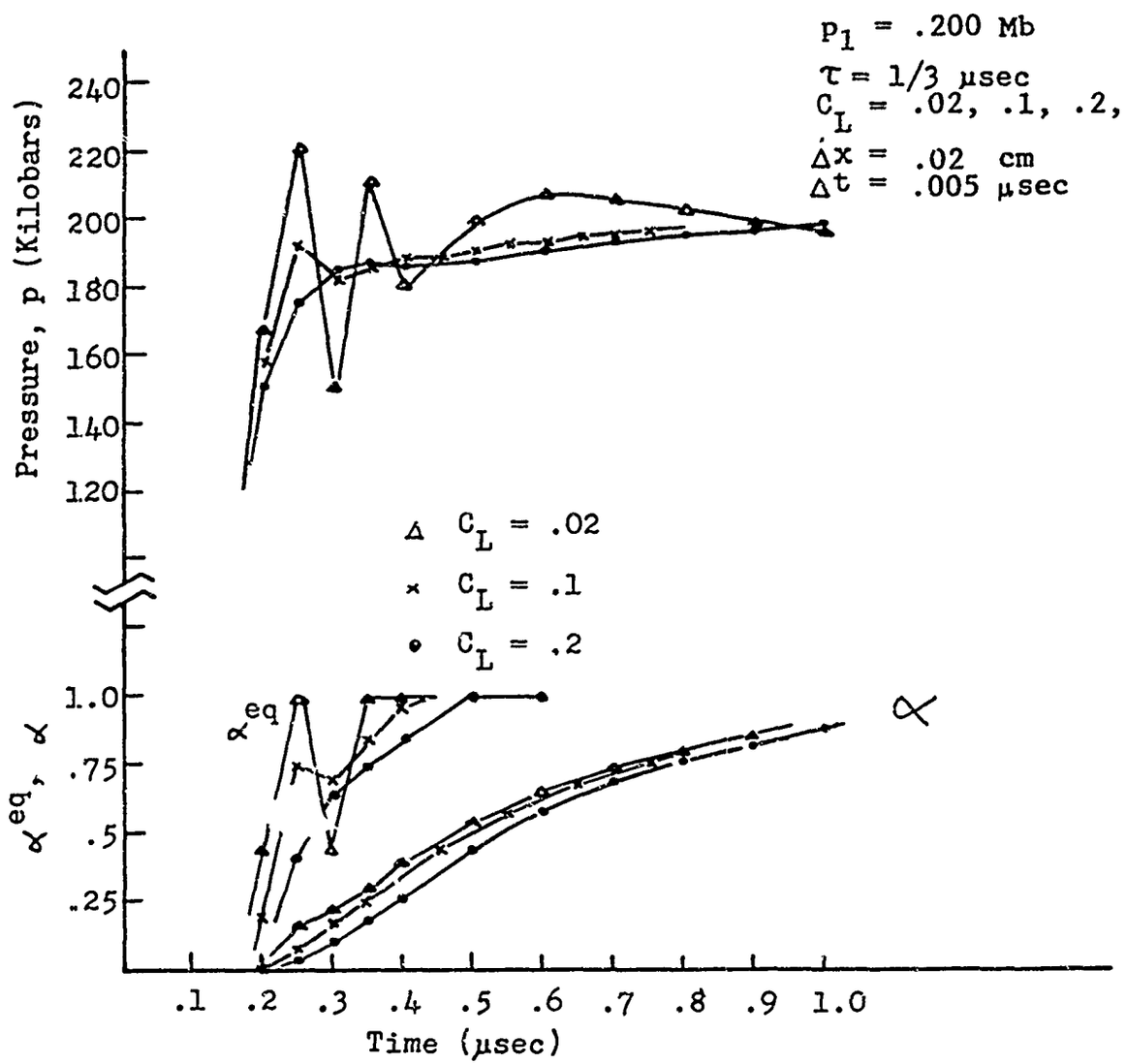

Fig.5.12--q and Speed of Transformation at Fifth Cell

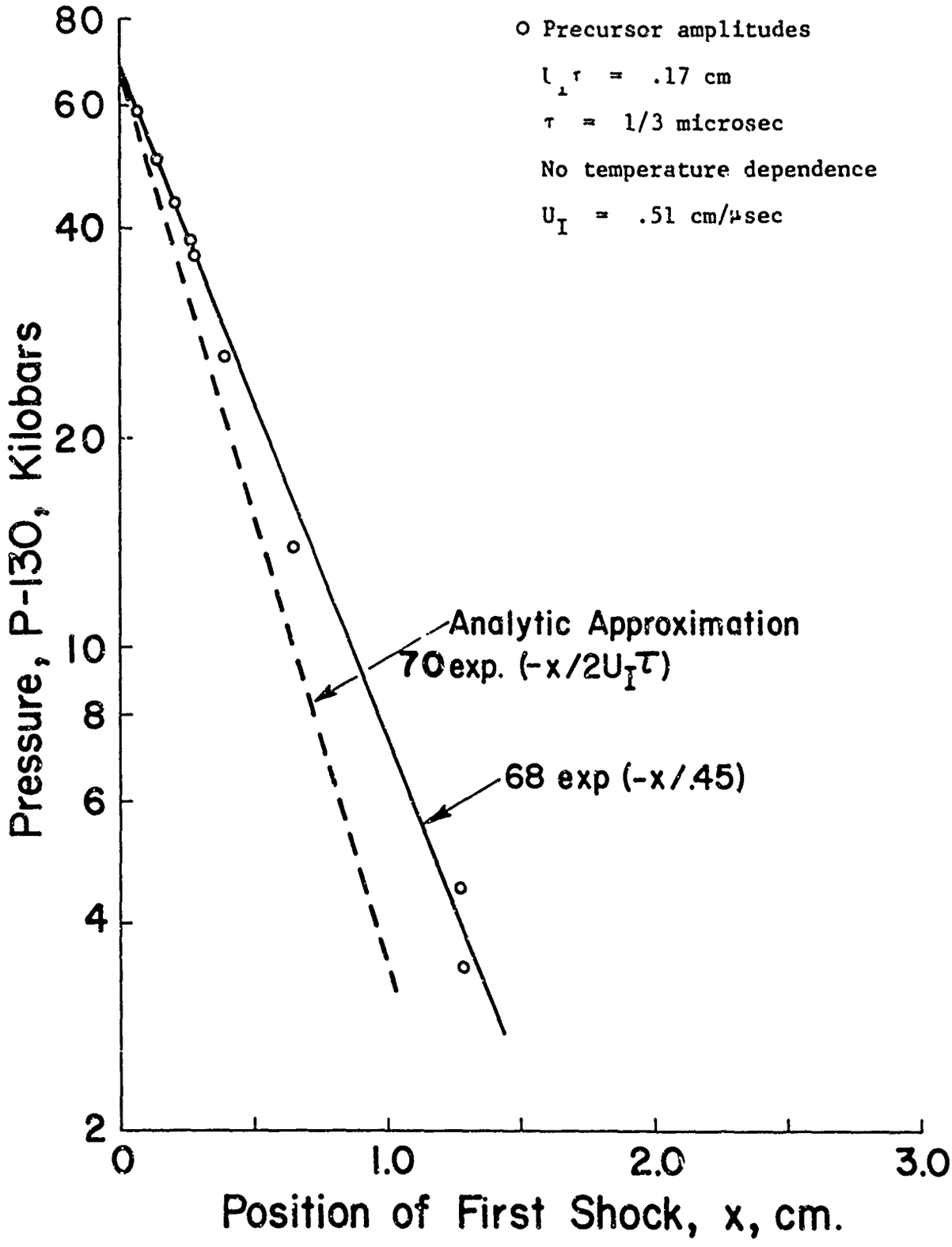

Fig. 5.13.--Decay of First Shock in Iron Resulting from Phase Transition.

If $v_1(p)$ is linear, then

$$\alpha_{eq} = \begin{cases} 1 \quad , & v_1 \le v_m - \Delta v \\ (v_m - v_1)/\Delta v = (p_m - p_1)(dv_1/dp)/\Delta v \ , & \\ \qquad v_m - \Delta v \le v_1 \le v_m & \\ 0 \quad , & v_m \le v_1 \end{cases}$$

Here v_m and p_m are pressure and volume where the Hugoniot first enters the mixed phase. These expressions yield

$$\begin{aligned} p_1 &= p_D + (x\,\Delta\,v/2U\tau)\ dp/dv_1 \ , \quad v_1 \le v_m - \Delta v \\ &= p_m + (p_D - p_m)\ \exp(-x/2U\tau) \ , \\ &\qquad\qquad v_m - \Delta v \le v_1 \le v_m \\ &= 0 \qquad v_m \le v_1 \end{aligned}$$

where $x = Ut$. Figure (5.17) shows that in the present case (p_D = driving pressure = 200 kbar), the central formula applies, therefore we should expect to find that

$$p_1 - 130 = 70 \exp(-x/2U\tau)$$

The difference between this curve and the numerical results, shown in Fig. 5.13, is due to non-linear effects.

In Figs. 5.5 and 5.11 there are arrows labelled A and B. These indicate the shock front position which would be predicted at the indicated times from the Rankine-Hugoniot jump conditions: A for the first shock, B for the second. The difference between this predicted arrival time and the one obtained in the

numerical integration arises because the shock profile has not reached its steady state or permanent regime. For the permanent regime, to which jump conditions apply, the locus of p+q vs v lies along two straight lines, OM and MC in Fig. 5.14. M represents the break in pressure between the first wave and the second, and the velocities of the first and second waves are proportional to the square roots of the slopes of these two lines. When the pressure is applied suddenly and the relaxation time is long, the state of an element will rise to a point on the extended metastable curve of phase 1, say C' in Fig. 5.14, and then proceed toward the equilibrium point C along an isobar. During the process of precursor decay, the locus will lie along intermediate curves such as OabC. In fact then the leading wave and the developing profile behind it propagate at first with a velocity proportional to the square root of the slope of the chord OC', only gradually approaching the smaller steady state velocities. Consequently the wave front position calculated by integration of the flow equations should always lie ahead of the position predicted by the jump conditions whenever the constitutive relations include rate or time dependent processes. Loci for p+q obtained in the calculations for several positions and two values of C_L are shown in Fig. 5.15. They do indeed display the behavior described in Fig. 5.14; moreover the locus is relatively independent of C_L.

It is possible to calculate the equilibrium Hugoniot curve for a material undergoing a phase change using only the jump conditions and an equation of state (17). However, once a

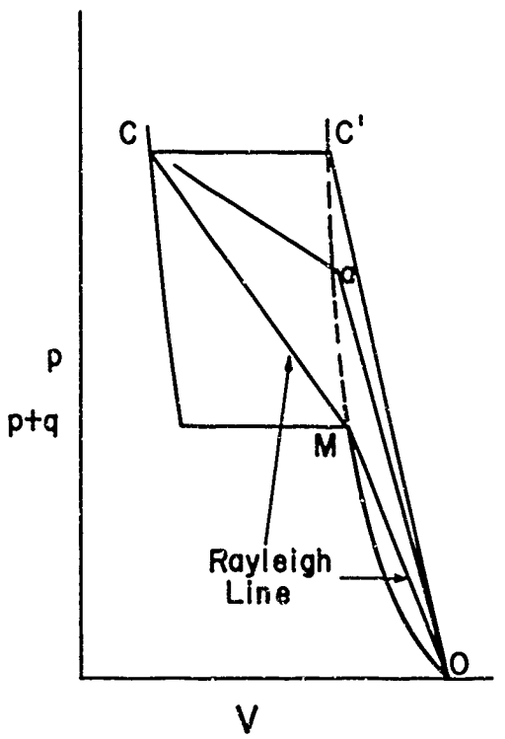

Fig. 5.14. --Pressure Profile and Total Stress with Respect to the Rayleigh Line.

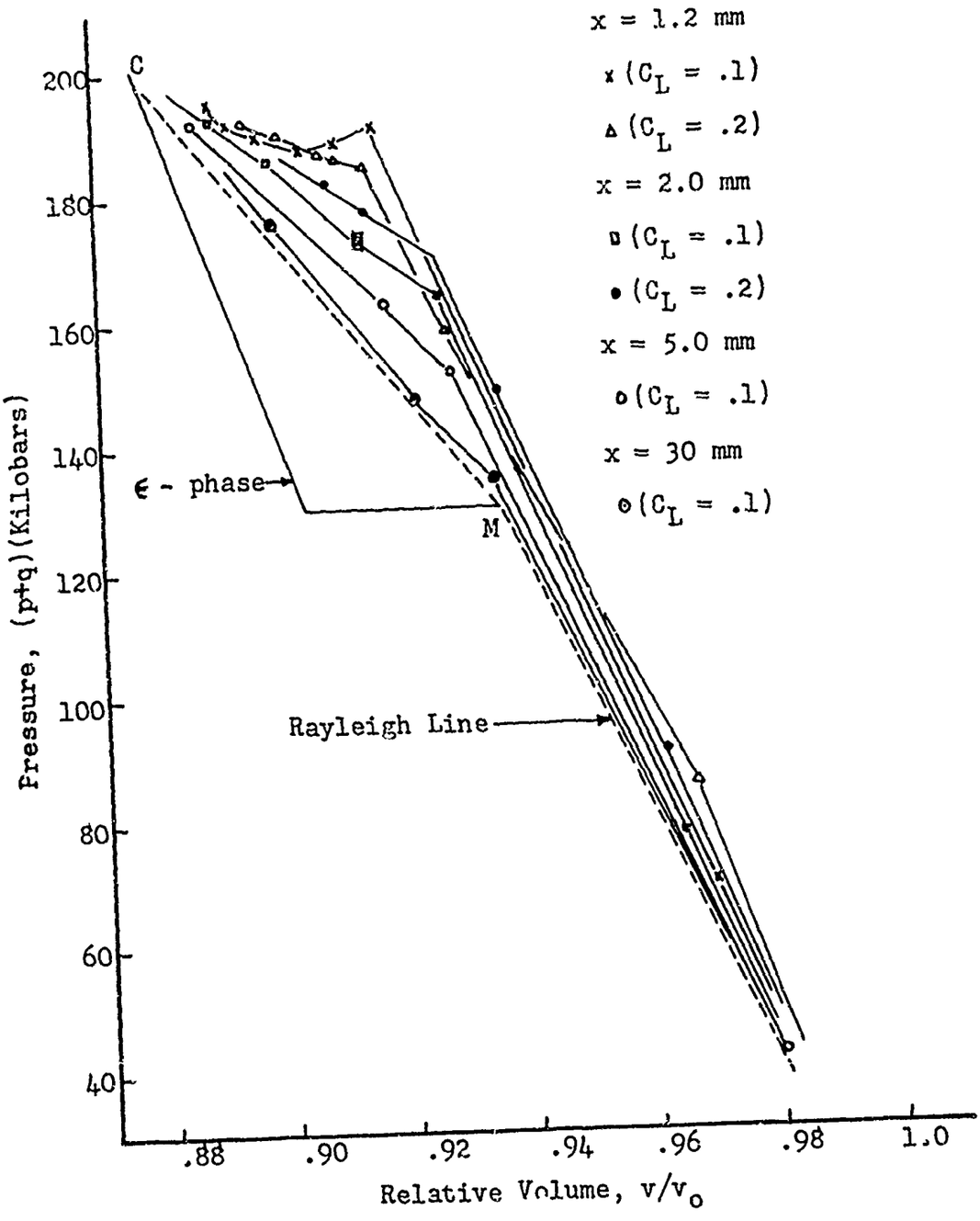

Fig. 5.15-- Total Stress (p+q) and Rayleigh Line

program is available for integrating the flow equations, as in this case, it turns out to be easier to run the program with a uniform driving pressure and tabulate p and v in the uniform region far behind the shock fronts than to do the equilibrium computation. That has been done and the results are shown in Fig. 5.16.

TI is the temperature independent solution (which is on the second phase isotherm), and TD1 and TD2 are temperature dependent solutions with different isothermal compressibilities (a_2 = 3.4 and a_2 = 2.4, respectively). The difference between TI and TD1 is due only to the temperature dependence in the equation of state. The reason TI lies above TD1 can be explained as follows: since dp/dT is negative in the coexistence region, the transition produces a temperature decrease. This decrease is found to be larger, except near the transition point, than the temperature rise in the first shock (about 20°), hence it gives a slight pressure drop for the temperature-dependent equation of state. Experimental values measured by Minshall (13) are indicated by crosses. The differences between these and the calculated curves are substantial. It is quite possible that a curve passing through points B and C can be developed by allowing v_2-v_1 to vary with p. Point A, however, appears to be unattainable within what are here believed to be reasonable limits of the thermodynamic and transition parameters.

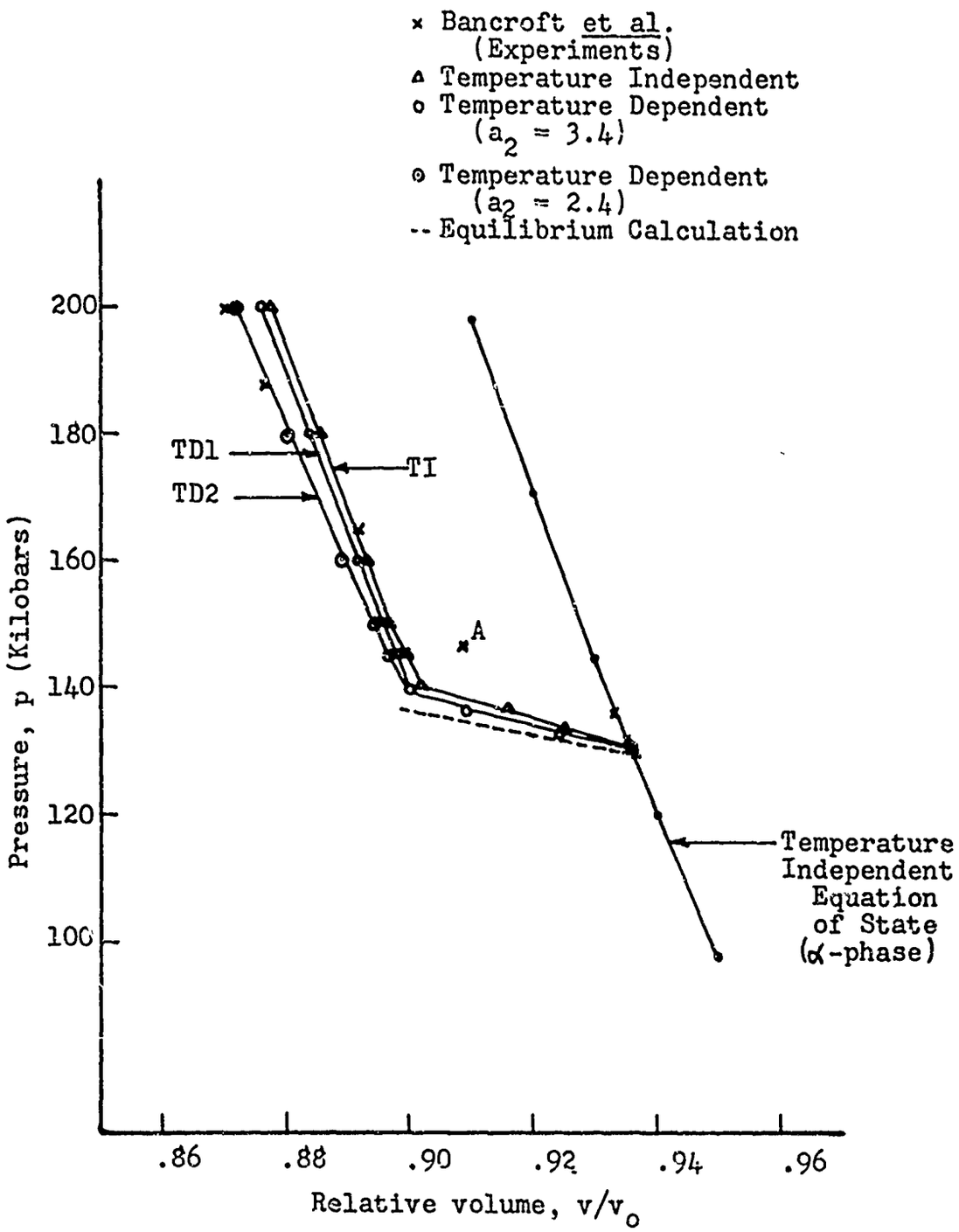

Fig. 5.16.--The Hugoniot Curve in and beyond the Coexistence Region.

5.32 Permanent Regime

After the shock of the last section has propagated far into the medium, the profiles of the first and second shocks are expected to become unchanging, though they continue to separate because of differing velocities. When this happens, these profiles should be described by a permanent regime solution to the flow equations (37). Such a solution is obtained here in order to determine how far the wave must travel to closely approach the permanent regime and to provide an independent check on the numerical integration for the transient case. We proceed by setting $(\partial/\partial t)x = 0$ for all variables in Eqs. (3.3)-(3.5) and (3.43). The resulting equations are, for the temperature independent case:

$$\rho u \, du/dx = -dp/dx \tag{5.15}$$

$$d(\rho u)/dx = 0; \quad \rho u = m \tag{5.16}$$

$$u d\alpha/dx = (\alpha^{eq}-\alpha)/\tau \tag{5.17}$$

$$v = v_1 + (v_2-v_1)\alpha \tag{5.18}$$

$$v_2(p) - v_1(p) = \text{const} \tag{5.19}$$

$$p = p(v_1) \tag{5.20}$$

Combining Eqs. (5.16) and (5.15) yields the Earnshaw relation:

$$p-p_o = \rho_o^2 U^2 (v_o-v) = m^2(v_o-v) \tag{5.21}$$

where U is shock velocity. Combining Eqs. (5.17), (5.18), (5.19) and (5.21) yields an equation for dp/dx in the transition region

$$dp/dx = m (v_1-v_2)(\alpha^{eq}-\alpha)/\tau(1+m^2 dv_1/dp)v \ . \tag{5.22}$$

From the definition of α^{eq} we have

$$\begin{aligned} \alpha^{eq} &= 0, \quad p \le p_o \\ &= (v-v_o)/(v_a-v_o), \quad p_o \le p \le p_a \qquad (5.23) \\ &= 1, \quad p_a \le p \end{aligned}$$

where p_o, p_a, v_a, v_o are defined in Fig. 5.18. Combining Eq. (5.23) with (5.18), (5.21), and (5.22) yields the following expressions for dp/dx:

$$dp/dx = m^3(v_o-v_1)/\tau(1+m^2dv_1/dp)(m^2v_o-p+p_o), \quad p_o \le p \le p_a \qquad (5.24)$$

$$dp/dx = m(m^2(2v_o-v_1-v_a) + p_o-p)/\tau(1+m^2dv_1/dp) \cdot (m^2v_o-p+p_o), \quad p_a \le p \le p_f \qquad (5.25)$$

Here v_1 is a known function of p, Eq. (5.20). Examination of Eqs. (5.24) and (5.25) shows that $dp/dx = 0$ at $p = p_o$ and $p = p_f$. In Eq. (5.22), $m < 0$ for a forward-facing shock, $\alpha^{eq} - \alpha > 0$, $v_1-v_2 > 0$, and $1 + m^2dv_1/dp > 0$, from Fig. 5.18. Therefore $dp/dx < 0$ throughout the transition. The qualitative features of dp/dx are shown in Fig. 5.18.

Eqs. (5.24) and (5.25) have been integrated for the iron transition, assuming that no temperature changes occur in the shock. The results are compared with the temperature-independent transient case in Fig. 5.19 for a driving pressure of .200 Mbar. The shock width, defined as $\Delta x = \Delta p/|dp/dx|_{max}$, is for this case about .3 cm. The steady velocity of the second shock with respect to the material ahead of it is U_{II} = 0.37 cm/μsec. The relaxation time assumed for the calculation

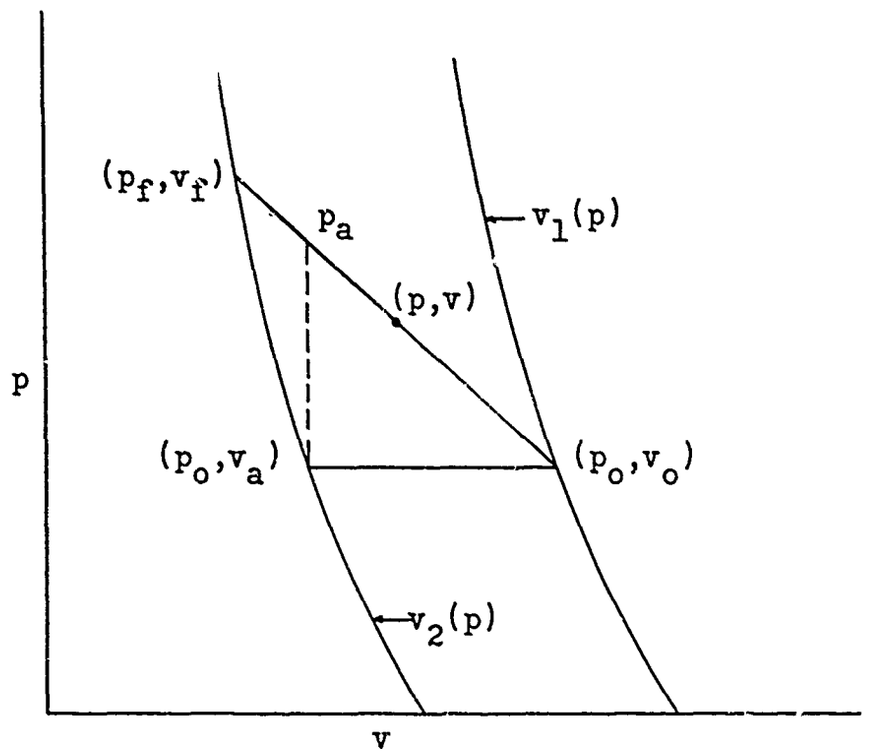

Fig. 5.17.--Path of the Permanent Regime Solution

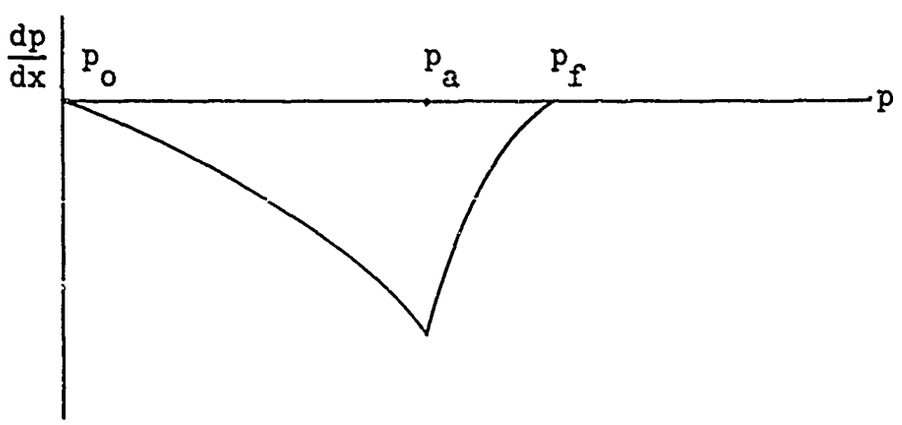

Fig. 5.18.--dp/dx for Permanent Regime Solution

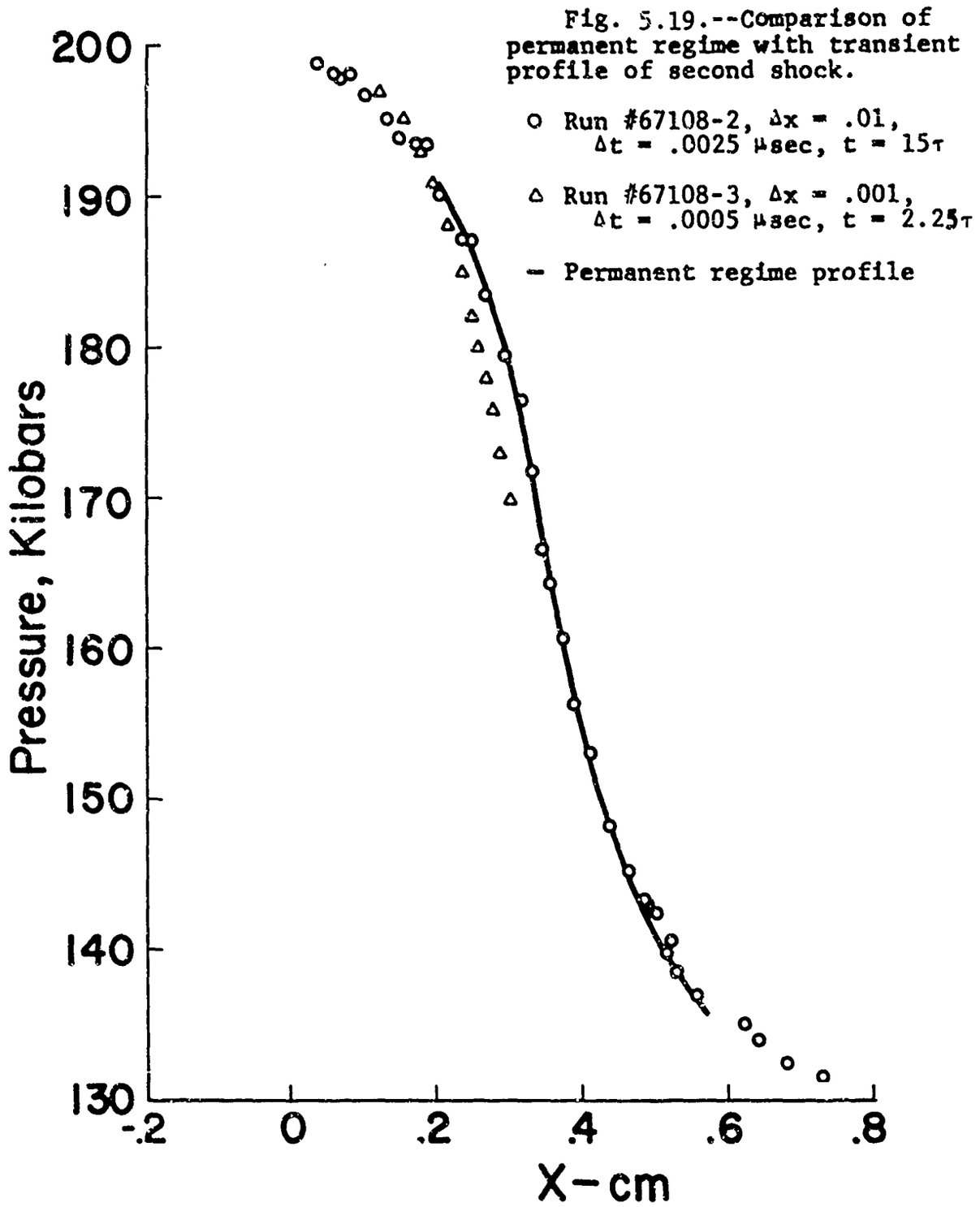

Fig. 5.19. --Comparison of Permanent Regime with Transient Profile of Second Shock.

is $\tau = 1/3$ μsec, so $\Delta x \approx 2.4\ U_{II}\tau$. Profiles obtained from the transient calculation at $t = 2.25\tau$, 15τ, 22.5τ are shown for comparison. The agreement is very good at 15τ. This agreement is additional evidence of the validity of the integration procedure for the transient case.

LITERATURE CITED

1. G. E. Duvall and G. R. Fowles. "Shock Waves," Ch. 9, Vol. 2 of High Pressure Physics and Chemistry, Academic Press, 1964. R. S. Bradley, Ed.

2. M. H. Rice, R. G. McQueen, and J. M. Walsh. "Compression of Solids by Strong Shock Waves," Solid State Physics, VI, Academic Press, 1958. F. Seitz and D. Turnbull, Eds.

3. The discussion in this section was stimulated by a conversation with Dr. Michael Cowperthwaite of Stanford Research Institute.

4. T. H. K. Barron. "Gruneisen Parameters for the Equation of State of Solids," Annals of Physics 1, 77 (Apr. 1957).

5. G. R. Fowles, Washington State University, private communication.

6. D. G. Doran. "Shock Waves in Metals," Ph.D. thesis, Washington State University, 1960.

7. George E. Duvall and Y. Horie. "Shock Induced Phase Transitions," Proceedings, Fourth Symposium on Detonation, Oct. 12-15, 1965. U.S. Naval Ordnance Laboratory, White Oak, Maryland. (U.S. Government Printing Office, 1967).

8. R. E. Duff and F. S. Minshall. Phys. Rev. 108, 1207 (1957).

9. P. W. Bridgman. Phys. Rev. 48, 893 (1935).

10. T. Takahashi and W. A. Bassett. Science, 145, 483 (1964).

11. C. B. Sclar. J. Geophys. Res. 67, 4049 (1962).

12. P. W. Bridgman. The Physics of High Pressure, G. Bell and Sons, 1958.

13. F. S. Minshall. "Dynamic Response of Iron Alloys" in Response of Metals to High Velocity Deformation, Interscience, 1961. P. G. Shewmon and V. F. Zackay, Eds.

14. S. A. Novikov et al. Soviet Physics JETP, 20, 545 (1964).

15. J. Wackerle. J. Appl. Phys. 33, 922 (1962).

16. B. A. Bilby and J. W. Christian. "The Mechanism of Phase Transformation in Metals," The Institute of Metals, London, 1956.

17. D. Turnbull. "Phase Changes," Solid State Physics, III, Academic Press, 1956. F. Seitz and D. Turnbull, Eds.

18. J. W. Christian. "Phase Transformation," Physical Metallurgy, North-Holland Publishing Co., 1965. R. W. Cahn, Ed.

19. R. Smoluchowski et al. Phase Transformations in Solids, John Wiley and Sons, 1951.

20. J. C. Fisher et al. Trans. Am. Inst. Mining Met. Engrs. 185, 691 (1949).

21. S. A. Kulin and M. Cohen. Trans. Am. Inst. Mining Met. Engrs. 188, 1139 (1950).

22. W. C. Leslie. "Deformation and Transformation Structures of Shock-Loaded Iron-Base Alloy." Paper presented at Second Intl. Symposium of Metals.

23. B. G. Koepke. "Strengthening Iron-Base Alloys by Shock Waves," ML TDR 64-282, Research Dept. of Rocketdyne, Canoga Park, California.

24. S. R. de Groot and P. Mazur. Non-Equilibrium Thermodynamics, North Holland Publishing Co., 1962, p. 23.

25. T. de Donder. L'Affinite, Gauthem-Villans, Paris, 1927.

26. J. O. Hirschfelder et al. Molecular Theory of Gases and Liquids, John Wiley and Sons, Inc., 1954, p. 709.

27. J. von Neumann and R. D. Richtmyer. J. Appl. Phys. 21, 232 (1950).

28. D. Bancroft et al. J. Appl. Phys. 27, 291 (1956).

29. H. D. Drickamer. Solid State Physics XVII, Academic Press, 1965. F. Seitz and D. Turnbull, Eds.

30. C. S. Smith. Trans. AIME 214, 574 (1958).

31. L. V. Al'tshuler et al. Soviet Physics JETP 11, 5731 (1960).

32. D. Dudley. Physics International Co., San Leandro, Calif. Private Communication.

33. L. V. Al'tshuler et al. Soviet Physics JETP 15, 65 (1962).

34. Smithsonian Physical Tables, Smithsonian Institute, 1954.

35. M. L. Wilkins. "Calculation of Elastic-Plastic Flow," Methods in Computational Physics, Academic Press, 1964. B. Alder, S. Fernbach, and M. Rotenberg, Eds.

36. R. D. Richtmyer. "Difference Methods for Initial Value Problems," Interscience, 1957, p. 227.

37. W. Band. J. Geophys. Res., 65, 695 (1960).

38. H. A. Bethe. "The Theory of Shock Waves for an Arbitrary Equation of State," S.R.D. Report No. 545 (1942).

39. H. J. McSkimin, P. Andreatch, and R. N. Thurston. J. Appl. Phys. 36, 1624-1632.

40. R. N. Thurston, McSkimin, H. J., and Andreatch, P. J. Appl. Phys. 37, 267-275.

41. F. W. Neilson, W. B. Benedick, W. P. Brooks, R. A. Graham, and G. W. Anderson. Les Ondes de Detonation (Editions du CNRS), 1961.

42. V. Gregson. Private Communication, 1963.

43. P. W. Bridgman. Collected Experimental Papers, Vol. VI, 160-3819, 1947.

44. O. L. Anderson. J. Phys. Chem. Solids 27, 547 (1966).

45. L. Knopoff. Chapter 5, High Pressure Physics and Chemistry, Academic Press. R. S. Bradley, Ed. (1963)

46. R. N. Thurston. Physical Acoustics, 1A, Academic Press. W. P. Mason, Ed. (1964).

47. W. P. Mason. Piezoelectric Crystals and Their Application to Ultrasonics, D. Van Nostrand, Inc. (1950).

48. G. R. Fowles. Thesis, Stanford, 1961.

49. G. R. Fowles. J. Appl. Phys. 32, 1475. (1961).

APPENDIX I

HEAT CAPACITY OF MIXTURE

Equation (31) of Reference (7) gives

$$C_{VM} = - T(\partial V/\partial P)_{SM} (dP/dT)^2 \tag{1}$$

where $(\partial V/\partial P)_{SM}$ is the slope of an equilibrium adiabat in the mixed phase region. Equation (16) of the same reference gives

$$(\partial V/\partial P)_{SM} = dV_1/dP - (dS_1/dT)(dT/dP)^2 - (V - V_1)(dT/dP)^2 \, d^2P/dT^2 \, . \tag{2}$$

Using the identities

$$T \, dS_1/dT = C_{V1} + T(\partial P/\partial T)_{V1} \, dV_1/dT$$

and

$$dV_1/dT = (\partial V_1/\partial T)_P + (\partial V_1/\partial P)_T \, dP/dT \, ,$$

Equations (1) and (2) can be transformed to yield

$$C_{VM} = C_{V1} - T(\partial P/\partial V_1)_T (dV_1/dT)^2 + T(V-V_1) \, d^2P/dT^2 \tag{3}$$

The first two terms of Equation (3) correspond to Equation (85) of Reference (38). The third term may be important if the state point is not near the boundary of phase I.

APPENDIX II

PROGRAM FOR CALCULATING WAVE FLOW IN ONE SPACE DIMENSION FOR PLANE, CYLINDRICAL, OR SPHERICAL GEOMETRY

A. Program Name: BURN

B. Program Description

This program is an adaptation of one written by John O. Erkman at Stanford Research Institute. It integrates the equations of flow through one space and one time dimension for arbitrary initial and boundary conditions. Integration is carried through shock fronts by means of an artificial viscosity. Initial and boundary conditions, input parameters and output statements are contained in subroutines so they may be readily altered.

Subroutine DECIDE contains the input parameters which define the problem. Comments in the Listing (Section C) should make this subroutine self-explanatory, except perhaps for the following:

S is an integer index used to label the various regions in the problem, S = 2,S1

BURN(S) is an index which defines the material in region S; for example if the geometry is spherical and the problem consists of a sphere of explosive surrounded by an Al shell, S1 = 3, BURN(2) = 1, BURN(3) = 4. Other values of BURN(S) are defined in the program listing.

ØPTIØN is an index defining the driving system for the problem. ØPTIØN = 1,2,3, or 4 for a pressure pulse applied to the left boundary.

TAU is a characteristic time parameter for the applied pressure. For its exact meaning, consult the listing of the MAIN program. It's units are microseconds.

LEFTP is in Megabars (Mb)

TQUIT, microseconds

Values of ZØN(S) and L(S) need be given for S = 2, S1.

The primary output consists of tables of values of particle velocity, pressure, etc., vs J for each time and cycle indicated in DESCRIBE.

C. Program Listing and Sample Output

```
//BURN EXEC FORTGCLG
//FORT.SYSIN DD *
C     THIS IS A ONE-DIMENSIONAL Q-CODE ADAPTED FROM ONE WRITTEN BY
C     JOHN O. ERKMAN OF SRI, WHO MODELED AFTER ONE WRITTEN BY
C     MARK WILKINS OF LRL.  AN APPROXIMATE DESCRIPTION CAN BE FOUND
C     IN "COMPUTATIONAL PHYSICS.  VOL. III," EDITED BY ALDER AND
C     FERNBACH AND ROTENBERG
C     THE PROBLEM IS SET UP IN SUBROUTINE "DECIDE."
C     THE MEANING OF KEY SYMBOLS IS DESCRIBED THERE.
      COMMON /C1ZON/ H(9),BURN(9),L(9),DX(9),S1,RHO(9)
      COMMON /C2TIME/ TIMES,CYCLE,DELT,DTN,DTMX,TLIMA(300),JCRIT,
     1  TQUIT,TAU
      COMMON /C3CTRL/ COUNTS,JSTAR,JPE,JPB,JQUIT,LAST,CYCLES
      COMMON /C4FLOW/ U(300),V(300),X(300),Q(300),P(300),E(300),QA,VN,
     1MASS(300),CSP(300)
      COMMON /C7GNRL/ ALP,OPTION,CONA,CQ,LEFTP
C
      INTEGER  H,BURN,S,S1,ZON,CYCLE,COUNTS,CYCLES,ALP,OPTION,H2,HS1,HS,
C
     1  BURNS,HS2
      REAL  L,MASS,LINEAR,LEFTP
C
      CALL DECIDE
C     THE FOLLOWING DO LOOPS ENDING AT STATEMENT 9 CALCULATE THE
C     POSITION OF THE J'TH CELL IN CM AND ITS MASS IN GRAMS.  RHO(S)=
C     DENSITY OF REGION S IN GRAMS/CC.
      DO 9 S=2,S1
      HS1=H(S-1)+1
      HS2=H(S)
      DO 9 J=HS1,HS2
      X(J+1)=X(J)+DX(S)
    9 MASS(J)=(X(J+1)**ALP-X(J)**ALP)*RHO(S)
C
C     THE VARIABLES IN THE FOLLOWING FOUR WRITE STATEMENTS HAVE BEEN
C     DEFINED IN SUBROUTINE DECIDE.
      WRITE(6,951)ALP,DELT,DTMX,CONA,CQ
      WRITE(6,952)CYCLES,COUNTS,JQUIT
  952 FORMAT('0','CYCLES',6X,'COUNTS',6X,'JQUIT'/I6,4X,I6,6X,I5)
      WRITE(6,957)S1,(BURN(S),S=2,S1)
      WRITE(6,961)TAU,LEFTP,U(1),OPTION
C
      IF (OPTION.EQ.6) CALL FLIER
      IF (OPTION.NE.6) JSTAR=5
C
      CALL WRITE1
C
      CQSQ=CQ**2
      CQSQ4=4.0*CQSQ
      LINEAR=1.0+CONA+CONA
C     "TIMES"=T, THE TIME VARIABLE, MEASURED FROM ZERO.
      TIMES=0.0
      CYCLE=0
C     "JCRIT"=NO. OF SPACE CELL FOR WHICH TLIMA(J) HAD ITS MINIMUM
C     VALUE IN THE PREVIOUS CYCLE.
      JCRIT=0
```

```
C       "LAST" IS AN INTEGER CONTROL PARAMETER WHICH DIRECTS THE
C       SUBROUTINE "WRITE" TO PERFORM A TERMINAL COMPUTATION AFTER THE
C       INTEGRATION HAS BEEN COMPLETED.
        LAST=0
C       "DTN" IS THE VALUE OF "DELT" CALCULATED IN THE CYCLE BEFORE LAST.
        DTN=DELT
        DELTI=DELT+DELT
C-----START OF TIME LOOP
C       PPEAK=MAXIMUM VALUE OF PRESSURE CALCULATED IN PREVIOUS CYCLE.
   40   PPEAK=0.0
C       TLIMB=TLIMA(JCRIT)=MINIMUM VALUE OF TLIMA(J).
        TLIMB=1.0
        TIMES=TIMES+DELT
        CYCLE=CYCLE+1
   50   J=1
        S=2
        J1=2
        JT=3
        PLEFT=0.0
C       COMMENT EVALUATE P FOR FIRST CELL AND U AND X ON LEFT BOUNDARY
        GO TO (51,52,53,54,60,60),OPTION
   51   IF(TIMES .LE. TAU) PLEFT=LEFTP
        GO TO 60
   52   IF(TIMES .LE. TAU) PLEFT=((1-TIMES/TAU)+1.0)*LEFTP
        GO TO 60
   53   PLEFT=LEFTP*EXP(-0.46*TIMES)
   54   CONTINUE
   60   IF(ALP.EQ.1)U(1)=-((P(1)+Q(1)-PLEFT)/(X(2)-X(1)))*V(1)*DELTI+U(1)
        XA=U(1)*DELT+X(1)
C-----START OF J-LOOP
   70   IF(J.GT.H(S)) S=S+1
   78   DENU=(X(JT)-X(J1))/V(J1)+(X(J1)-X(J))/V(J)
   79   U(J1)=(DELTI*(P(J)-P(J1)+Q(J)-Q(J1)))/DENU+U(J1)
   80   X(J)=XA
        XA=DELT*U(J1)+X(J1)
        IF(J .EQ. H(S1)) X(J1)=XA
        IF(ABS(U(J1)) .LT. 5.0E-5) U(J1)=0.0
        VN=(XA**ALP-X(J)**ALP)/MASS(J)
        DELU=U(J1)-U(J)
        DELX=XA-X(J)
C
C-----GET Q FOR SHOCK
C       "QA"=NEW VALUE OF ARTIFICIAL VISCOUS STRESS; Q(J) IS "OLD" VALUE.
   87   QA=-DELU*(CQSQ*ABS(DELU)+CONA*CSP(J))/VN
        IF(QA .LT. 0.0) QA=0.0
C       "TLIMA(J)=TIME PARAMETER USED IN CALCULATING THE VALUE OF DELT
C       FOR THE NEXT TIME STEP.  AT THIS POINT VN, THE NEW VALUE OF
C       SPECIFIC VOLUME, AND QA ARE AVAILABLE, SO THE INFORMATION REQUIRED
C       FOR CALCULATING PRESSURE IN CELL J,P(J),ENERGY,F(J), ETC. IS AT
C       HAND.  THESE CALCULATIONS ARE MADE IN SUBROUTINES B_EQST(S,J),
C       WHICH ARE ENTRY POINTS IN B_INIT(S).  CONTROL IS TRANSFERRED TO
C       SUBROUTINE EQST(S,J), AND FROM THIS IT IS TRANSFERRED TO THE
C       APPROPRIATE B_EQST(S,J).
        TLIMA(J)=DELX/(LINEAR*CSP(J)+CQSQ4*ABS(DELU))
        CALL EQST(S,J)
```

```
      IF(ABS(P(J)) .LE. 1.0E-5) P(J)=1.0134E-6
      V(J)=VN
      Q(J)=QA
      IF(TLIMA(J).GE.TLIMB) GO TO 129
      JCRIT=J
      TLIMB=TLIMA(J)
  129 IF(P(J)+Q(J).LE.PPEAK) GO TO 131
      PPEAK=(P(J)+Q(J))
C     "JPMAX" IS THE VALUE OF J FOR WHICH PPEAK TAKES ITS MAXIMUM VALUE.
      JPMAX=J
  131 J=J+1
      J1=J+1
      JT=J1+1
C     "JSTAR" IS A VALUE OF J AHEAD OF THE WAVE FRONT AT WHICH COMPUTING
C     STOPS PREPARATORY TO ADVANCING TIME BY ANOTHER INCREMENT.  JSTAR
C     IS ADVANCED BY UNITY WHENEVER PARTICLE VELOCITY, U(JSTAR),
C     BECOMES NON-NEGLIGIBLE.
      IF(J.LE.JSTAR+1) GO TO 70
C-----TEST TO ADVANCE JSTAR
      IF(ABS(U(JSTAR+1)).GT.1.0E-5) JSTAR=JSTAR+1
      IF((CYCLE.EQ.CYCLE ).OR.(TIMES.GE.TQUIT).OR.(J.EQ.JQUIT))GO TO 169
      IF(CYCLE.GT.10)GO    20
C     TO CHANGE FREQUENCY OF PRINT-OUT, A STATEMENT CAN BE INSERTED
C     HERE:  "IF (CYCLE.GT. K) COUNTS=MN" WHERE "K" AND "MN" ARE
C     INTEGERS TO BE CHOSEN BY THE PROGRAMMER.
      IF(MOD(CYCLE,COUNTS).NE.0) GO TO 180
      GO TO 170
  169 LAST=1
  170 JPB=1
      JPE=JSTAR+2
      CALL WRITE
  180 DTNH1=0.6*TLIMB
      IF(DTNH1/DELT.GT.1.1) DTNH1=1.1*DELT
      IF(DTNH1.GT.DTMX) DTNH1=DTMX
      DTN=DELT
      DELT=DTNH1
      DELTI=DTN+DELT
      GO TO 40
C
  951 FORMAT(1H1,6X,3HALP,9X,4HDELT,11X,4HDTMX,11X,4HCONA,12X,2HCQ/7X,I1
     -,4F15.6)
  957 FORMAT(1H0,8X,2HS1,5X,8HBURN(1)../8X,I2,9X,9I5/2X)
  961 FORMAT(1H0,5X,3HTAU,16X,5HLEFTP,14X,4HU(1),15X,6HOPTION/3E19.8,I8)
      END
      SUBROUTINE DECIDE
C
      COMMON /C1ZON/ H(9),BURN(9),L(9),DX(9),S1,RHO(9)
      COMMON /C2TIME/ TIMES,CYCLE,DELT,DTN,DTMX,TLIMA(300),JCRIT,
     1  TQUIT,TAU
      COMMON /C3CTRL/ COUNTS,JSTAR,JPE,JPB,JQUIT,LAST,CYCLES
      COMMON /C4FLOW/ U(300),V(300),X(300),Q(300),P(300),E(300),QA,VN,
     1 MASS(300),CSP(300)
      COMMON /C7GNRL/ ALP,OPTION,CONA,CQ,LEFTP
      DIMENSION ZON(9)
C
```

```
      INTEGER  H,BURN,S,S1,ZON,CYCLE,COUNTS,CYCLES,ALP,OPTION,H2,HS1,HS,
     1  BURNS,HS2
      REAL  L,MASS,LINEAR,LEFTP
C
C     CHOOSE GEOMETRY.  ALP IS AN INTEGER LABEL WHICH IS TO BE SET
C     ACCORDING TO THE GEOMETRY OF THE PROBLEM.
C     X IS THE EULERIAN SPACE COORDINATE.  THE INITIAL VALUE AT T=0
C     OF THE LEFT BOUNDARY OF CELL 1 IS SET HERE.  THE POSITIONS OF
C     OTHER CELL BOUNDARIES ARE CALCULATED IN MAIN FROM THE NUMBER OF
C     ZONES AND THE DIMENSIONS OF THE PROBLEM.
C     FOR CYLINDRICAL AND SPHERICAL PROBLEMS, LEFT BOUNDARY IS
C     INTERPRETED AS INNER BOUNDARY.
C         ALP = 1 FOR PLANE GEOMETRY
C         ALP = 2 FOR CYLENDRICAL GEOMETRY
C         ALP = 3 FOR SPHERICAL GEOMETRY
      ALP=1
C-----CHOOSE COORDINATES OF FIRST CELL
      X(1)=0.0
C-----NUMBER OF REGIONS PLUS ONE (NOT TO EXCEED 9)
C     THIS PROGRAM CAN BE RUN WITH SEVERAL REGIONS OF DIFFERENT
C     MATERIALS.  THE NUMBER OF SUCH REGIONS IS DENOTED BY AN INTEGER
C     S1-1.  THIS PECULIAR CONVENTION ARISES BECAUSE OF A CHARACTERISTIC
C     OF FORTRAN--ZERO INDICES ARE NOT ALLOWED.  EACH DISTINCT REGION IS
C     DENOTED BY AN INTEGER LABEL S.  S=2 IS THE LEFT-MOST REGION, S=3
C     THE NEXT TO THE RIGHT, ETC. UP TO S1.
C     EACH REGION IS DIVIDED INTO A NUMBER OF SPACE ZONES OR CELLS,
C     ZON(S).  THE NUMBER OF CELLS UP TO AND INCLUDING REGION S
C     (STARTING WITH THE LEFTMOST REGION) IS H(S)=SUM(ZON(K)),
C     K=2 TO S, INCLUSIVE.
      S1=2
C ----MATERIAL IN REGIONS
C     "BURN(S)" IS AN INTEGER LABEL WHICH DEFINES THE MATERIAL OF
C     REGION S.
C         BURN(S) = 1 FOR EXPLOSIVE
C         BURN(S) = 2 FOR VOID
C         BURN(S) = 3 FOR LIQUID
C         BURN(S) = 4 FOR SOLID
C         BURN(S) = 5 FOR PHASE TRANSITION
      BURN(2)=5
C-----SET OPTION
C     "OPTION" IS AN INTEGER LABEL WHICH DESCRIBES THE TYPE OF PROBLEM
C     TO BE SOLVED.  IF OPTION=1,2, OR 3, THE PROBLEM IS ONE IN WHICH
C     A SPECIFIED PRESSURE IS APPLIED TO THE LEFT HAND BOUNDARY.  IF
C     OPTION=5, AN EXPLOSIVE REGION IS INCLUDED AND ITS DETONATION
C     PROVIDES THE DRIVING FORCE.  OPTION=6 MEANS THAT THE FIRST REGION
C     (S=2) IS A FLYER PLATE WHICH HAS JUST COLLIDED WITH THE SECOND
C     REGION (S=3) AT THE START OF THE PROBLEM.  WHEN THIS HAPPENS,
C     EACH CELL IN REGION 1 (S=2) IS GIVEN THE FLYER PLATE VELOCITY
C     U(1), EXCEPT THE ONE ADJACENT TO REGION 2(S=3) THIS CELL AND THE
C     FIRST CELL IN REGION 2 (S=3) ARE GIVEN VELOCITIES U(1)/2 FOR
C     SMOOTHING PURPOSES.  WHEN OPTION=1, THE TIME DURATION, TAU, OF
C     THE APPLIED PRESSURE MUST BE SET.  FOR A CONSTANT PRESSURE APPLIED
C     AT T=0, SET TAU EQUAL TO A LARGE NUMBER, SAY 500 (MICROSECONDS).
C     FOR OPTION=2, TIME TAU IS THE TIME AT WHICH THE APPLIED PRESSURE
C     EQUALS ZERO IN A LINEAR RAMP.  OPTION=3 HAS A BUILT-IN TIME
```

```
C     CONSTANT.  THE PEAK APPLIED PRESSURE IN EACH CASE IS "LEFTP" IN
C     MEGABARS.
C         OPTION = 1 GIVES SQUARE PULSE
C         OPTION = 2 GIVES LINEAR PULSE
C         OPTION = 3 GIVES EXPONENTIAL
C         OPTION = 4 UNASSIGNED
C         OPTION = 5 GIVES NO PULSE (FOR EXPLOSION)
C         OPTION = 6 GIVES NO PULSE (FOR FLYER PLATE)
      PTION=1
C-----IF OPTION = 1 OR 2, SET TAU
      TAU=500.0
C-----IF OPTION = 6, SET U(1) (FOR FLYER PLATE)
      U(1)=0.0
C-----IF OPTION = 1,2, OR 3, SET LEFTP (PRESSURE ON LEFT BOUNDARY)
      LEFTP=0.200
C-----VISCOSITY COEFFICIENT (CQ FOR QUADRATIC AND CONA FOR LINEAR)
      CONA=0.1
      CQ=2.0
C-----LENGTH OF RUN MAY BE DETERMINED BY SETTING ANY OR ALL OF NEXT
C     WHEN CYCLE=CYCLES OR TIMES=TQUIT OR J=JQUIT, COMPUTATION WILL
C     STOP, WHICH EVER OCCURS FIRST.
C     J IS THE INTEGER LABEL OF THE SPACE CELLS.  J=1 AT THE LEFTMOST
C     CELL OF THE LEFTMOST REGION AND RUNS TO H(S1), THE RIGHTMOST CELL
C     OF THE RIGHTMOST REGION.
C              CYCLES= NUMBER OF INCREMENTS IN TIME
C         TQUIT (PROPAGATION TIME)
C         JQUIT (NUMBER OF LAST CELL)
      CYCLES=100
      TQUIT=260
      JQUIT=25
      JQUIT=250
C-----THE NUMBER OF ZONES IN REGION K IS ZON(K)
      ZON(2) =50
C-----THE THICKNESS OF REGION K IN CM. IS L(K)
      L(2)=5.0
C-----DELT IS STARTING VALUE FOR DELTAT
C     "DELTAT" IS THE TIME-INCREMENT FROM ONE CYCLE TO THE NEXT,
C     MICROSECONDS.
      DELT=.05
C-----DTMX IS UPPER LIMIT FOR DELTAT
      DTMX=.05
C-----PRINTOUTS OF CYCLES IS MODULO COUNTS
C     "COUNTS" CONTROLS PRINTING,  IF COUNTS=5, THE STANDARD FLOW
C     VARIABLES U,P,Q,E,V, ETC. ARE PRINTED OUT EVERY FIFTH CYCLE, ETC.
C     FREQUENTLY "COUNTS" IS SET =1 IN "DECIDE", THEN AFTER THE FIRST
C     FEW CYCLES INCREMENTED TO 10 OR 20.
      COUNTS=1
C     H(S) IS AN INTEGER LABEL EQUAL TO THE NUMBER OF SPACE CELLS TO
C     THE LEFT OF AND INCLUDING REGION S.
      H(1) = 0
      DO 12 S=2,S1
      DX(S) = L(S)/FLOAT(ZON(S))
   12 H(S)=H(S-1) + ZON(S)
C-----CALL ROUTINES TO SET INITIAL REGIONS
C     AT THIS POINT CONTROL IS TRANSFERRED TO B_INIT(S) FOR S=2 TO S1,
```

```
C     WHERE _ IS AN INTEGER FROM 1 TO 5, CORRESPONDING TO THE VALUE
C     OF BURN(S).  FOR EXAMPLE IF S1=4 AND BURN(2)=1, BURN(3)=4, AND
C     BURN(4)=3, THEN B1INIT(2), B4INIT(3), B3INIT(4) ARE CALLED IN
C     TURN: I.E., THE NEXT THREE STATEMENTS WOULD BE:  "CALL B1INIT(2)",
C     "CALL B4INIT(3)", "CALL B3INIT(4)".
      CALL B5INIT(2)
C
      RETURN
  102 FORMAT (10I4)
  906 FORMAT(23I3)
  907 FORMAT(7(14F5.2/))
      END
      SUBROUTINE EQST(S,J)
C
      COMMON /C1ZON/ H(9),BURN(9),L(9),DX(9),S1,RHO(9)
      COMMON /C2TIME/ TIMES,CYCLE,DELT,DTN,DTMX,TLIMA(300),JCRIT,
     1  TQUIT,TAU
      COMMON /C4FLOW/ U(300),V(300),X(300),Q(300),P(300),E(300),QA,VN,
     1 MASS(300),CSP(300)
C
      INTEGER  H,BURN,S,S1,ZON,CYCLE,COUNTS,CYCLES,ALP,OPTION,H2,HS1,HS,
     1  BURNS,HS2
C
      BURNS=BURN(S)
      GO TO (101,102,103,104,105,106,107,108,109),BURNS
  101 CALL B1EQST(S,J)
  102 RETURN
  103 CALL B3EQST(S,J)
      RETURN
  104 CALL B4EQST(S,J)
      RETURN
  105 CALL B5EQST(S,J)
      RETURN
  106 RETURN
  107 RETURN
  108 RETURN
  109 RETURN
      END
      SUBROUTINE FLIER
C
      COMMON /C1ZON/ H(9),BURN(9),L(9),DX(9),S1,RHO(9)
      COMMON /C3CTRL/ COUNTS,JSTAR,JPE,JPB,JQUIT,LAST,CYCLES
      COMMON /C4FLOW/ U(300),V(300),X(300),Q(300),P(300),E(300),QA,VN,
     1 MASS(300),CSP(300)
C
      INTEGER  H,BURN,S,S1,ZON,CYCLE,COUNTS,CYCLES,ALP,OPTION,H2,HS1,HS,
     1  BURNS,HS2
C
      REAL  L,MASS,LINEAR,LEFTP
C
      JSTAR=H(2)+2
      H2=H(2)
      DO 43 J=1,H2
   43 U(J+1)=U(1)
      U(H2+1)=0.5*U(H2+1)
```

```
      RETURN
      END
      SUBROUTINE B1INIT (S)
C     THIS SUBROUTINE IS A DUMMY WHICH ALLOWS FOR FUTURE EXPANSION
      GO TO 12
      ENTRY B1EQST(S,J)
      GO TO 101
   12 CONTINUE
  101 CONTINUE
      RETURN
      END
      SUBROUTINE B3INIT (S)
C     THIS SUBROUTINE IS A DUMMY WHICH ALLOWS FOR FUTURE EXPANSION
      GO TO 14
      ENTRY B3EQST(S,J)
      GO TO 121
   14 CONTINUE
  121 CONTINUE
      RETURN
      END
      SUBROUTINE B4INIT (S)
C     THIS SUBROUTINE IS A DUMMY WHICH ALLOWS FOR FUTURE EXPANSION
      GO TO 13
      ENTRY B4EQST(S,J)
      GO TO 90
   13 CONTINUE
   90 CONTINUE
      RETURN
      END
      SUBROUTINE B5INIT(S)
C     THIS SUBROUTINE IS WRITTEN SPECIFICALLY FOR IRON WITH A SHOCK-
C     INDUCED PHASE TRANSITION.
C     THE PARAMETERS ARE DEFINED IN APPENDIX II OF "EQUATION OF STATE
C     IN SOLIDS," BY G. E. DUVALL, G. R. FOWLES, AND Y. HORIE, SUMMARY
C     REPORT ON CONTRACT NO. DA-04-200-AMC-1702(X), BALLISTICS RESEARCH
C     LABORATORY, ABERDEEN PROVING GROUND, MD., FEB., 1967.
C
      COMMON /C1ZON/ H(9),BURN(9),L(9),DX(9),S1,RHO(9)
      COMMON /C2TIME/ TIMES,CYCLE,DELT,DTN,DTMX,TLIMA(300),JCRIT,
     1  TQUIT,TAU
      COMMON /C4FLOW/ U(300),V(300),X(300),Q(300),P(300),E(300),QA,VN,
     1 MASS(300),CSP(300)
      COMMON /C5THER/ TMP(300),ENT(300)
      COMMON /C6TEMP/ ET,PT
      COMMON /B5DATA/ VO(9),A1,A2,A3,DV(9),TAUO,NSA(300),PM,GAMM1(9),
     1  FRACT2(300),V1(300),XEQ(300),VP,V2
C     VP = SPECIFIC VOLUME AT WHICH HUGONIOT INTERSECTS PHASE BDRY
C
      INTEGER  H,BURN,S,S1,ZON,CYCLE,COUNTS,CYCLES,ALP,OPTION,H2,HS1,HS,
     1  BURNS,HS2
      REAL  L,M,LINEAR,LEFTP
C
      GO TO 14
      ENTRY B5EQST(S,J)
      GO TO 121
```

```
C
C  ENTRY POINT TO INITIALIZE BURN 5*************************************
C
C
   14 RHO(S)=7.84
      A1=1.667
      A2=3.4
      A3=0.0
      DV(S)=-.004
      PM=.130
      CV1=.45E-05
      CVMIX=.46E-05
      GAMM1(S)=1.6
      EO=0.0
      TO=300.0
      DPDTMX=-6.5E-05
      TAUO=3.0
C
      VO(S)=1.0/RHO(S)
      VP=VO(S)/(1.0+(-A1+SQRT(A1**2.+4.0*A2*PM))/(2.0*A2))
      V2=VP+DV(S)
      WRITE(6,960) RHO(S),A1,A2,A3,DV(S),PM,CV1,DX(S),CVMIX,GAMM1(S),EO,
     1 TO,DPDTMX,TAUO,H(S),L(S)
      CSPS=.5
      HS1=(H(S-1)+1)
      HS2=H(S)+2
      DO 39 J=HS1,HS2
      V(J)=VO(S)
   39 U(J+1)=0.0
      Q(J)=0.0
      P(J)=1.0134E-6
      TLIMA(J)=DELT
      CSP(J)=CSPS
      V1(J)=VO(S)
      FRACT2(J)=0.0
      E(J)=0.0
      ENT(J)=0.0
      TMP(J)=TO
      NSA(J)=1
      XEQ(J)=0.0
   39 CONTINUE
      RETURN
C
C  ENTRY POINT TO SET EQUATIONS OF STATE FOR BURN5*********************
C
  121 NSW=NSA(J)
      GO TO (220,221),NSW
C-----MATERIAL IS IN PHASE 1
  220 ETAM1=(VO(S)/VN)-1.0
      PT=A1*ETAM1+A2*ETAM1**2
      CSP(J)=(A1*VO(S)+2.*A2*VO(S)*(VO(S)/VN-1.)+3.*A3*VO(S)*(VO(S)/VN-
     1 1.)**2.)**.5
      ET=E(J)-0.5*(P(J)+PT+QA+Q(J))*(VN-V(J))
      IF(ABS(PT).LT.1.0E-5)PT=0.0
      IF(PT.GE.PM)CALLZMIX(S,J)
```

```
      P(J)=PT
      E(J)=ET
      RETURN
  222 CALL ZMIX(S,J)
      E(J)=ET
      P(J)=PT
      RETURN
C
  960 FORMAT(1H0,5X,3HRHO,12X,2HA1,12X,2HA2,12X,2HA3,12X,2HDV,12X,2HPM,
     1 11X,3HCV1,12X,5HDX(S),/1X,8E14.6,/1H0,4X,5HCVMIX,9X,5HGAMM1,11X,
     2 2HEO,12X,2HTO,10X,6HDPDTMX,11X,4HTAUO,11X,4HH(S),11X,4HL(S),/
     3 6F14.6,4X,I7,3X,E14.6)
      END
      SUBROUTINE ZMIX(S,J)
C
C     THIS SUBROUTINE SUITABLE FOR COMPRESSION PHASE ONLY
C
      COMMON /C1ZON/ H(9),BURN(9),L(9),DX(9),S1,RHO(9)
      COMMON /C2TIME/ TIMES,CYCLE,DELT,DTN,DTMX,TLIMA(300),JCRIT,
     1  TQUIT,TAU
      COMMON /C4FLOW/ U(300),V(300),X(300),Q(300),P(300),E(300),QA,VN,
     1 MASS(300),CSP(300)
      COMMON /C6TEMP/ ET,PT
      COMMON /B5DATA/ VO(9),A1,A2,A3,DV(9),TAUO,NSA(300),PM,GAMM1(9),
     1  FRACT2(300),V1(300),XEQ(300),VP,V2
C
      INTEGER  H,BURN,S,S1,ZON,CYCLE,COUNTS,CYCLES,ALP,OPTION,H2,HS1,HS,
     1  BURNS,HS2
      REAL  L,MASS,LINEAR,LEFTP
C
C
      NSA(J)=2
      XO=FRACT2(J)
      XEQO=XEQ(J)
      CA=TAUO*DELT
      IF(VN.GT.VP) GO TO 2
      IF (VN.GT.V2) GO TO 3
      XEQN=1.0
      GO TO 6
    2 XEQN=0.0
      GO TO 6
    3 XEQN=1.0+(VN-V2)/DV(S)
    6 CONTINUE
      XN=(XO*(1.0-CA/2.0)+0.5*(XEQO+XEQN)*CA)/(1.+CA/2.0)
      IF(XN.LT.0.0) XN=0.0
      VT= VN-XN*DV(S)
      EMU1=(VO(S)/VT)-1.0
      PT=A1*EMU1+A2*EMU1**2.
      CSP(J)=(A1*VO(S)+2.*A2*VO(S)*(VO(S)/VN-1.)+3.*A3*VO(S)*(VO(S)/VN-
     1 1.)**2.)**.5
      ET=E(J)-0.5*(PT+P(J)+QA+Q(J))*(VN-V(J))
      V1(J)=VT
      FRACT2(J)=XN
      XEQ(J)=XEQN
      RETURN
```

```
      END
      SUBROUTINE WRITE
      COMMON /C1ZON/ H(9),BURN(9),L(9),DX(9),S1,RHO(9)
      COMMON /C2TIME/ TIMES,CYCLE,DELT,DTN,DTMX,TLIMA(300),JCRIT,
     1  TQUIT,TAU
      COMMON /C3CTRL/ COUNTS,JSTAR,JPE,JPB,JQUIT,LAST,CYCLES
      COMMON /C4FLOW/ U(300),V(300),X(300),Q(300),P(300),E(300),QA,VN,
     1 MASS(300),CSP(300)
      COMMON /C5THER/ TMP(300),ENT(300)
      COMMON /C7GNRL/ ALP,OPTION,CONA,CQ,LEFTP
      COMMON /B5DATA/ VO(9),A1,A2,A3,DV(9),TAUO,NSA(300),PM,GAMM1(9),
     1  FRACT2(300),V1(300),XEQ(300),VP,V2
C
      INTEGER  H,BURN,S,S1,ZON,CYCLE,COUNTS,CYCLES,ALP,OPTION,H2,HS1,HS,
     1  BURNS,HS2
C
      REAL  L,MASS,LINEAR,LEFTP
C
      GO TO 14
      ENTRY WRITE1
      GO TO 121
   14 WRITE(6,302)
      WRITE(6,304)TIMES,DELT,DTN,CYCLE,JCRIT
      WRITE(6,306)
      S=2
      IF( JPB.EQ.1 .AND. JSTAR.GT.H(2)+10 ) JPB=H(2)
      DO 330 J=JPB,JPE
      IF(J.GT.H(S)) S=S+1
  310 WRITE(6,318)J,U(J),V(J),P(J),E(J),Q(J),FRACT2(J),V1(J),X(J),TMP(J)
     1,TLIMA(J)
  330 CONTINUE
C-----NEXT TWO STATEMENTS (COMMENTS) ARE TO BE USED IF GRAPHING IS DESIRED
      CALL MANUAL(1.25*LEFTP,0.)
      CALL GRAPH1(P,JPE)
      IF(LAST.EQ.1)CALL EXIT
      RETURN
  121 WRITE(6,862)
      DO 46 J =1,2
   46 WRITE(6,962)J,U(J),V(J),P(J),E(J),Q(J),FRACT2(J),V1(J),X(J),      T
     -MP(J),TLIMA(J)
      DO 57 S=2,S1
      HS1=H(S)-1
      HS2=H(S)+2
      DO 57 J=HS1,HS2
   57 WRITE(6,962)J,U(J),V(J),P(J),E(J),Q(J),FRACT2(J),V1(J),X(J),      T
     -MP(J),TLIMA(J)
      RETURN
  302 FORMAT(1H1)
  304 FORMAT(10X,6HTIME= ,E14.8,4X,6HDELT= ,E14.8,4X,5HDTN= ,E14.8,4X,7H
     -CYCLE= ,I5,4X,7HJCRIT= ,I5/5X)
  306 FORMAT(2X,1HJ,6X,1HU,9X,1HV,9X,1HP,9X,1HE,9X,1HQ,7X,6HFRACT2,6X,
     1   2HV1,9X,1HX,9X,3HTMP,6X,5HTLIMA//5X)
  318 FORMAT(I4,8F10.6,F7.1,E13.5)
  962 FORMAT(2X,1HJ,6X,1HU,9X,1HV,9X,1HP,9X,1HE,9X,1HQ,7X,6HFRACT2,6X,
     1   2HV1,9X,1HX,9X,3HTMP,6X,5HTLIMA//2X)
```

```
962 FORMAT(I4,8F10.6,F7.1,E13.5)
  3 FORMAT(1H0,2X,6HTIMF= ,E14.8,4X,5HUFS= ,F14.8,4X,5HXFS= ,E14.8,4X,
   -7HCYCLE= ,I4,3X,7HJPMAX= ,I4,3X,7HJCRIT= ,I4/2X)
    END
    SUBROUTINE GRAPH4(A,B,C,D,N)
C
    COMMON /C3CTRL/ COUNTS,JSTAR,JPE,JPB,JQUIT,LAST,CYCLES
    COMMON /C4FLOW/ U(300),V(300),X(300),Q(300),P(300),E(300),QA,VN,
   1 MASS(300),CSP(300)
    COMMON /C7GNRL/ ALP,OPTION,CONA,CQ,LEFTP
C
    REAL  L,MASS,LINEAR,LEFTP
    DIMENSION A(N), B(N), C(N), D(N), POINT(4), GRAPH(122)
    DATA POINT/1HA,1HB,1HC,1HD/
    DATA MSWTCH,BLANK,PERIOD/0,1H ,1H./
    M=4
    IF(MSWTCH.EQ.1) GO TO 50
    AMAX=D(1)
    AMIN=D(1)
    DO 1 I=1,N
    IF(AMAX.LT.D(I)) AMAX=D(I)
  1 IF(AMIN.GT.D(I)) AMIN=D(I)
    GO TO 2
    ENTRY GRAPH3(A,B,C,N)
    M=3
    IF(MSWTCH.EQ.1) GO TO 50
    AMAX=C(1)
    AMIN=C(1)
  2 DO 3 I=1,N
    IF(AMAX.LT.C(I)) AMAX=C(I)
  3 IF(AMIN.GT.C(I)) AMIN=C(I)
    GO TO 4
    ENTRY GRAPH2(A,B,N)
    M=2
    IF(MSWTCH.EQ.1) GO TO 50
    AMAX=B(1)
    AMIN=B(1)
  4 DO 5 I=1,N
    IF(AMAX.LT.B(I)) AMAX=B(I)
  5 IF(AMIN.GT.B(I)) AMIN=B(I)
    GO TO 6
    ENTRY GRAPH1(A,N)
    M=1
    IF(MSWTCH.EQ.1) GO TO 50
    AMAX=A(1)
    AMIN=A(1)
  6 DO 7 I=1,N
    IF(AMAX.LT.A(I)) AMAX=A(I)
  7 IF(AMIN.GT.A(I)) AMIN=A(I)
 50 SC=(AMAX-AMIN)/120.
    WRITE(6,100) AMIN,AMAX,SC,(PERIOD,I=1,121)
100 FORMAT(1H1,17HRANGE OF GRAPH IS,F15.8,8H THROUGH,F15.8//1X,17HSCAL
   1ING FACTOR IS,F15.8//105X,21H111111111111111111111/15X,111H1111111
   211122222222223333333333444444444455555555556666666666777777777888
   388888889999999999000000000011111111112/6X,120H123456789012345678901
```

```
     4123456789012345678901234567890123456789012345678901234567890123456
     5789012345678901234567890123456789 0/5X,121A1)
      DO 8 I=1,N
      DO 17 J=1,121
   17 GRAPH(J)=BLANK
      GO TO (9,10,11,12),M
   12 K4=(D(I)-AMIN)/SC+1.
      IF(K4.LT.0.OR.K4.GT.122) K4=122
   11 K3=(C(I)-AMIN)/SC+1.
      IF(K3.LT.0.OR.K3.GT.122) K3=122
   10 K2=(B(I)-AMIN)/SC+1.
      IF(K2.LT.0.OR.K2.GT.122) K2=122
    9 K1=(A(I)-AMIN)/SC+1.
      IF(K1.LT.0.OR.K1.GT.122) K1=122
      GO TO (13,14,15,16),M
   16 GRAPH(K4)=POINT(4)
   15 GRAPH(K3)=POINT(3)
   14 GRAPH(K2)=POINT(2)
   13 GRAPH(K1)=POINT(1)
      IF(GRAPH(121).NE.BLANK) GRAPH(120)=GRAPH(121)
      WRITE(6,101) I,(GRAPH(I1),I1=1,120)
  101 FORMAT(2X,I3,1H.,120A1)
    8 CONTINUE
      MSWICH=0
      RETURN
      ENTRY MANUAL(A1,A2)
      AMAX=A1
      AMIN=A2
      MSWTCH=1
      RETURN
      END
/*
/*
```

For numerical output of this problem, refer to Vol. II of this report filed in the Document Library of Ballistics Research Laboratories.

D. List of Labels

DECIDE

DX(S) = Eulerian space interval in region S at t = 0

= L(S)/ZØN(S)

H(S) = no. of cells from left boundary through region S

$$= \sum_{L=2}^{S} \text{ZØN}(L)$$

B5INIT(S)

RHØ(S) = density at zero pressure in region S

A1,A2,A3 = coefficients in Eq. (4.5)

DV(S) = $v_2(p,T) - v_1(p,T)$

PM = pressure at which the Hugoniot in phase I intercepts the phase boundary

CV1 = C_{v1}

CVMIX = $C_{v,m}$

GAMM1(S) = Γ

EØ = internal energy at the foot of the Hugoniot

TØ = T_o

DPDTMX = $(\partial p/\partial T)_{v,m}$

TAUØ = $1/\tau$, Eq. (5.11)

VP = specific volume in phase I at p = PM = $v_1(pM,T)$

V2 = $v_2(pM,T)$

CSPS = starting value for sound speed

J = index for space grid

V(J) = v_j

U(J) = U_j

Q(J) = q_j

P(J) = p_j

TLIMA(J) = value of Δt_j for next time step

CSP(J) = sound speed in cell J

E(J) = E_j

ENT(J) = s_j

TMP(J) = T_j

NSA(J) = switching index

= 1, phase I

= 2, mixed phase

= 3, phase II

MAIN

X(J) = x_j (Fig. 5.2)

MASS(J) = mass of cell J

JSTAR = cell label just ahead of shock front at which computation stops for each time cycle

TIMES = t

CYCLE = number of times t has been incremented

JCRIT = value of J for which TLIMA is minimum

LAST = switching index for halting program after writing last output.

PPEAK = maximum computed pressure in each cycle

TLIMB = TLIMA(JCRIT)

PLEFT = pressure applied to left boundary

DFNU = mass in cell J+1

XA = $x(t + \Delta t)$

VN = $v(t + \Delta t)$

QA = $Q(t + \Delta t)$

JPMAX = value of J at which p is maximum

ZMIX

FRACT(J) = α_j

XEQ(J) = α_j^{eq}

V1(J) = $v_{1j}(p,T)$

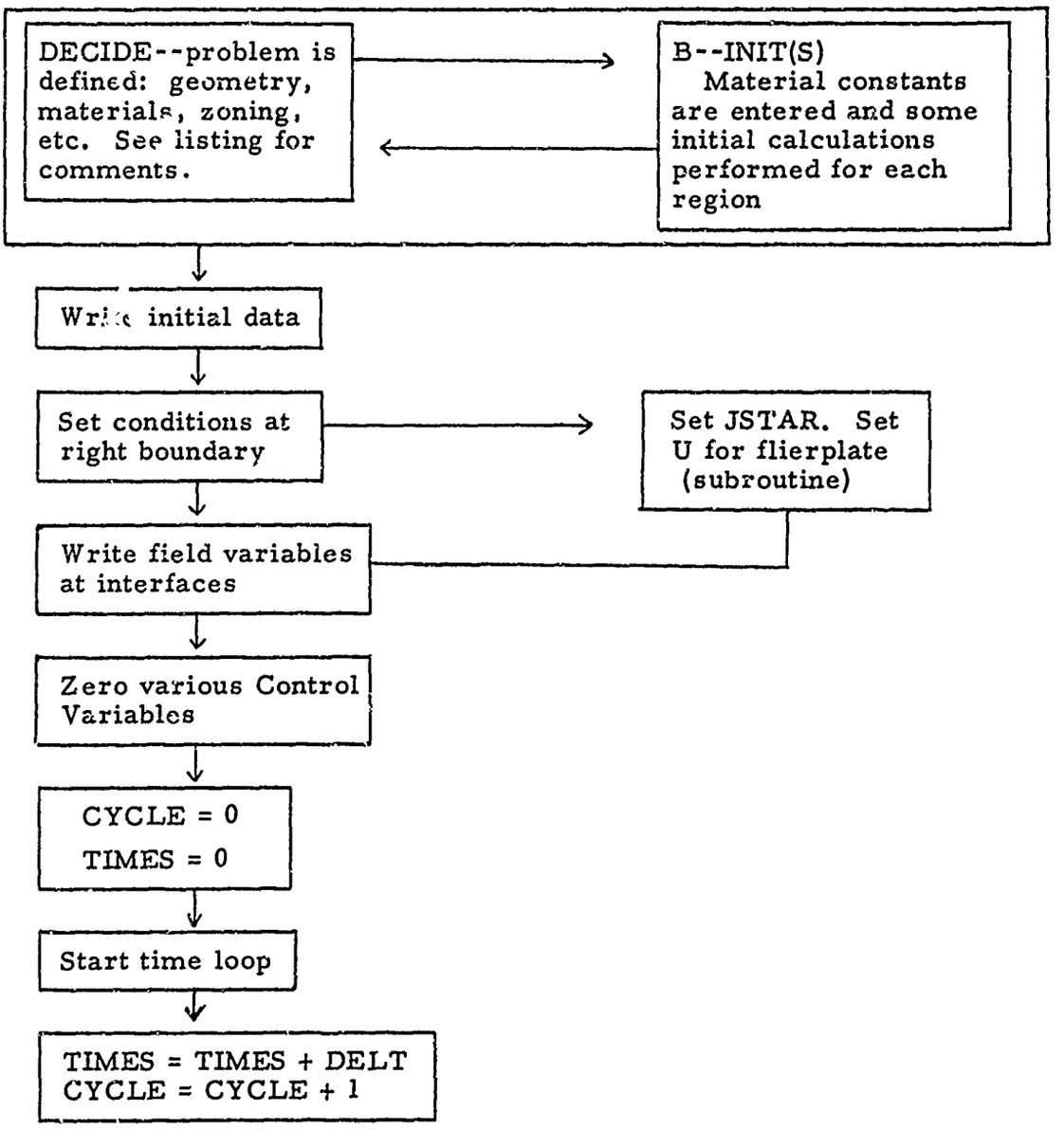

Fig. 1.--FLOW CHART FOR BURN

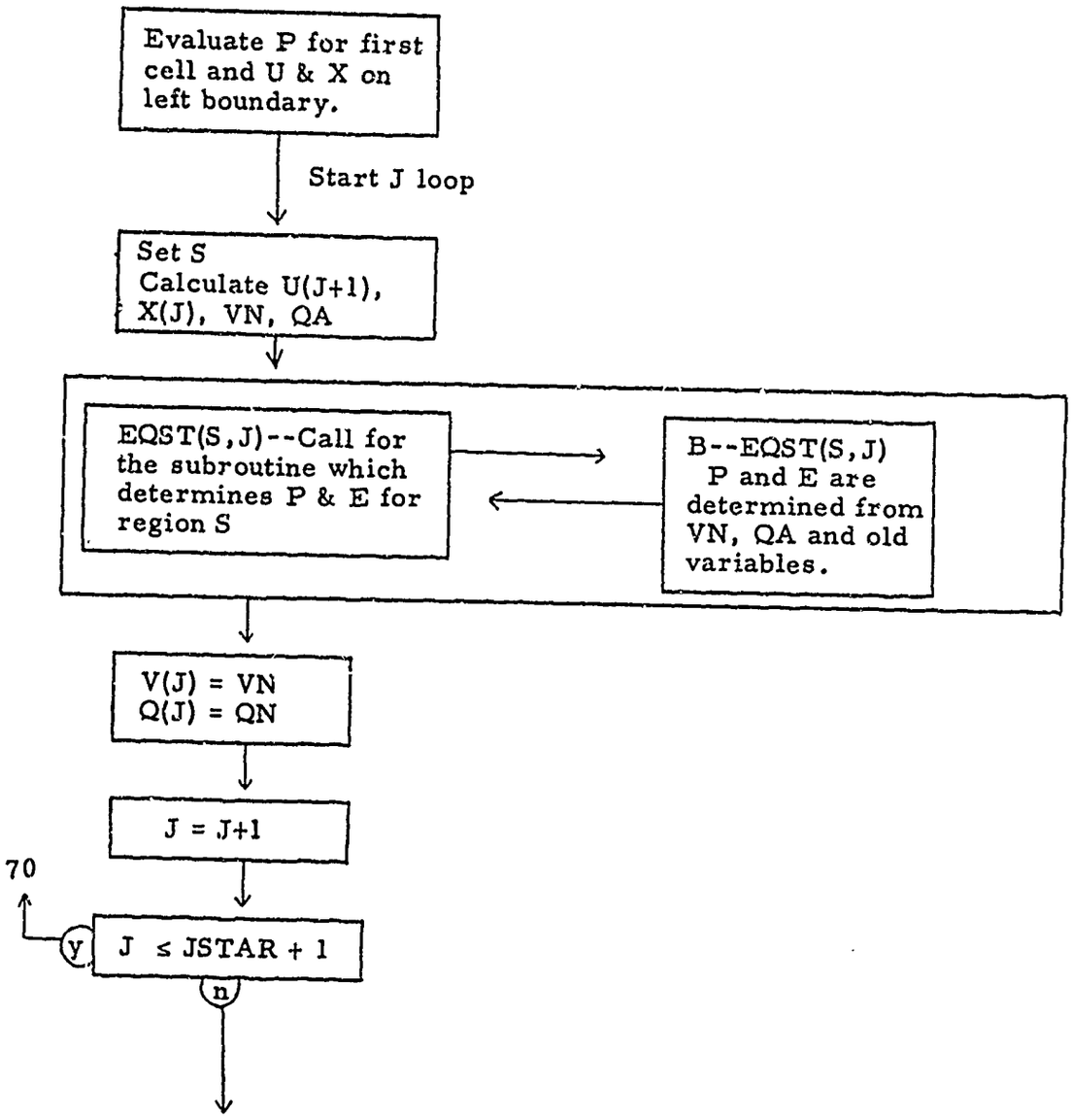
Evaluate P for first cell and U & X on left boundary.
Start J loop
Set S
Calculate U(J+1), X(J), VN, QA
EQST(S,J)--Call for the subroutine which determines P & E for region S
B--EQST(S,J)
P and E are determined from VN, QA and old variables.
V(J) = VN
Q(J) = QN
J = J+1
70
y
J ≤ JSTAR + 1
n

Fig. 1. (b)

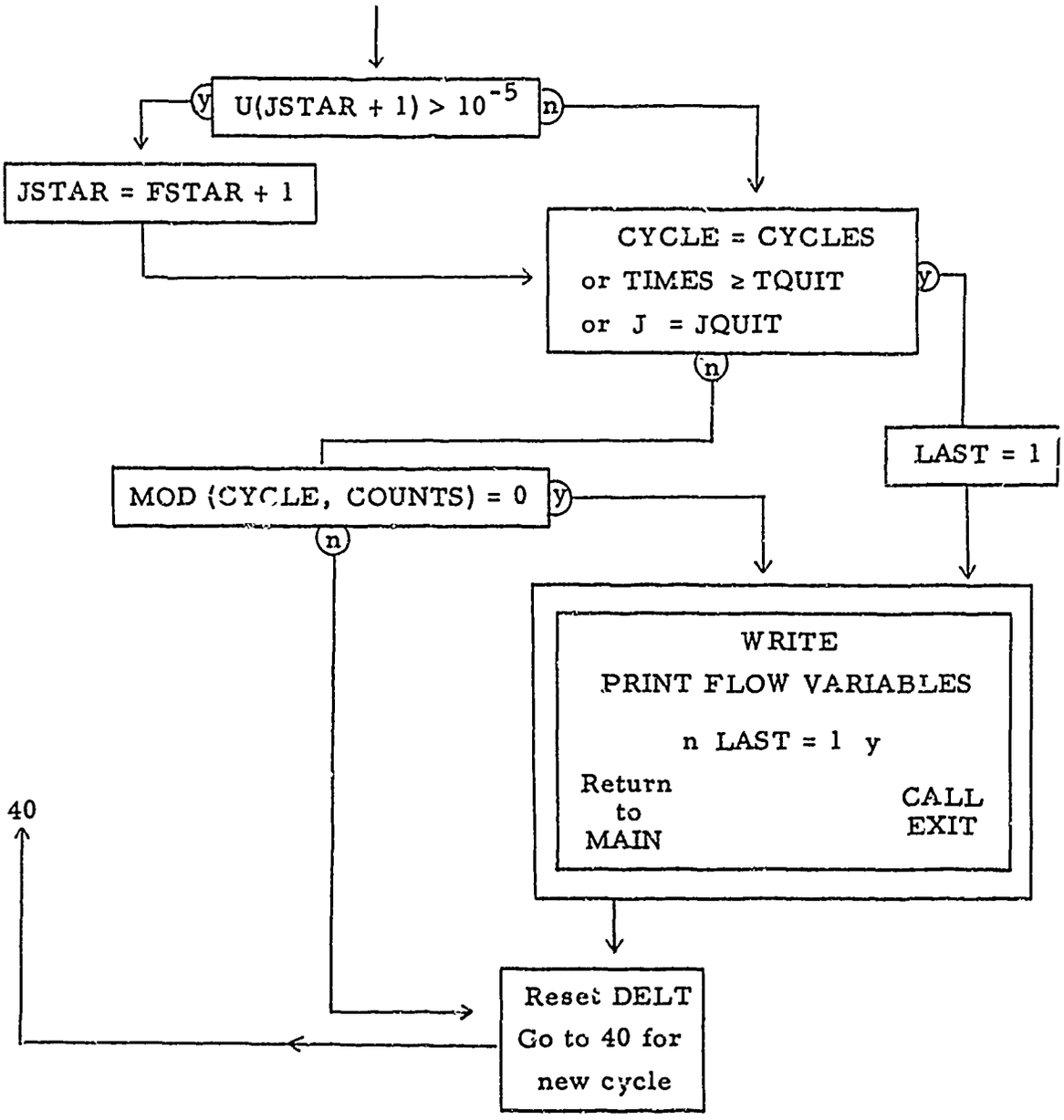
U(JSTAR + 1) > 10^-5
y
n
JSTAR = FSTAR + 1
CYCLE = CYCLES
or TIMES ≥ TQUIT
or J = JQUIT
y
n
LAST = 1
MOD (CYCLE, COUNTS) = 0
y
n
WRITE
PRINT FLOW VARIABLES
n LAST = 1 y
Return to MAIN
CALL EXIT
40
Reset DELT
Go to 40 for new cycle

Fig. 1. (c)

Unclassified
Security Classification

DOCUMENT CONTROL DATA - R & D

Security classification of title, body of abstract and indexing annotation must be entered when the overall rep. (In classified)

1. ORIGINATING ACTIVITY (Corporate author)
Washington State University
Department of Physics, Shock Dynamics Laboratory
Pullman, Washington 99163

2a. REPORT SECURITY CLASSIFICATION
UNCLASSIFIED

2b. GROUP

3. REPORT TITLE
EQUATIONS OF STATE IN SOLIDS (U)

4. DESCRIPTIVE NOTES (Type of report and inclusive dates)
Technical Summary Report No. 1 February 1967

5. AUTHOR(S) (First name, middle initial, last name)
Duvall, George E.,
Fowles, G. Richard,
Horie, Yasuyuki

6. REPORT DATE
February 1967

7a. TOTAL NO. OF PAGES

7b. NO. OF REFS
49

8a. CONTRACT OR GRANT NO.
DA-04-200-AMC-1702(X)

b. PROJECT NO.

c.

d.

9a. ORIGINATOR'S REPORT NUMBER(S)
SDL 67-01

9b. OTHER REPORT NO(S) (Any other numbers that may be assigned this report)

10. DISTRIBUTION STATEMENT
This document has been approved for public release and sale; its distribution is unlimited.

11. SUPPLEMENTARY NOTES

12. SPONSORING MILITARY ACTIVITY
U.S. Army
Ballistics Research Laboratories
Aberdeen Proving Ground, Maryland

13. ABSTRACT
A procedure is described for developing simple approximate equations of state of liquids from Hugoniot P-V relations determined in shock wave measurements. This is applied to a number of liquids and a table of coefficients is given.

The formalism of irreversible thermodynamics is applied to time-dependent phase transitions in iron and an approximate set of constitutive relations is obtained in a form suitable for numerical integration with the equations of continuum dynamics. These are applied in an approximate form to study the development of the two-wave structure in iron caused by the α-ε phase transition.

Finite strain theory is applied to the analysis of shock wave data for quartz, and the results supply enough information to estimate some of the fourth-order elastic constants.

DD FORM 1 NOV 65 1473

Unclassified
Security Classification

Security Classification

14 KEY WORDS	LINK A ROLE	LINK A WT	LINK B ROLE	LINK B WT	LINK C ROLE	LINK C WT
shock waves						
equations of state						
quartz--elastic constants						
liquids--equations of state						
phase transitions						
solids--phase transitions						
pressure induced phase transitions						
phase-transitions--effects on shock waves						
phase transitions--kinetics						
kinetics of phase transitions						

Security Classification